P-ISSN 0126-3188
E-ISSN 2443-3926

BRIN
BADAN RISET
DAN INOVASI NASIONAL

METALURGI

VOLUME 39 No 1 2024

SCIENTIFIC JOURNAL ACCREDITATION NO.3/E/KPT/2019

National Research and Innovation Agency

BRIN
BADAN RISET
DAN INOVASI NASIONAL

Publisher :
National Research and Innovation Agency (BRIN)
KST B.J Habibie Serpong, Tangerang Selatan, Banten, Indonesia, 15314

E-mail: metalurgi@brin.go.id

Science and technology magazine, regularly published every year; one volume consists of 3 editions

METALURGI

VOLUME 39 NUMBER 1 2024

P-ISSN 0126-3188
E-ISSN 2443-3926

ACCREDITATION: SK No. 72/E/KPT/2024

PREFACE

The author gives thanks to Allah for bestowing His blessing and direction, allowing the **Metalurgi Journal Volume 39, Edition 1**, **2024** to be successfully published.

The first article results from Soesaptri Oediyani and colleagues research activities on *The Added Value of Copper and Silver Metal from Printed Circuit Boards Waste Using Davis Tube with Variations of Size and Magnetic Intensity*. Vita Astini and colleagues presented the second article, *Influence of Electrolyte Molarity and Applied Voltage on the Purification of Ferronickel by Electrolysis Method*. Haviz Aulia and colleagues reviewed *Surface Modification of Composite Coating for Marine Application: A Short Review* in the following article. For the fourth article, Rahadian Nopriantoko reviewed *Green Approaches to Extractive Metallurgy: A Novel Synthesis of Sustainable Practices*. The fifth article by Fadhli Muhammad and his colleagues discussed *Microstructural Stability and High-Temperature Oxidation Behavior of* $Al_{0.25}$*CoCrCuFeNi High Entropy Alloy*.

The publication of this volume in Metalurgi Journal will benefit the advancement of research in Indonesia.

EDITORIAL

METALURGI

ISSN 0126 – 3188 Vol. 39 No. 1, 2024

Keywords sourced from articles. This abstract is reproduced without permission or fee.

Soesaptri Oediyani, Rahman Faiz Suwandana, Tiara Triana, Dewi Kusumaningtyas, Adjie Pradana, Zuhrainis Syaifara (Department of Metallurgy, Sultan Ageng Tirtayasa University)

Metalurgi, Vol. 39 No. 1, 2024

The Added Value of Copper and Silver Metal from Printed Circuit Boards Waste using Davis Tube with Variations of Size and Magnetic Intensity

The widespread use of electronic devices has led to a significant increase in electronic waste, including PCB (printed circuit board) waste. PCBs contain valuable metals like copper and silver, which can be reclaimed and reused. Recently, there has been a growing demand for urban mining processes to extract electronic waste PCB FR-2 (Flame Retardant-2) from laptops and computers. During the urban mining process, PCB FR-2 waste undergoes various physical treatments such as dismantling, crushing, and concentration processes. One of the concentration processes involves magnetic separation using a Davis tube. This study aims to investigate the effects of size and magnetic intensity variations on the recovery of copper and silver levels in FR-2 PCB waste. The magnetic concentration process was carried out using different size ranges (-63+100#, -100+150#, -150#) and magnetic intensities (1000 G, 2000 G, 3000 G). The results indicated that the most effective size for separating copper and silver is -63+100# and the optimal magnetic intensity is 1000 G. This resulted in copper and silver content of 45.66% and 0.162%, with recoveries of 80.135% and 62.505% respectively.

Keywords: Davis tube, electronic waste, magnetic separation, PCB FR-2, recovery

METALURGI

ISSN 0126 – 3188 Vol. 39 No. 1, 2024

Keywords sourced from articles. This abstract is reproduced without permission or fee.

Vita Astini[a] , Selvia Meirawati[b], Sulistia Nengsih[b], Arif[b], Hasriyanti[b], Johny Wahyuadi Mudaryoto Soedarsono[a], Anne Zulfia[a] ([a]Department of Metallurgy and Materials Engineering, University of Indonesia; [b]Department of Mining Engineering, Sembilanbelas November University)

Metalurgi, Vol. 39 No. 1, 2024

Influence of Electrolyte Molarity and Applied Voltage on the Purification of Ferronickel by Electrolysis Method

The current advancements in the automotive industry highlight the critical need for electric vehicles, which require a reliable supply of nickel for battery production. A potential nickel source is Ferronickel's local content, which can be used as a secondary resource. However, research on converting smelted Ferronickel into electrolytic nickel is still limited. This study aims to examine the effects of electrolyte molarity and applied voltage during the electrolysis process for refining Ferronickel. The molarities of HCl employed in this research are 0.1, 0.25, 0.5, 0.75, and 1 M for 2 hours. Additionally, the molarities of HCl are set at 2, 3, and 4 M for 6 hours. Further experiments were performed using varying voltages of 1, 2, 4, 6, and 8 V while keeping the solution concentration constant at 1 M and maintaining an electrolysis duration of 2 hours. The electrolysis solution was subsequently analyzed using the AAS (atomic absorption spectrophotometry) test. The results indicated that higher molarity levels were associated with increased current, resulting in faster reaction rates and greater solubilization of nickel metal. The Ni concentration rose with higher molarity, increasing from 76.50 mg/L in .25 M HCl to 91.88 mg/L in 1 M HCl. In contrast, the Fe concentration remained nearly constant across various molarity levels, ranging from 11.81 mg/L in .25 M HCl to 11.95 mg/L in 1 M HCl, suggesting a minimal influence of molarity below 1 M. Fe exhibited a strong positive correlation with increasing electrolyte molarity, showing a significant rise in concentration from 49.06 g/L at 2 M to 90.17 g/L at 4 M. Ni showed a more modest response to elevated molarity, with concentrations increasing from 11.95 g/L at 2 M to 22.70 g/L at 4 M. The Ni concentration increased with the applied voltage up to 6 V, reaching 95.57 mg/L, but then decreased to 77.67 mg/L at 8 V, indicating that the optimum voltage is 6 V. The Fe concentration displayed slight fluctuations but remained relatively stable across different voltage levels, measuring 11.81 mg/L at 1 V and 12.28 mg/L at 8 V, indicating that the applied voltage does not significantly influence Fe concentration in the solution.

Keywords: Ferronickel, electrolysis, molarity, applied voltage, concentration

METALURGI

ISSN 0126 – 3188 Vol. 39 No. 1, 2024

Keywords sourced from articles. This abstract is reproduced without permission or fee.

Hafiz Aulia, Rini Riastuti, Rizal Tresna Ramdhani (Department of Metallurgical and Materials Engineering, University of Indonesia)

Metalurgi, Vol. 39 No. 1, 2024

Surface Modification of Composite Coating for Marine Application: A Short Review

Corrosion is a prevalent phenomenon that significantly contributes to the deterioration of materials in offshore applications. The aggressive nature of marine corrosion is primarily attributed to the high salt content and the low electrical resistivity of seawater. While corrosion cannot be entirely eliminated, its reaction can be slowed down. Applying protective coatings is an effective and widely utilized method to protect metal surfaces from corrosion. These coatings act as a protective barrier that separates the metal from its surrounding environment, effectively retarding the corrosion rate. According to ISO 12944, the most commonly used generic coating systems for marine service include alkyd, acrylic, ethyl silicate, epoxy, vinyl ester, polyurethane, polyaspartic, and polysiloxane. The latest innovations in marine coatings still employ a layer-by-layer coating method, involving primer coats, intermediate coats, and top coats, depending on the desired thickness. Marine structures exposed to atmospheric conditions are commonly coated with one or two layers of epoxy. For enhanced performance, a more expensive system involving a layer of zinc-rich primer, followed by epoxy and aliphatic polyurethane coatings, may be utilized. Coating systems for atmospheric conditions are frequently employed in intertidal and splash zones. On the other hand, immersion zones of marine structures are typically coated with one or two layers of 100% solid epoxy or three layers of solvent-borne epoxy. The use of a single polymer as a generic coating has limitations. Incorporating fillers is a widely employed technique to enhance the characteristics of polymers, thereby transforming them into composites. In marine coatings, fillers are still limited to glass flakes and powder. Poor dispersion and agglomeration might reduce the effectiveness of fillers in the matrix, which decreases the adhesion properties. The fillers must be surface-modified before application. This review provides a comprehensive and critical analysis of the current research status of composite coatings that serve as candidates to be used in marine coating applications.

Keywords: Corrosion, marine coating, composite, surface modification

METALURGI

ISSN 0126 – 3188 Vol. 39 No. 1, 2024

Keywords sourced from articles. This abstract is reproduced without permission or fee.

Rahadian Nopriantoko **(**Mechanical Engineering, Krisnadwipayana University)

Metalurgi, Vol. 39 No. 1, 2024

Green Approaches to Extractive Metallurgy: A Novel Synthesis of Sustainable Practices

The realm of extractive metallurgy, a cornerstone for diverse industrial applications, has traditionally grappled with environmental challenges stemming from conventional extraction methods. This thorough literature review delves into the realm of innovative green approaches within extractive metallurgy, with the overarching goal of synthesizing sustainable practices. The introduction casts a spotlight on the environmental quandaries associated with traditional metallurgical practices, underscoring the imperative for ecologically friendly alternatives. The research methodology meticulously entails a comprehensive review of peer-reviewed literature, applying stringent criteria to handpick studies that delve into sustainable metallurgical practices. The results and discussion section intricately categorizes and dissects an array of green approaches in metal extraction, including bioleaching, ionic liquids, supercritical fluid extraction, green hydrometallurgy, electrochemical methods, and hybrid processes, providing nuanced insights into their efficacy and sustainability. Through the lens of case studies, the study sheds light on recent strides made by industries that have wholeheartedly embraced these sustainable practices, with a keen focus on unraveling their consequential environmental and economic impacts. Moreover, the study conscientiously addresses the challenges encountered in the adoption of green metallurgy and adeptly identifies latent opportunities for further development in this transformative field. The findings resonate with a resounding call for the widespread adoption of sustainable practices within extractive metallurgy, emphasizing their profound implications for both industrial application and the trajectory of future research endeavors. This expanded exploration underscores the pivotal role of environmentally conscious approaches in reshaping the landscape of extractive metallurgy, paving the way for a more sustainable and responsible future.

Keywords:Green, extraction, metallurgy, eco-friendly, sustainability

METALURGI

ISSN 0126 – 3188 Vol. 39 No. 1, 2024

Keywords sourced from articles. This abstract is reproduced without permission or fee.

Fadhli Muhammad[a], Ernyta Mei Lestari[a], Tria Laksana Achmad[a], Akhmad Ardian Korda[a], Budi Prawara[b], Djoko Hadi Prajitno[c], Bagus Hayatul Jihad[d], Muhamad Hananuputra Setianto[d], and Eddy Agus Basuki[a] ([a]Department of Metallurgical Engineering, Faculty of Mining and Petroleum Engineering, Institut Teknologi Bandung, [b]Research Centre for Advanced Materials, National Research and Innovation Agency, [c]Research Organization for Nuclear Technology, National Research and Innovation Agency, [d]Research Centre for Rocket Technology, Research Organization for Aeronautics and Space, National Research and Innovation Agency

Metalurgi, Vol. 39 No. 1, 2024

Microstructural Stability and High Temperature Oxidation Behavior of Al0.25CoCrCuFeNi High Entropy Alloy

$Al_{0.25}$CoCrCuFeNi is a high-entropy alloy composed of transition metals, specifically designed for high-temperature applications owing to its favorable mechanical properties, high melting point, and excellent high-temperature resistance. This alloy has been identified as a promising material for space exploration, particularly in the fabrication of combustion chambers and rocket nozzles by the National Aeronautics and Space Agency. Ongoing alloy development involves modifying the elemental composition. This study reduced aluminum content in the equiatomic AlCoCrCuFeNi alloy to $Al_{0.25}$CoCrCuFeNi, followed by isothermal oxidation treatments at 800, 900, and 1000°C. A series of experiments were conducted to investigate the microstructure stability and oxidation behavior of the $Al_{0.25}$CoCrCuFeNi alloy. The alloying elements were melted using a single DC electric arc furnace, followed by homogenization at 1100°C for 10 hours in an inert atmosphere. Subsequently, samples were cut into coupons for isothermal oxidation testing at the desired temperatures for 2, 16, 40, and 168 hours. The oxidized samples were characterized using XRD (x-ray diffraction), SEM (scanning electron microscopy) equipped with EDS (energy-dispersive X-ray spectroscopy), optical microscopy, and Vickers hardness testing. The as-homogenized alloy consisted of two constituent phases: an FCC (face-centered cubic) phase in the dendritic region and a copper-rich FCC phase in the inter-dendritic region. The oxides formed during the oxidation process included Al_2O_3, Cr_2O_3, Fe_3O_4, CoO, CuO, NiO, and spinel oxides $(Co, Ni, Cu)(Al, Cr, Fe)_2O_4$), with distinct formation mechanisms at each temperature.

Keywords: High-entropy alloy, isothermal oxidation, FCC structure, high temperature, phase stability

Metalurgi (2024) 1: 1 - 6

METALURGI
Majalah Ilmu dan Teknologi
p-ISSN 0126-3188 | e-ISSN 2443-3926
ejurnalmaterialmetalurgi.lipi.go.id

THE ADDED VALUE OF COPPER AND SILVER METAL FROM PRINTED CIRCUIT BOARDS WASTE USING DAVIS TUBE WITH VARIATIONS OF SIZE AND MAGNETIC INTENSITY

Soesaptri Oediyani*, Rahman Faiz Suwandana, Tiara Triana, Dewi Kusumaningtyas, Adjie Pradana, Zuhrainis Syaifara

Department of Metallurgy, Sultan Ageng Tirtayasa University
Jl. Jenderal Sudirman Km 3, Banten, Indonesia 42435
*E-mail: E-mail: s_oediyani@untirta.ac.id

Received: 12-02-2024, Revised: 04-03-2024, Accepted: 27-03-2024

Abstract

The widespread use of electronic devices has led to a significant increase in electronic waste, including PCB (printed circuit board) waste. PCBs contain valuable metals like copper and silver, which can be reclaimed and reused. Recently, there has been a growing demand for urban mining processes to extract electronic waste PCB Flame Retardant-2 (FR-2) from laptops and computers. During the urban mining process, PCB FR-2 waste undergoes various physical treatments such as dismantling, crushing, and concentration processes. One of the concentration processes involves magnetic separation using a Davis tube. This study aims to investigate the effects of size and magnetic intensity variations on the recovery of copper and silver levels in FR-2 PCB waste. The magnetic concentration process was carried out using different size ranges (-63+100#, -100+150#, -150#) and magnetic intensities (1000 G, 2000 G, 3000 G). The results indicated that the most effective size for separating copper and silver is -63+100# and the optimal magnetic intensity is 1000 G. This resulted in copper and silver content of 45.66% and 0.162%, with recoveries of 80.135% and 62.505% respectively.

Keywords: *Davis tube, electronic waste, magnetic separation, PCB FR-2, recovery*

1. INTRODUCTION

Advances in technology have led to an increase in the need for electronic equipment among the public so the production process of electronic devices is continuously in demand. However, this electronic equipment has a usage time limit which can cause e-waste to increase [1]. In 2016, global production of e-waste reached around 44.7 tons, while in 2021 the number increased by 17%, which is around 52.2 million tons and it can be estimated that by the end of 2030, total e-waste in the world could reach 74.7 million tons [2]-[3]. Things that can be done to take advantage of the ever-increasing amount of electronic waste can be reprocessing or urban mining. Many studies have been carried out to treat electronic waste, to obtain valuable metals contained in it such as gold and silver [2]. One part of an electronic device that contributes about 3% of all electronic waste is PCB (printed circuit board). PCB is a circuit board in a variety of electronic devices such as cell phones, computers, and televisions. The components on the PCB are made of polymer, metal, ceramic, and glass-based materials. PCB contains about 40% metal in all its components. Based on this, PCB is considered to have high economic value, so it is considered for reprocessing [2]. PCBs were included in electronic waste which contains the metal elements of Cu by 10-14.3% and Fe by 4.5-28% [4].

The three main stages applied to the process of extracting precious metals from PCBs are dismantling concentration, and purification. Magnetic separation was the commonly employed concentration process. Magnetic separation is carried out with two variables, i.e.,

DOI : 10.55981/metalurgi.2024.747

Metalurgi is Sinta 2 Journal (https://sinta.kemdikbud.go.id/journals/profile/3708) accredited by Ministry of Education, Culture, Research, and Technology, Republic Indonesia

particle size and gauss/magnetic intensity. The use of the magnetic concentration method (magnetic separation) was effective in the process of extracting precious metals from PCBs because magnets can separate metals with different magnetic properties [5]. Particle size is critical in PCB waste treatment, influencing the distribution of metal content across various size fractions [4]. The finer the PCB sample size used, the higher the valuable metal content obtained.

2. MATERIALS AND METHODS

The material used in this research was FR-2 PCB (printed circuit board) waste from computers and laptops. In this study, the dismantling was carried out which was then followed by comminution and magnetic separation. In the dismantling process, the electrical components were separated manually using a screwdriver, pliers, and a hammer. Furthermore, the comminution process consists of two stages, crushing and grinding to reduce PCB size. In the crushing process, a hammer mill was used up to 18# PCB size. In the grinding process, a pulverizer mill was used to reduce the PCB size. Then the sieving process is carried out with sizes -63+150#, -100+150#, and -150#. The XRD (x-ray diffraction) and XRF (x-ray fluorescence) analyses were also carried out for initial sample characterization. The next process was magnetic separation using a Davis tube with a magnetic intensity of 1000 G, 2000 G, and 3000 G and variations in size -63+100#, -100+150#, and -150#. The recovered samples from the Davis tube were further analyzed by XRF.

3. RESULT AND DISCUSSION

3.1 Sieve Analysis of FR-2 PCB Waste

Sieve analysis was conducted in a dry state, and a graph in Fig. 1 shows the relationship between particle size in micrometers and the cumulative percentage pass. This sieve analysis aims to ensure that 80% of the passing particles are of the desired size.

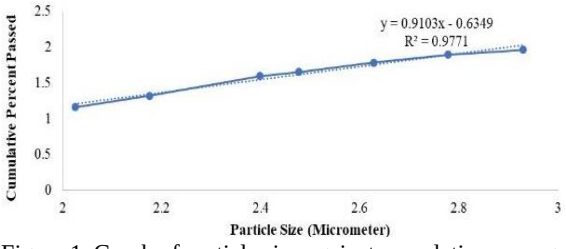

Figure 1. Graph of particle size against cumulative passage

Based on the graph, it appears that 80% of the initial samples did not pass through the 63#, 100#, and 150# sieves. Therefore, it is necessary to regrind the samples using a pulverizer mill.

3.2 XRD Characterization

The FR-2 PCB (printed circuit board) sample was tested using XRD (x-ray diffraction) characterization, and the results were obtained in Fig. 2. In Figure 2, it can be seen, that the dominant phases in the PCB used consist of copper and tin. The result is also supported by Anshu Priya's 2018 research which identified copper as the dominant metal element in PCB FR-2 [6]. On the other hand, tin is the main metal in the soldering process on PCBs, so the Sn content is also high [7].

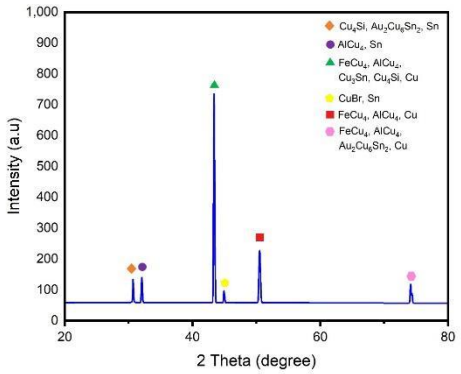

Figure 2. The constituents contained in PCBs

3.3 XRF Characterization

The results of the XRF (x-ray fluorescence) characterization test can be seen in Table 1 which depicts the highest elements content, such as copper, silicon, bromine, calcium, and aluminum.

Table 1. XRF characterization result of FR-2 PCB waste

Component	Grade (%)	Component	Grade (%)
Cu	54.03	Pb	0.71
Si	17.83	S	0.44
Br	8.57	Ag	0.24
Ca	7.44	Zn	0.17
Al	6.38	Ni	0.07
Sn	2.77	Sr	0.02
Fe	1.07	Sb	0.02

Copper l is the most dominant metal in PCBs because it has good electrical conductivity [8]. While silicon and calcium are non-metallic elements found in PCBs. Both elements were used as fiberglass materials for PCB parts [9]. Bromine was an element used in PCB boards such as paint, rubber, or PVC electrical insulation. Bromine has the function of reducing the flammability of PCB boards [8]. Silver and

tin were used in solder to suppress the use of toxic lead [8]. Iron and nickel were used as construction elements for contact transformer magnetic cores [8].

3.4 Effect of Size Variation on Copper Content in Non-Magnetic Materials

The particle size is one of the factors that can affect the concentration in the magnetic separation process [10]. Figure 3 shows the effect of sample size on copper and silver content. The copper content is increased when it reaches the size of -100+150# at the magnetic intensity of 2000 and 3000 G. However, at this size, the copper content decreased at 1000 G. According to Wills, the finer the materials, the easier to separate them from impurities [10]. Deviations from expected results observed at size fractions between -100+150# under 1000 G, particularly in the context of decreased copper content, might be attributed to suboptimal release efficiencies caused by copper adhesion to the solder holding layer. The solder holding layer on the PCB is a permanent epoxy resin-based coating applied to the PCB shaping process. The copper was still attached or locked with other materials (gangue) which can only be separated with further comminution [11]. These results were also supported by Otsuki et al, who stated that on PCB boards there was a high probability of metal bonding with other materials such as metal, plastic, fiberglass, or resin in different particle sizes. In coarser sizes, metals are prone to bonding with other materials, whereas in finer sizes, the possibility of a metal still bonding with other materials is low [12]. Further comminution is also needed because based on the ductile nature of copper, it shows low grind-ability [13]. Therefore, to liberate copper with other components and increase its levels, it is necessary to carry out further comminution.

Table 2. Copper and silver content in magnetic materials

Magnet Intensity (G)	Particle Size (#)	Copper (%)	Silver (%)
2000	-150	36.97	0.144
3000		47.89	0.133

The reduction in copper content at a specific size during the magnetic concentration process using a Davis tube is influenced by various factors. These include the degree of release and forces such as magnetic intensity, gravity, and friction acting on the Davis tube. These forces can impact the outcome of the concentration process. [14]. The larger copper particles can get stuck in the magnetic material at the center of the tube, causing them to be trapped among the magnetic elements. Svoboda [15] suggests that at higher concentrations, fluid forces are less effective for larger copper particles, so they cannot push the copper to the non-magnetic output. The metal content was increased at -150# with conditions of 1000 and 2000 G, whereas at this size with a magnetic intensity of 3000 G, the content was decreased. The increase of copper content at -150# is supported by Wills, that fine-size samples will get higher levels [10]. The finer particles can cause a degree of liberation increase and the valuable minerals will be easily separated from the impurities [10]. The size reduction process carried out to be a finer size can optimize the degree of liberation of copper from impurities (gangue) such as epoxy resin [11]. The increase in copper content at fine sizes can also be affected by the fluid flow during this magnetic separation. The finer the particle size, can cause the fluid push to become stronger than the working magnetic force [15]. In finer size, copper is easily carried away by fluid flow. During the concentration process, small metal particles were carried by the fluid flow and deposited into a non-magnetic container. Anomalous findings at size -150# under a 3000 G magnetic intensity condition may result from copper becoming trapped by the magnet and entering the magnetic output due to the strong magnetic intensity. This is further confirmed by the significant copper content in the magnetic output, as indicated in Table 2, at 47.89%.

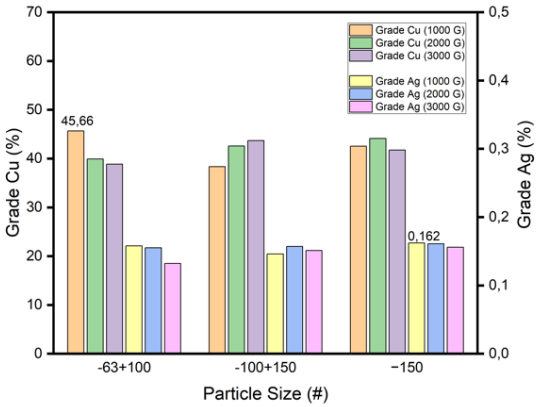

Figure 3. Effect of particle size on copper and silver metal content in non-magnetic materials

3.5 Effect of Size Variation on Silver Metal Content in Non-Magnetic Materials

The silver content obtained from this study can be seen in Fig. 3. The silver content continues to increase with the finer particles. The research by Wills [10] stated that the finer the size, the more valuable minerals will be free from impurities. The increased content of silver

at a fine size was also caused by silver on the PCB board which is in the form of a thin layer [16]. Apart from this, the low content of silver facilitates the process of reducing the size of silver in PCB FR-2 waste [13]. The results of this study can be caused by the influence of the fluid used during the wet magnetic separation process. The fine size can cause the fluid force to be greater than the working magnetic force [15]. This is because silver with a smooth size and a flat shape on the PCB is easier to push by the fluid flow and not attracted by the intensity of the magnet which will then go to a non-magnetic material container.

3.6 Effect of Magnetic Intensity on Copper and Silver Content in Non-Magnetic Materials

In Figure 4 it can be seen the effect of the magnetic intensity on the levels of copper and silver. Copper and silver levels were concluded as fluctuating results. This is because the levels of copper and silver increase at a magnetic intensity of 2000 G and then decrease at a magnetic intensity of 3000 G. The increased levels of copper and silver in non-magnetic materials with a magnetic intensity of 2000 G can be caused by the dominance of low magnetic (diamagnetic) metals on FR-2 PCB waste samples. The dominance of low magnetic metals will cause impurities resulting from the magnetic concentration process. These impurities can be in the form of high-diamagnetic material at both outputs from the magnetic concentration process [10]. This is supported by the high levels of copper and silver in magnetic materials. The predominance of diamagnetic metals on FR-2 PCBs, for example, copper, tin, zinc, and silver, can be seen in Table 1.

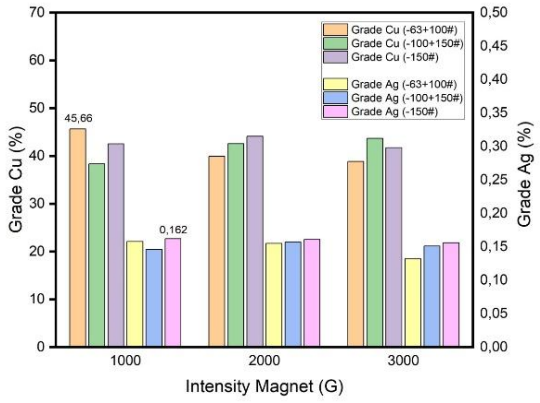

Figure 4. Effect of magnetic intensity on copper and silver content in non-magnetic materials

The decreased levels of copper and silver at a magnetic intensity of 3000 G can be caused by a high magnetic intensity. The high intensity of the magnet can increase the strength of the magnet to attract materials with low magnetic properties into the magnetic material output. This causes a decrease in weakly magnetic metals in the output of non-magnetic materials [10]. In other words, it can be concluded that with a magnetic intensity of 3000 G, a lot of copper and silver are attracted to the magnet and become a magnetic material output. The following research by Yamato [17] that the higher the magnetic intensity used, the material with low magnetic properties will be carried over to the magnetic material output.

The varying levels of copper and silver obtained could be due to clumping during the concentration process. Clumping prevents the material from coming into contact with the magnet during the magnetic concentration process. Clumping may occur because the PCB FR-2 material is hydrophobic, causing it to clump when dissolved in water [18].

3.7 Copper and Silver Recovery in Non-Magnetic Materials Using Davis Tube

The highest recovery of copper (80.135%) and silver (62.505%) was achieved at a magnetic intensity of 1000 G. While the documented prevalence of these key elements in FR-2 PCBs, as highlighted by Anshu Priya [6], may indeed facilitate their recovery, it appears that an alternative mechanism is in operation in this context.

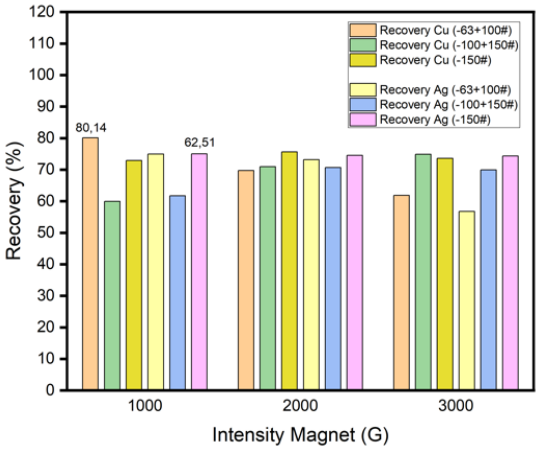

Figure 5. Copper and silver recovery in non-magnetic materials

Despite the hypothesis that strong magnetic attraction is needed to achieve high recovery of these weakly magnetic metals, the high recovery at 1000 G seems to be due to their repulsion from the magnet and subsequent settling in the non-magnetic container. This is consistent with the observation that high magnetic intensity can

impede the recovery of non-magnetic materials [17].

The ideal magnetic intensity of 1000 G for the recovery of copper and silver is likely due to a balance between maximizing the capture of the main elements in the PCB and minimizing the repulsive effects of the magnet on these weak magnetic metals. Although this intensity is close to achieving the theoretical maximum recovery of 100% [19], further research is necessary to fully comprehend the connection between magnetic intensity, metal properties, and recovery efficiency in this separation process.

4. CONCLUSION

The size of particles influences how quickly valuable minerals are separated from impurities. During magnetic concentration, the highest levels of copper and silver were obtained at particle sizes of -63+100# and -150# respectively. The strength of the magnetic field affects the separation of materials based on their magnetic properties. The highest levels of copper and silver were found at a magnetic intensity of 1000 G, with levels of 45.66% and 0.162% respectively. The recovery of metals is impacted by the metal content and the mass of valuable minerals obtained. The best recoveries of copper and silver are 80.135% and 62.505% at a magnetic intensity of 1000 G.

ACKNOWLEDGMENT

The author would like to thank the Geoservices Laboratory for assisting in providing a place and tools for this research.

REFERENCES

[1] H. M. Veit, T. R. Diehl, A. P. Salami, J. S. Rodrigues, A. M. Bernardes, and J. A. S. Tenório, "Utilization of magnetic and electrostatic separation in the recycling of printed circuit boards scrap," *Waste Management*, vol. 25, no. 1, pp 67-74, 2005. Doi:10.1016/j.wasman.2004.09.009.

[2] C. M. de Oliveira, R. Bellopede, A. Tori, G. Zanetti, and P. Marini, "Gravity and electrostatic separation for recovering metals from obsolete printed circuit board," Materials, vol. 15, no. 5, 2022. Doi: 10.3390/ma15051874.

[3] P. R. Yaashikaa, B. Priyanka, P. S. Kumar, S. Karishma, S. Jeevanantham, and S. Indraganti, "Chemosphere a review on recent advancements in recovery of valuable and toxic metals from e-waste using bioleaching approach," *Chemosphere*, vol. 287, pp 132230, 2022. Doi:10.1016/j.chemosphere.2021.132230.

[4] X. N. Zhu, C. C. Nie, S. S. Wang, Y. Xie, H. Zhang, X. J. Lyu, J. Qiu, and L. Li, "Cleaner approach to the recycling of metals in waste printed circuit boards by magnetic and gravity separation," *Journal of Cleaner Production*, vol. 248, pp 119235, 2019. Doi:10.1016/j.jclepro.2019.119235.

[5] L. H. Yamane, V. T. de Moraes, D. C. R. Espinosa, and J. A. S. Tenório, "Recycling of WEEE: Characterization of spent printed circuit boards from mobile phones and computers," *Waste Management*, vol. 31, no. 12, pp 2553-2558, 2011. Doi:10.1016/j.wasman.2011.07.006.

[6] Anshu Priya and S. Hait, "Comprehensive characterization of printed circuit boards of various end-of-life electrical and electronic equipment for beneficiation investigation," *Waste Management*, vol. 75, pp. 103-123, 2018. Doi:10.1016/j.wasman.2018.02.014.

[7] J. Hao, X. Wang, Y. Wang, F. Guo, and Y. Wu, "Optimization kinetic studies of tin leaching from waste printed circuit boards and selective tin recovery from Its pregnant solution," *Metals*, vol. 12, no. 6, 2022. Doi:10.3390/met12060954.

[8] J. Szałatkiewicz, "Metals content in printed circuit board waste," *Polish Journal of Environmental Studies*, vol. 23, no. 6, pp 2365-2369, 2014.

[9] H. Jianjun, J. Shi, M. Yuedong, and L. Zhengzhi, "DC arc plasma disposal of printed circuit board system of the DC arc plasma disposal of solid waste," *Plasma Science & Technology*, vol. 6, 2004.

[10] T. Napier-Munn and B. A. Wills, *Wills' Mineral Processing Technology*, 7th ed., 2005. Doi:10.1016/b978-075064450-1/50000-x.

[11] H. A. Noorliyana, K. Zaheruddin, and H. Kamarudin, "A study of liberation and separation process of metals from printed circuit boards (PCBS) scraps," *Key Engineering Materials*, pp 123-127, 2014. Doi:10.4028/www.scientific.nen/KEM.594-595.123.

[12] A. Otsuki, L. D. La Mensbruge, A. King, S. Serranti, L. Fiore, and G. Bonifazi, "Non-destructive characterization of mechanically processed waste printed circuit boards - particle liberation analysis," *Waste Management*, vol. 102, pp 510-519, 2020. Doi:10.1016/j.wasman.2019.11.006.

[13] A. Priya and S. Hait, "Characterization of particle size-based deportment of metals in various waste printed circuit boards towards metal recovery," *Cleaner Materials*, vol. 1, pp. 100013, 2021. Doi:10.1016/j.clema.2021.100100.
[14] B. R. Arvidson and D. Norrgran, 2014, *Magnetic separation*, Mineral Processing and Extractive Metallurgy: 100 Years of Innovation," vol. M, no. 2, pp 223-233. Doi:10.1201/9781003139638-41.
[15] J. Svoboda and T. Fujita, "Recent developments in magnetic methods of material separation," *Minerals Engineering*, vol. 16, no. 9, pp 785-792, 2003. Doi:10.1016/S0892-6875(03)00212-7.
[16] M. Kaya, "Recovery of metals and nonmetals from electronic waste by physical and chemical recycling processes," *Waste Management*, vol. 57, pp 64-90, 2016. Doi:10.1016/j.wasman.2016.08.004.
[17] M. Yamato and T. Kimura, "Magnetic processing of diamagnetic materials," *Polymers*, vol. 12, no. 7, pp 1-23, 2020. Doi:10.3390/polym12071491.
[18] O. O. Oluokun and I. O. Otunniyi, "Chemical conditioning for wet magnetic separation of printed circuit board dust using octyl phenol ethoxylate," *Separation and Purification Technology*, vol. 240, pp. 116586, 2020. Doi :0.1016/j.seppur.2020.116586.
[19] C. Gasparrini, "General principles of mineral processing," in *Gold and Other Precious Metals*. 1993. Doi:10.1007/978-3-642-77184-2_6.

Metalurgi (2024) 1: 7 - 14

METALURGI
Majalah Ilmu dan Teknologi
p-ISSN 0126-3188 | e-ISSN 2443-3926
ejurnalmaterialmetalurgi.lipi.go.id

INFLUENCE OF ELECTROLYTE MOLARITY AND APPLIED VOLTAGE ON THE PURIFICATION OF FERRONICKEL BY ELECTROLYSIS METHOD

Vita Astini[a] , Selvia Meirawati[b], Sulistia Nengsih[b], Arif[b], Hasriyanti[b], Johny Wahyuadi[a] Mudaryoto Soedarsono[a], Anne Zulfia[a,*]

[a]Department of Metallurgy and Materials Engineering,University of Indonesia
Kampus Universitas Indonesia Depok, Indonesia 16424
[b]Department of Mining Engineering, Sembilanbelas November University
Jl. Pemuda No. 339, Kolaka, Indonesia 93517
*E-mail: anne.zulfia@ui.ac.id

Received: 08-12-2023, Revised: 20-03-2024, Accepted: 29-04-2024

Abstract

The current advancements in the automotive industry highlight the critical need for electric vehicles, which require a reliable supply of nickel for battery production. A potential nickel source is Ferronickel's local content, which can be used as a secondary resource. However, research on converting smelted Ferronickel into electrolytic nickel is still limited. This study aims to examine the effects of electrolyte molarity and applied voltage during the electrolysis process for refining Ferronickel. The molarities of HCl employed in this research are 0.1, 0.25, 0.5, 0.75, and 1 M for 2 hours. Additionally, the molarities of HCl are set at 2, 3, and 4 M for 6 hours. Further experiments were performed using varying voltages of 1, 2, 4, 6, and 8 V while keeping the solution concentration constant at 1 M and maintaining an electrolysis duration of 2 hours. The electrolysis solution was subsequently analyzed using the AAS (atomic absorption spectrophotometry) test. The results indicated that higher molarity levels were associated with increased current, resulting in faster reaction rates and greater solubilization of nickel metal. The Ni concentration rose with higher molarity, increasing from 76.50 mg/L in .25 M HCl to 91.88 mg/L in 1 M HCl. In contrast, the Fe concentration remained nearly constant across various molarity levels, ranging from 11.81 mg/L in .25 M HCl to 11.95 mg/L in 1 M HCl, suggesting a minimal influence of molarity below 1 M. Fe exhibited a strong positive correlation with increasing electrolyte molarity, showing a significant rise in concentration from 49.06 g/L at 2 M to 90.17 g/L at 4 M. Ni showed a more modest response to elevated molarity, with concentrations increasing from 11.95 g/L at 2 M to 22.70 g/L at 4 M. The Ni concentration increased with the applied voltage up to 6 V, reaching 95.57 mg/L, but then decreased to 77.67 mg/L at 8 V, indicating that the optimum voltage is 6 V. The Fe concentration displayed slight fluctuations but remained relatively stable across different voltage levels, measuring 11.81 mg/L at 1 V and 12.28 mg/L at 8 V, indicating that the applied voltage does not significantly influence Fe concentration in the solution.

Keywords: *Ferronickel, electrolysis, molarity, applied voltage, concentration*

1. INTRODUCTION

A substantial supply of nickel is required as a battery raw material to support the government's domestic electric vehicle production initiative. One potential source of nickel is local-content ferronickel (FeNi), which can be utilized as a secondary resource. However, FeNi applications are currently limited. It is primarily used as a raw material for stainless steel production. To date, ferronickel has not been effectively utilized for other purposes [1]-[4].

According to United States Patent No. 3,755,113 [4] and findings published by Moussoulos [5], the production process of electrolytic nickel from ferronickel

DOI : 10.55981/metalurgi.2024.742

Metalurgi is Sinta 2 Journal (https://sinta.kemdikbud.go.id/journals/profile/3708) accredited by Ministry of Education, Culture, Research, and Technology, Republic Indonesia

demonstrates that ferronickel products with a nickel content of 80-85% can be purified to 99.95% Ni through the electrorefining method. This process can significantly expand the market potential of ferronickel, which is currently predominantly utilized in stainless steel manufacturing. However, there are limitations, including the requirement that a Feni anode with a minimum Ni content of 80% be used to obtain high nickel with high purity by electrorefining.

Feni extracted from Ni laterite ore with a pyrometallurgical process has a Ni content of around ± 20%. So, in both studies, the anode from Feni was not used; it made its anode material with a composition of Ni above 80%. Therefore, a precise method is needed to convert Feni into Ni electrolytic with the available Feni Anode.

Several studies have been conducted [6–9] to separate Ni from other metals. Chen et al.[6] Crushed and calcined the battery and dissolved it with acetic acid and water. Ni and Cd dissolve as Ni(CHCOO) and Cd(CHCOO), while Fe(CHCOO)OH is insoluble in water. So, that method can be used to separate Ni and Fe.

The ferronickel refining process using the electrolysis method uses an electrolyte solution as a conductor medium to conduct electric current between the anode and the cathode. The electrolyte solution can also be a catalyst to accelerate the reaction rate. The molarity of the electrolyte solution used can affect the process that occurs in electrolysis and the quality of the results obtained.

This study utilized HCl (hydrochloric acid) as the electrolyte solution. HCl was chosen due to its strong acid properties, which allow complete ionization in solution. This characteristic makes HCl an effective catalyst within the electrolyte solution, facilitating a rapid reaction rate through enhanced ionic conductivity and efficient electrochemical kinetics [10].

This study focuses on the influence of electrolyte molarity and applied voltage in the electrolysis process for refining ferronickel (FeNi). The electrolyte solution's concentration and applied voltage can significantly impact electrolysis. Thus, when employing electrolysis methods in ferronickel refining, it is crucial to consider the effects of electrolyte molarity and applied voltage to achieve optimal refining results.

2. MATERIALS AND METHODS

2.1 Sample and Electrolyte Preparation

This research aims to obtain secondary nickel (Ni) and cobalt (Co) resources through the electrorefining of ferronickel shot. Ferronickel shot from PT Antam Tbk. is available in two composition variations: LCS (low carbon shot) and HCS (high carbon shot). Based on XRF (x-ray fluorescence) analysis, the composition of the HCS samples is in Table 1.

Tabel 1. Composition of ferronickel shot

Element	Composition (wt.%)
Fe	77.369
C	1.140
Ni	18.490
Co	0.340
Mn	0.040
Cr	0.890
Si	0.430
P	0.017
S	1.275
Cu	0.009

Ferronickel was cast into blocks with 11 x 1 x 0.5 cm dimensions to use as the anode in the electrolysis process (Fig. 1). The cast ferronickel samples were cut into pieces according to predetermined dimensions. Subsequently, the samples were cleaned of impurities using a grinding machine and weighed to determine their mass before the electrolysis reaction.

Figure 1. Ferronickel anode

Electrodes serve as conductive media that allow electric current to flow from one medium to another. Typically made from metals like copper, silver, tin, or zinc, electrodes can also be composed of non-metallic conductive materials like graphite[11]. In this study,

graphite was used as the cathode, while the ferronickel block was used as the anode. The cathode uses graphite (C) as a cylinder with a length of 11 cm and a diameter of 1 cm.

The electrolyte solution was prepared by diluting 37% HCl in distilled water. HCl, a strong acid commonly used in industry, is an effective electrolyte in solution [12]. The molarities of HCl used in this research are 0.1, 0.25, 0.5, 0.75, and 1 M.

2.2 Electrolysis Process

Various concentrations of HCl were employed to investigate the influence of electrolyte molarity on the electrolysis process. The electrolysis was conducted in a 250 ml glass beaker containing 200 ml of the prepared electrolyte solution. A ferronickel block served as the anode, while graphite was used as the cathode, both immersed in the electrolyte. The HCl molarities studied were 0.1, 0.25, 0.5, 0.75, and 1 M. The anode and cathode were connected to the positive and negative terminals of a Dekko PS-3030Q rectifier, respectively, with an applied voltage of 1 V. The electrolysis was carried out for 2 hours. Additional experiments were conducted using higher HCl molarities of 2, 3, and 4 M, with an applied voltage of 2 V and an extended electrolysis duration of 6 hours.

Subsequent experiments were performed at varying voltages of 1, 2, 4, 6, and 8 V to elucidate the effect of applied voltage on electrolysis while maintaining a constant HCl concentration of 1 M and an electrolysis duration of 2 hours.

2.3 Quantitative Determination of Chemical Element

AAS (atomic absorption spectrophotometry) is a chemical analysis instrument that uses the principle of energy absorbed by atoms to analyze the concentration of analytes in a sample. By absorbing energy, electrons in the atom are quickly excited to a higher orbital [13].

The parameters varied in this research include the concentration of the HCl electrolyte solution, precisely 0.1, 0.25, 0.5, 0.75, and 1 M, and the applied voltage that is 1, 2, 4, 6, and 8V. After electrolysis, the solution was filtered using filter paper to separate it from impurities. The filtered solution was then transferred to a 100 ml bottle for analysis using AAS to determine its elemental composition.

For the experiments conducted with higher HCl molarities of 2, 3, and 4 M under an applied voltage of 2 V and an electrolysis duration of 6 hours, the electrolyte was characterized using a 725 ICP-OES (inductively coupled plasma optical emission spectroscopy) instrument.

3 RESULT AND DISCUSSION

3.1 The Effect of Electrolyte Molarity

The electrolysis results for each sample varied according to the concentration levels used. The electrolyte solutions are depicted in Fig. 2. Observations indicate that higher molarity levels correspond to increased current. Consequently, the electric current in each sample varied with the molarity concentration, leading to a faster reaction rate and increased solubilization of nickel metal.

Figure 2. Electrolysis solution

Based on the standard reduction potential at 25 ^{o}C, the Ni reaction in Equation 1 and for Fe oxidation reaction in Equation 2 [14].

$$Ni^{+} + 2e^{-} \rightarrow Ni \qquad E^{o} = -0.250 \text{ V} \quad (1)$$

$$Fe^{++} + 2e^{-} \rightarrow Fe \qquad E^{o} = -0.440 \text{ V} \quad (2)$$

The relationship between the standard reduction potentials of Ni and Fe and the rate of electrolysis at an anode composed of Fe and Ni with a graphite cathode is governed by the relative tendencies of these metals to undergo oxidation. Iron, having a more negative standard reduction potential (-0.44 V) compared to nickel (-0.25 V), is more susceptible to oxidation. Consequently, during the electrolytic process, the oxidation of iron at the anode typically proceeds faster than that of nickel under equivalent conditions.

Figure 3 shows dissolved Ni and Fe resulting from electrolysis at a 1 V voltage measured using AAS based on differences in electrolyte molarity. Fe concentration remains almost constant across different molarity levels, with only slight fluctuations. In 0.25 M HCl, it is 11.81 mg/l, and in 1 M HCl, it is 11.95 mg/l. This stability suggests that the electrolyte's molarity does not significantly influence the Fe

concentration if the concentration of HCl is below 1 M.

The apparent increase in Ni concentration with higher molarity levels suggests that Ni ions are more readily dissolving into the solution as the molarity increases. The lowest Ni concentration is 76.50 mg/L in 0.25 M HCL; the highest is 91.88 mg/L in 1 M HCl. This could indicate that higher molarity electrolytes enhance the solubility of Ni or that Ni ions are being more effectively released into the solution due to stronger electrolyte interactions. Higher molarity electrolytes can play a crucial role in enhancing the solubility of nickel ions or facilitating the more effective release of nickel ions into a solution due to more robust interactions with the electrolyte [15]-[17].

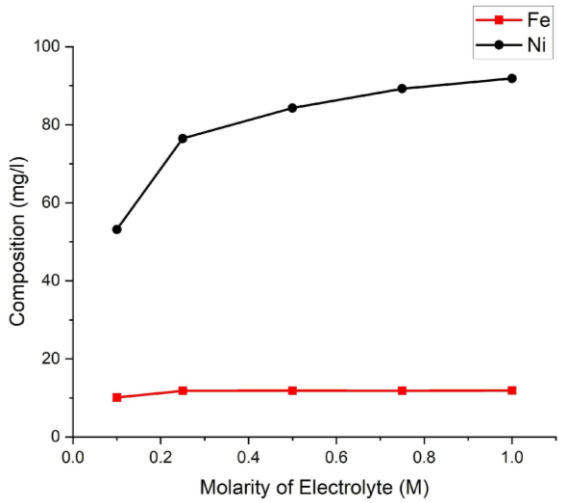

Figure 3. Dissolved Ni and Fe resulting from electrolysis at a 1 V for 2 h voltage were measured using AAS based on differences in electrolyte molarity

Passivation of iron in weak acid media greatly lowers the reaction rates due to the protective oxide layer that develops on the iron surface. This layer prevents further electrochemical activity, hence reducing the dissolution of iron.

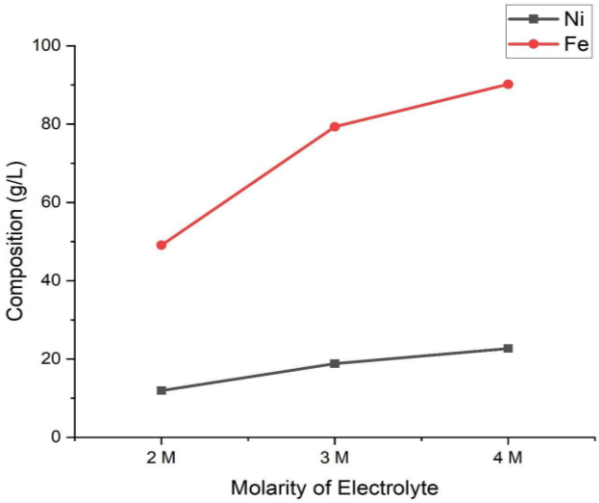

Figure 4. Dissolved Ni and Fe resulting from electrolysis at 2 V for 6 h were measured using 725 ICP-OES based on differences in electrolyte molarity

In contrast, the same acid environment is less aggressive for nickel since it does not form any protective passive layer under these conditions. Consequently, nickel becomes more sensitive to oxidation and dissolution during electrolysis; hence, its higher concentration in solution [18]-[19].

Figure 4 describes the effect of electrolyte molarity on the composition of Ni and Fe in the solution, measured in grams per liter (g/L). The data demonstrate distinct responses of Ni and Fe to changes in the molarity of the electrolyte. For Fe, a positive correlation is observed between the molarity of the electrolyte and the Fe concentration in the solution. Specifically, at 2 M molarity, the Fe concentration is approximately 49.06 g/L.

This concentration increases to about 79.31 g/L at 3 M and 90.17 g/L at 4 M molarity. The trend suggests a linear relationship between the electrolyte molarity and the Fe concentration, indicating that higher molarity levels facilitate more significant dissolution or deposition of Fe in the solution. This phenomenon could be attributed to enhanced ionization or increased availability of Fe ions in higher molarity conditions [20]-[21].

The Ni concentration shows a more modest increase with the electrolyte molarity. At 2 M molarity, the Ni concentration is around 11.95 g/L. The increases to approximately 18.82 g/L at 3 M molarity and to about 22.70 g/L at 4 M. The increment is relatively smaller than Fe, suggesting that Ni is less sensitive to changes in electrolyte molarity. This behavior might be due to the intrinsic electrochemical properties of Ni, such as its standard electrode potential, and because the anode contains almost four times higher percentation of Fe than Ni.

3.2 The Effect of Applied Voltage

The Fe concentration shows slight fluctuations but remains relatively stable across different voltage levels (Fig. 5). In 1 V, it is 11.81 mg/L, and in 8 V, it is 12.28 mg/L, indicating that the applied voltage does not heavily influence the concentration of Fe in the solution. This suggests that voltage changes do not significantly impact Fe ions solubility in 1 M HCl and 2 H electrolysis.

The Ni concentration increases with the applied voltage up to 6V, after which it decreases at 8V. In 6 V, it is 95.57 mg/L, and in 8 V, it is 77.67 mg/L. This indicates a more

complex relationship between Ni concentration and applied voltage in 1 M HCl and 2 H electrolysis. The initial increase suggests that higher voltage enhances the solubility or release of Ni ions into the solution [22]-[23]. However, the decrease at 8V may imply a too-rapid reaction because of a too-high voltage, affecting Ni ion concentration at higher voltages [24].

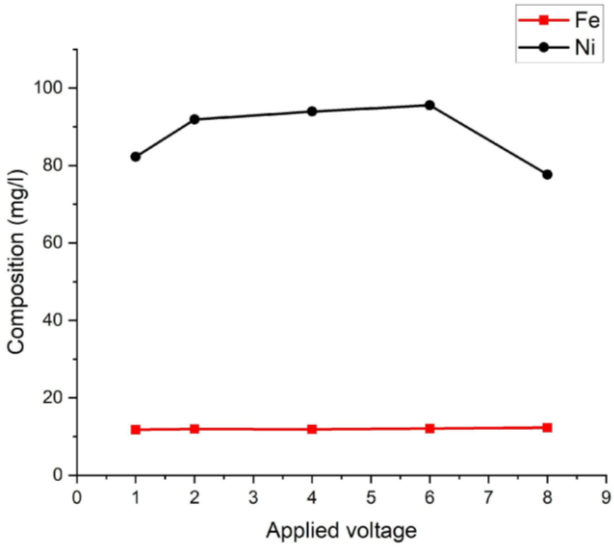

Figure 5. Dissolved Ni and Fe resulting from electrolysis at 1 M HCl for 2 h were measured using AAS based on differences in applied voltage

3.2 Precipitation with NaOH

After the electrolysis process, a filtrate containing metal ions such as Ni^{2}+, Fe^{2}+, Co2+, and others is obtained. The deposition experiment commences with the oxidation of the filtrate solution using hydrogen peroxide (H_2O_2).

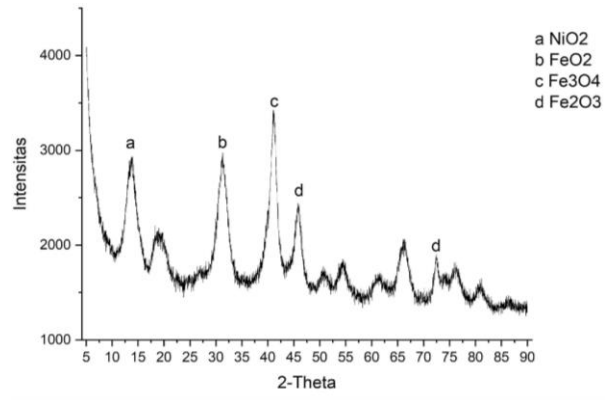

Figure 6. XRD patterns illustrate the precipitates generated at a consistent pH of 4 with reaction temperatures of 50°C, resulting from electrolysis in 2 M HCl at 2 V for 11 hours, with oxidation by H_2O_2 measured using XRD

This oxidation step, crucial for converting Fe^{2}+ ions to Fe^{3}+, is carefully controlled over approximately 1 hour. Following oxidation, the filtrate is subjected to precipitation by adding NaOH and adjusting the pH to approximately 4. Subsequent filtration is then performed to separate the filtrate enriched with Ni^{2}+ and Co^{2}+ ions from the Fe residue. At 50°C precipitation temperature (Fig. 6), the residue exhibits peaks, indicating a mixed-phase composition. Peaks labeled b, c, and d suggest the presence of FeO_2, Fe_3O_4, and Fe_2O_3, with Fe_2O_3 being the dominant phase. Also, there is a small peak of NiO.

Controlling pH and temperature is very important to separate Ni from Fe and other metals that are contained in ferronickel.

4. CONCLUSION

In this investigation, higher molarity levels were associated with increased current, which resulted in faster reaction rates and increased nickel metal solubilization. Ni concentrations increased with increasing molarity, from 76.50 mg/L in 0.25 M HCl to 91.88 mg/L in 1 M HCl. In contrast, Fe content remained fairly constant across multiple molarity levels, ranging from 11.81 mg/L in 0.25 M HCl to 11.95 mg/L in 1 M HCl, demonstrating that molarity has no effect below 1 M. Fe concentration increases significantly as electrolyte molarity increases, from 49.06 g/L at 2 M to 90.17 g/L at 4 M. Ni responds more modestly to changes in high molarity, with concentrations increasing from 11.95 g/L at 2 M to 22.70 g/L at 4 M. The less obvious increase in Ni concentration can be attributed to its intrinsic electrochemical features, such as standard electrode potential, as well as the anode's nearly four-fold higher Fe percentage than Ni. The Ni concentration rises with the applied voltage up to 6 V, reaching 95.57 mg/L, but drops to 77.67 mg/L at 8 V. The initial increase indicates that increased voltage improves the solubility or release of Ni ions into the solution. However, the decline at 8 V could indicate that a high voltage induces an extremely quick response, affecting Ni ion concentration at higher voltages. So, the ideal voltage is 6 volts. The Fe content changes somewhat but remains very consistent across voltage levels.

ACKNOWLEDGMENT

Universitas Indonesia has supported this paper through the PUTI Postgraduate Grant Grant with contract number NKB-246/UN2.RST/HKP.05.00/2023, and PT ANTAM Tbk. have provided the FeNi material.

REFERENCES

[1] S. Mulshaw and A. Gardner. Nickel outlook - Appendices 2022. USA: Wood Mackenzie, 2022, pp.3-10.
[2] S. Mulshaw and A. Gardner. Global Nickel Investment Horizon Outlook Q3. USA : Wood Mackenzie, 2022, pp. 6-22.
[3] IEA. Securing supplies for an electric future. France: IEA, 2022, pp. 6-12.
[4] I. Entsev, N. Kuntshev, G. Haralamplev, and D. Petrov. " Method for electrorefining of nickel". U.S. Patent 3 755 113, Aug. 28, 1973.
[5]L. Moussoulos, "A process for the production of electrolytic nickel from ferronickel," *Metall. Trans. B*, vol. 6, no. 4, pp. 641-645, 1975.
[6] K. Chen, W. Chester, J. K. Collins, B. P. Kiely, F. Luo, L. D. O'Mahony, R. P. Phillipson, and F. Shanahan, " Method for separating iron from nickel and/or cadmium from a waste containing the same". U.S Patent 5 728 1854, 1998.
[7] Y. Xue, Y. Hua, J. Ru, C. Fu, Z. Wang, J. Bu, and Y. Zhang, "High-efficiency separation of Ni from Cu-Ni alloy by electrorefining in choline chloride-ethylene glycol deep eutectic solvent," J. *Adv. Powder Technol.*, vol. 32, no. 6, pp. 2791-2797, 2021.
[8] F. Crundwell and M. Moats, "Extractive metallurgy of nickel, cobalt and platinum group metals," USA : Elsevier, 2011, pp. 1-18. Doi:10.1016/B978-0-08-096809-4.10002-4
[9] R. R. Moskalyk and A. M. Alfantazi, "Nickel sulfide smelting and electrorefining practice: A review," *Miner. Process. Extr. Metall. Rev*., vol. 23, no. 3-4, pp. 141-180, 2002. Doi: 10.1080/08827500306893
[10] A. W. Noviana, "Analisis pengaruh variasi jenis elektrode dan katalis terhadap produksi hidrogen dengan metode elektrolisis air laut dari kawasan mangrove," Bachelor Thesis. Muslim Negeri Maulana Malik Ibrahim University. pp. 48-59, 2022.
[11] S. Fariya and S. Rejeki, "Pemanfaatan elektrolit air laut menjadi cadangan sumber energi listrik sebagai penerangan pada sampan," *J. Sains dan Teknol*., vol. 10, no. 1, pp. 44-58, 2015.
[12]S. Anwar, "Analisis tipe dan konsentrasi jembatan garam pada karakteristik elektrik pembangkit listrik berbahan elektrolit air laut," *Front. Neurosci*., vol. 14, no. 1, pp. 1-13, 2021.
[13]S. Sugito and S. D. Marliyana, "Uji performa spektrofotometer serapan atom thermo ice 3000 terhadap logam Pb menggunakan CRM 500 dan CRM 697 di UPT laboratorium terpadu UNS," *Indones. J. Lab.*, vol. 4, no. 2, pp. 67, 2021. Doi: 10.22146/ijl.v4i2.67438.
[14]Cynthia G. Zoski. Handbook of Electrochemistry. USA: Elsevier, 2007, pp. 815-817.
[15] L. Trotochaud, S. Young, J. Ranney, and S. Boettcher, "Nickel–iron oxyhydroxide oxygen-evolution electrocatalysts: the role of intentional and incidental iron incorporation," *J. Am. Chem. Soc.*, vol. 136, no. 18, pp. 6744-6753, 2014. Doi: 10.1021/ja502379c.
[16] J. Li and C. Barile, "Reversible electrodeposition of Ni and Cu for dynamic windows," *J. Electrochem. Soc.*, vol. 168, no. 9, p. 092501, 2021. Doi: 10.1149/1945-7111/ac2022.
[17] L. Liu, L. Twight, J. Fehrs, Y. Ou, D. Sun, and S. Boettcher, "Purification of residual Ni and Co hydroxides from Fe-free alkaline electrolyte for electrocatalysis studies," *Chem Electro Chem*, vol. 9, no. 15, 2022. Doi: 10.1002/celc.202200279.
[18] I. Bösing, "Modeling electrochemical oxide film growth-passive and transpassive behavior of iron electrodes in halide-free solution," *NPJ Materials Degradation*, vol. 7, *(1)*, pp. 53, 2023. Doi: 10.1038/s41529-023-00369-y.
[19] R. Fayaz, I. Bösing, F. La Mantia, M. Baune, M. Hanafi, and T. Gesinget, "Deoxidation electrolysis of hematite in alkaline solution: impact of cell configuration and process parameters on reduction efficiency", *Chem Electro Chem*, vol. 10, no. 22, 2023. Doi:10.1002/celc.202300451.
[20] S. Yasnur, S. Saha, A. Ray, M. Das, A. Mukherjee, and S. Das, "Effect of electrolyte concentration on electrochemical performance of bush like α-Fe_2O_3 nanostructures," *Chemistry Select*, vol. 6, no. 29, pp. 9823-9832, 2021. Doi: 10.1002/slct.202101641.
[21] K. Jeerage and S. Stavis, "Rapid synthesis and correlative measurements of electrocatalytic nickel/iron oxide nanoparticles," *Scientific Reports*, vol. 8, 2018. Doi: 10.1038/s41598-018-22609-x.
[22]Q. Zhou, M. Zhang, B. Zhu, and Y. Gao, "Investigation of the stability and hydrogen evolution activity of dual-atom catalysts on

nitrogen-doped graphene," *Nanomaterials*, vol. 12, no. 15, pp. 2557, 2022. Doi: 10.3390/nano12152557.
[23]X. Ou, T. Liu, W. Zhong, X. Fan, X. Guo, and X. Huang, "Enabling high energy lithium metal batteries via single-crystal Ni-rich cathode material co-doping strategy," *Nat. Commun.*, vol. 13, no. 1, 2022. Doi: 10.1038/s41467-022-30020-4.
[24] C. Liao, F. Li, and J. Liu, "Challenges and modification strategies of Ni-rich cathode materials operating at high-voltage," *Nanomaterials*, vol. 12, no. 11, pp. 1888, 2022. Doi: 10.3390/nano12111888.

Metalurgi (2024) 1: 15 - 36

METALURGI
Majalah Ilmu dan Teknologi
p-ISSN 0126-3188 | e-ISSN 2443-3926
ejurnalmaterialmetalurgi.lipi.go.id

SURFACE MODIFICATION OF COMPOSITE COATING FOR MARINE APPLICATION: A SHORT REVIEW

Hafiz Aulia*, Rini Riastuti, Rizal Tresna Ramdhani
[b]Department of Metallurgical and Materials Engineering, University of Indonesia
Kampus UI, Kukusan, Depok, Indonesia 16424
*E-mail: hafizaulia1907@gmail.com

Received: 08-02-2024, Revised: 06-03-2024, Accepted: 15-05-2024

Abstract

Corrosion is a prevalent phenomenon that significantly contributes to the deterioration of materials in offshore applications. The aggressive nature of marine corrosion is primarily attributed to the high salt content and the low electrical resistivity of seawater. While corrosion cannot be entirely eliminated, its reaction can be slowed down. Applying protective coatings is an effective and widely utilized method to protect metal surfaces from corrosion. These coatings act as a protective barrier that separates the metal from its surrounding environment, effectively retarding the corrosion rate. According to ISO 12944, the most commonly used generic coating systems for marine service include alkyd, acrylic, ethyl silicate, epoxy, vinyl ester, polyurethane, polyaspartic, and polysiloxane. The latest innovations in marine coatings still employ a layer-by-layer coating method, involving primer coats, intermediate coats, and top coats, depending on the desired thickness. Marine structures exposed to atmospheric conditions are commonly coated with one or two layers of epoxy. For enhanced performance, a more expensive system involving a layer of zinc-rich primer, followed by epoxy and aliphatic polyurethane coatings, may be utilized. Coating systems for atmospheric conditions are frequently employed in intertidal and splash zones. On the other hand, immersion zones of marine structures are typically coated with one or two layers of 100% solid epoxy, or three layers of solvent-borne epoxy. The use of a single polymer as a generic coating has limitations. Incorporating fillers is a widely employed technique to enhance the characteristics of polymers, thereby transforming them into composites. In marine coatings, fillers are still limited to glass flakes and powder. Poor dispersion and agglomeration might reduce the effectiveness of fillers in the matrix, which decreases the adhesion properties. The fillers must be surface-modified before application. This review provides a comprehensive and critical analysis of the current research status of composite coatings that serve as candidates to be used in marine coating applications.

Keywords: *Corrosion, marine coating, composite, surface modification*

1. INTRODUCTION

Metal is the primary raw material utilized in product design and construction structure within the manufacturing industry, where material processing techniques play a crucial role. It is important to conduct a thorough study of metallic materials before they are used in industrial applications, to maximize their efficiency and effectiveness [1]. Steel and alloys are commonly employed materials in marine construction, playing a crucial role in the fabrication of marine structures. Steel undergoes classification to ensure its appropriateness for specific applications in the marine environment. The classification of steel allows for the identification of its unique properties, facilitating a better understanding of its potential uses. Steel is classified based on various factors, including composition, manufacturing techniques, finishing methods, microstructure, strength, heat treatment, and product form [2].

The ocean-based economy encompasses a diverse array of industries, including fishing, coastal tourism, shipping, offshore energy, marine manufacturing, maritime infrastructure, and ocean-related services [3]. Among these diverse activities, the offshore energy and mineral resources sectors stand out as the largest industries

DOI : 10.55981/metalurgi.2024.746

Metalurgi is Sinta 2 Journal (https://sinta.kemdikbud.go.id/journals/profile/3708) accredited by Ministry of Education, Culture, Research, and Technology, Republic Indonesia

that heavily rely on metal for constructing platform structures, docks, pipelines, and ships.

Energy is one of the elements needed to realize a prosperous country. Energy is also a determinant of a country's sustainable development. Therefore, the need for energy is a must, and its sustainability must be maintained [4]. The utilization of offshore structures is paramount for the energy and economic sectors of multiple countries, as these structures primarily serve as drilling platforms to extract precious oil and gas reserves from beneath the ocean floor [5].

Materials, particularly metals, often encounter environments that induce deterioration. This process, known as corrosion, occurs when metals react with their surrounding environment, leading to changes in their properties and a significant reduction in performance [6]. The damage inflicted by corrosion on offshore structures is influenced by various factors. Statistical data shows that marine corrosion is responsible for approximately 30% of failures in ships and marine machinery, resulting in annual costs surpassing $1.8 trillion [7]. The marine environment's high salinity and low electrical resistance exacerbate its corrosive nature [8]. The presence of chloride in seawater can cause the depassivation of several metals and alloys, including stainless steel, aluminum alloys, and titanium alloys, even in the absence of oxygen. Furthermore, chloride can also be found in the marine atmosphere, posing a risk of corrosion to materials and structures that are not submerged [9]. Corrosion occurs when a material, typically a metal or alloy, undergoes a chemical or electrochemical reaction with its surroundings, resulting in the deterioration of the material and its properties. This degradation can be categorized as either chemical or electrochemical, depending on the environmental factors involved. Additionally, corrosion can be classified based on the surface morphology of the affected material or the underlying causes that contribute to the corrosion process. The two most prevalent types of corrosion are uniform corrosion, which affects the entire surface uniformly, and localized corrosion, which occurs in specific areas [10]. Corrosion is a thermodynamic system of metal and its environment, which strives to reach equilibrium. The system is in equilibrium when the metal has formed oxides or other more stable chemical compounds [11]. Corrosion cannot be stopped completely, but the reaction can be slowed down. Various methods can be employed to prevent corrosion, such as treating the metal surface, modifying the corrosive environment, regulating the electrochemical reaction that triggers corrosion, attacking corrosion with corrosion, applying protective coatings to the metal, and alloying the metal [2]. However, corrosion prevention methods using coatings are widely used and popular to protect metals from corrosion [12]. Coating serves as an effective strategy for corrosion protection by establishing a barrier that effectively isolates the metal from its surrounding environment [13]. This specialized layer is specifically designed to hinder any interactions between the substrate and destructive environments such as moisture, water, and other chemical compounds [14]. Safeguarding crucial infrastructure against the ravages of corrosion is a paramount concern in numerous industries. In the marine, pipelines and structure platforms face relentless challenges from harsh conditions and persistent exposure to corrosive elements, leaving them highly susceptible to the destructive forces of corrosion [15]. Applying protective coatings to these structures doesn't just stop leaks, it also extends their useful life and keeps them structurally sound. Coatings that guard against corrosion are essential in the maritime industry [16]. The salty ocean environment poses a constant threat to the durability of ships, platforms, and other marine structures. The constant contact with corrosive seawater causes these vessels and facilities to degrade at a faster rate compared to structures in less harsh conditions. This relentless exposure to the corrosive nature of the marine environment accelerates the corrosion process, leading to the need for more frequent maintenance and repair [17]. A protective coating is essential for preserving assets from corrosive surroundings, extending their useful life, lowering maintenance costs, and guaranteeing operational safety [18]. These protective layers effectively shield structures in diverse marine environments, such as atmospheric, submerged, splash, and tidal zones [12].

The protection against corrosion is accomplished through several processes, such as the shielding effect, providing a sacrificial layer, and the ability to repair itself. The shielding effect develops a protective covering that isolates metals from external conditions, blocking any direct contact or interaction between the metal and corrosive agent [18]. Creating a protective layer will obstruct impurities and other damaging elements into the underlying substrate [19]. Sacrificial protection works by adding a metal with a higher electrochemical potential than the metal protected into the coating [20]. Due to their high reactivity, they are designed to be corroded before the metal they protect. The self-healing properties are activated through the addition of

additives or materials that have the ability to mend themselves when faced with minor damage or scratches occurring [21].

Corrosion poses a significant challenge to the long-term economic success and environmental responsibility of a wide variety of industries, and the associated economic impacts, safety risks, and environmental damage highlight the urgent need to develop effective corrosion prevention methods. Protective coatings serve as an important primary protection mechanism, safeguarding materials, infrastructure, and ecosystems from the harmful effects of corrosion.

To tackle these obstacles, a range of techniques have been devised. The main aim of these methods is to improve particular characteristics like corrosion tolerance, wear tolerance, surface hardness, electrical insulation, thermal insulation, water repellency, and wettability [22]. These methods offer different approaches for applying coatings onto different substrates. Vapor-based chemical deposition is a process where gaseous materials interact to form a solid coating on a surface. This involves the chemical reactions of vapor-phase components, which culminate in the creation of a solid layer on the substrate. Physical Vapor Deposition employs physical processes like evaporation or sputtering to deposit a thin layer onto the substrate. Microarc Oxidation generates a ceramic coating through the electrochemical oxidation of metal. Thermal spraying entails projecting a liquid or semi-liquid material onto the substrate's surface. The sol-gel technique forms a layer through the hydrolysis and condensation of a precursor solution. The polymer coating is first applied in a liquid state, and then undergoes a hardening process to become a solid protective layer [23]-[24]. This text explores techniques used to alter the surface properties of fillers, aiming to strengthen the bond between fillers and matrices. The impact of surface modification techniques on the effectiveness of composite coatings was investigated.

2. GENERIC IN MARINE COATING

The marine environment is characterized by a higher presence of corrosive elements compared to natural conditions [24]. The high concentration of chloride particles in ocean water is the main factor behind this phenomenon. These chloride ions can penetrate and weaken the protective layer that shields the substrate, making them susceptible to localized corrosion, such as pitting [26]-[27]. Reliability and durability are critical for steel structures that are exposed to environmental attacks, particularly those situated close to the coast or off-shore (marine environments). It is therefore vital that the protective coating applied can provide protection from harmful elements. ISO 12944 is a set of instructions and recommendations on the various types of paints and protective coatings suitable for safeguarding steel structures. This international standard outlines the essential requirements and best practices for selecting, applying, and maintaining effective anti-corrosion systems for steel-based constructions. The extent to which the steel structure is exposed to corrosive conditions determines the level of protection required and the paint or coating system that is recommended for use [27].

Coating formulations typically consist of solvent, resin, pigment, filler, and additives. Once administered onto the base metal, these formulations create a seamless, uniform coating that safeguards against cracking and structural deterioration caused by stress, water infiltration, and natural wear and tear. For protective coatings to be deemed effective, they must exhibit minimal permeability, excellent corrosion resistance, and high adhesive to warrant their performance [28].

The Society for Protective Coatings serves as the preeminent authority and resource in the protective coatings industry, providing essential knowledge and guidance on preparing surfaces, choosing the right coatings, applying, and following environmental and safety rules. Within the marine coatings sector, manufacturers offer a diverse range of generic coating options tailored to the specific requirements of various marine applications [29]. This short article only discusses coating selection and application.

Sailors navigating on the wide sea often rely on protective coatings to shield their vessels from the sun's harsh rays and the corrosive marine environment. These coatings commonly feature single or double-layer epoxy, with the number of layers determined by the desired thickness of the protective barrier. Additionally, an aliphatic polyurethane layer is added to shield the epoxy from the harmful ultraviolet rays of the sun. In cases where the structure is not subjected to direct sunlight, two or more layers of epoxy may be employed. Alternatively, a slightly more expensive system comprising a zinc-rich primer coat, an epoxy coat, and an aliphatic polyurethane coat could provide enhanced performance in harsher environments.

Protective coatings intended for exposure to atmospheric conditions are often applied in areas where water regularly contacts the surface, like the shoreline and areas subject to splashing, to shield against deterioration. Within these specific regions, it is common practice to employ a flake-

filled epoxy coating to enhance resistance to impacts and abrasions. Furthermore, the application of Monel coating, which extends around 20 feet beneath the water's surface, serves the purpose of inhibiting the growth of marine fouling organisms and preventing corrosion on the steel substrate.

Marine structures often have immersion areas that are protected by either a single, double, or three layers of solid epoxy. Epoxy coatings that have been cured with polymeric amide solvent are renowned for their exceptional resistance to water and their capability to withstand partially cleaned steel surfaces. Coal tar epoxy coatings, which are renowned for their superior water resistance, are commonly used in a single or double-layer coating system for surfaces that are submerged [29].

According to ISO 12944, the marine setting is classified as having the most severe level of corrosiveness, denoted as Cx extreme. To shield structures from deterioration in this setting, it's crucial to use a coating that boasts robust mechanical attributes, endurance against abrasion, insulating capabilities, and chemical resilience. Commonly utilized materials for marine coatings include epoxy, polyurethanes, vinyl esters, and alkyds [27]. The latest innovations in marine coatings still use a layer-by-layer coating method (primer coats, intermediate coats, and top coats) depending on thickness. In marine coatings, fillers are still limited to glass flakes and powder [30]-[31]

Epoxy resins are renowned for their remarkable ability to offer effective barrier protection in various environments [31]. The hydrophilic nature of epoxy, attributed to the presence of polar epoxy groups, can be influenced by the combination of hydrophilic or hydrophobic polymers, thereby affecting the equilibrium properties of the resulting polymer [32]. The efficacy of epoxy as a coating is influenced by the presence of water, consequently impacting the overall performance on coating performance [33]. Epoxy is a highly popular thermosetting resin that finds extensive use due to its exceptional physical and chemical characteristics. These qualities encompass the lack of volatile components throughout the curing stage, the capacity to cure across a broad temperature spectrum, and the potential to attain regulated cross-linking. In the past century, epoxy has become a staple in the coatings industry or structural applications. This is largely due to their exceptional capabilities, which are further enhanced when paired with aliphatic amine curing agents [34]. Epoxy is widely acknowledged as the most extensively utilized anti-corrosion coating due to its exceptional mechanical characteristics, wear resistance, insulating capabilities, and stability in both acidic and alkaline environments [35]-[36]. These qualities make epoxy a preferred choice for various applications, as it can withstand extreme conditions. However, epoxy coatings do possess certain limitations, when cured coating can create tiny holes, weakening the coating. Additionally, these coatings may not withstand environmental factors well, becoming less durable and adhering poorly over time, potentially leading to deterioration [37]-[38]. Improving the effectiveness of coatings is essential in resolving the difficulties at hand. Ensuring these coatings operate optimally is key to addressing the prevailing concerns. Several methods can be employed to improve epoxy properties, such as polymer synthesis, incorporating additives, and utilizing new curing agents [39]. The incorporation of fillers has also emerged as a common technique to enhance polymer properties and transform them into composites [40]. In the realm of marine coatings, fillers are currently limited to glass flakes and powder [29]-[30]. Incorporating supplementary fillers enhances both the frictional and structural attributes of composite coatings [41]. GO, CNT, and nanoparticles are commonly used as fillers to reinforce these layers. The improvements in properties are credited to the interactions between the filler substances and the surrounding material, which involve covalent, hydrogen, and physical bonds [42]. The enhanced mechanical characteristics of composite coatings play a crucial role in their ability to inhibit the formation and spread of cracks, ultimately leading to improved coating performance [43]. However, the filler must be uniformly dispersed within the polymer matrix to achieve these improved properties. In cases where the dispersion is inadequate, agglomeration occurs, weakening the bond and causing separation between the filler and matrix, a phenomenon known as particle debonding. The effectiveness of the coating is significantly influenced by its adhesive characteristics. The quality of the coating is determined by the connection between the coating and the underlying surface. When the coating and the surface integrate seamlessly, it indicates strong adhesion, resulting in a smooth transition. Conversely, poor adhesion is reflected in a rough transition between the coating and the surface [42].

3. SURFACE MODIFICATION

Determining the effectiveness of modifying the filler's surface can be accurately done by studying how well it interacts with the surrounding matrix material. Improving the filler's ability to blend

seamlessly with the matrix is crucial for enhancing the corrosion resistance of the composite. Analyzing the WCA (water contact angle) and surface energy provides important insights into the hydrophilic (water-attracting) nature of the fillers [44]. Several existing surface modification techniques are available.

3.1 Physical Vapor Deposition

Applying thin film coatings is achieved through a method called PVD. This process involves the manipulation of materials at the atomic level within a vacuum environment. While PVD shares similarities with CVD (chemical vapor deposition), there are notable distinctions between the two methods. In PVD, solid precursors or materials are utilized for the deposition process, whereas CVD introduces the precursor in a gaseous form into the reaction chamber [44]-[45]. PVD presents numerous benefits. It enables the application of extremely thin layers of materials, generating coatings with visually appealing characteristics. Additionally, these coatings demonstrate improved resistance against deterioration from corrosion and physical wear [46]-[47].

3.2 Chemical Vapor Deposition

Chemical processes happen right on or close to the surface of a hot material in a method called CVD. The vapor transforms and solidifies, creating a physical substance that settles out of the gaseous state. The resulting solid materials can exhibit diverse structures, such as single crystals or thin layers. Through careful control of different factors, such as the composition and temperature of the underlying surface, the setup of the gas mixture fueling the reaction, and the speed at which the gas flows, it becomes achievable to design materials with a wide range of physical, friction-related, and chemical characteristics [48]-[49].

CVD offers several notable benefits, such as its capacity to enhance corrosion and wear resistance. Additionally, it enables the deposition of diverse materials with distinct microstructures. Furthermore, CVD can be conducted under low and ambient pressures [50]-[51]. However, there are certain limitations associated with this process. It requires the use of a heat-resistant substrate and an ultra-high vacuum environment. Additionally, there is a tendency for some wastage of the coating material during the CVD process [50]-[52].

3.3 Micro-Arc Oxidation

MAO is an innovative electrochemical technique that utilizes rapid micro-arc discharges to create porous ceramic coatings on various transition metals and their alloys, including aluminum, titanium, magnesium, and zirconium. This process involves subjecting the metal surface to high-voltage electrical discharges in an electrolyte solution, resulting in the formation of a ceramic layer with unique properties [53]-[56]. When the applied voltage exceeds the dielectric breakdown voltage of the ceramic/oxide layer, a micro-arc discharge is initiated. This phenomenon occurs due to the high voltage causing the breakdown of the dielectric material, leading to the discharge of electrical energy in the form of a micro-arc [57]-[60]. The distinctive feature of MAO lies in its ability to provide a porous substrate-based oxide layer, which cannot be achieved through conventional manufacturing techniques. This unique characteristic sets MAO apart from other traditional methods, offering a specialized oxide layer that enhances the material's properties and performance in various applications [62].

3.4 Electrodeposition

Electrodeposition coating is an electrochemical process that allows for the formation of a uniform metallic coating with an even thickness distribution on a conductive substrate. The selection of the substrate and deposition material is crucial as they serve as the cathode and anode within the electrochemical cell [63].

3.5 Sol-gel

The sol-gel technique is a commonly employed method for the deposition of thin layers, typically less than 10 millimeters in thickness. This approach, in contrast to conventional thin film fabrication techniques, offers enhanced control over the chemical composition and microstructural properties of the deposited layers. Additionally, the sol-gel method facilitates the production of uniform films, reduces the solidification temperature requirements, and provides the advantage of utilizing simpler and more cost-effective equipment [64].

3.6 Thermal spray

Thermal spray coating is a technique where manufacturers liquefy specially designed parts by applying intense heat like plasma, electricity, or burning chemicals. This transforms the materials into a protective layer. These layers are created by melting specific components through the application of heat from sources [64]-[66]. The

thermal spray coatings can be classified into five main sections based on the different energy sources utilized during the procedure. These categories encompass energy derived from flammable gases, the power of motion, electrical sparks, radiation, and liquid fuels. Each of these energy forms holds a pivotal part in shaping the overall efficiency and excellence of the thermal spray coating procedure.

Thermal coating can generate layers with diverse thicknesses, ranging from a mere 20 micrometers to several millimeters. This method stands out for its ability to achieve high deposition rates over large surface areas, surpassing other coating processes. Researchers have investigated an assortment of covering substances. The chosen coating substance is carefully heated until it transforms into a semi-liquid or molten form, ready to be applied. The metal arrives in powdered, bar-shaped, or wire-like forms, and is then rapidly accelerated, typically at speeds between 100 and 1500 meters per second, towards the target surface. This high-speed motion causes the metal to break apart into tiny droplets, which then cling to the target, building up the desired coating layer [68].

Diverse methods have been engineered to modify the characteristics of material surfaces, including PVD, CVD, sol-gel processing, MAO, electroplating techniques, thermal spraying, and several additional approaches. These techniques offer various benefits, such as enhanced protection against corrosion and wear, increased hardness, the ability to insulate electricity and heat, water-repelling properties, and improved wetting characteristics [22]. Each of these surface modification techniques has its characteristics depending on the application.

Table 1. Advantages and disadvantages of various surface modification techniques

Method	Advantages	Disadvantages	Ref
PVD	● Adjusting corrosion and visual appeal, while also boosting durability and applying a thin protective layer, can be effectively achieved and modified.	● High vacuum conditions are necessary, as abrasion can compromise the corrosion resistance of materials in polymer deposition applications, making damage control a challenging task.	[45], [46], [47], [48]
CVD	● Shielding against wear and tear, blending various substances with unique inner structures, and operating in both low and standard air pressures are critical factors in many industrial endeavors and uses.	● A high level of vacuum is required, along with a substrate that can withstand high temperatures, and minimal wastage of the coating material is necessary for this process.	[49], [50], [51], [52], [53]
MAO	● Exceptional hardness and outstanding corrosion resistance, combined with a porous framework that is well-suited for use in biological settings, as well as a diverse array of porosity levels spanning the entirety of the material's thickness.	● Primarily associated with valve metals such as aluminum, titanium, tungsten, chromium, and others.	[54], [55], [56], [57], [58], [59], [60], [61], [62]
ELD	● Applications for ornamentation, resistance to corrosion, high-temperature resistance, and abrasion.	● The effectiveness is heightened when paired with conductive metals.	[63]
Sol-gel	● Affordable.	● Manage the thickness and slow cycle time.	[64]
Plasma spray	● Restoration of polymers, rubber, metals, and engineered fibers through surface repair. Enhanced substrate adhesion, corrosion and wear resistance, and non-stick coating. Eco-friendly method for fiber	● Low-temperature techniques involving substrate surface modification necessitating heat energy are used on stuff unreactive at natural pressure. Extended exposure to plasma results in fiber damage through the creation of	[69]

	surface modification without environmental pollution.	deeper holes on the fiber surface. Procedures at low temperatures induce alterations on the substrate surface, necessitating a heat source, and are employed for substances unreactive under atmospheric natural pressure.	
Cold spray	● In contrast to alternative thermal spraying techniques, this method is both straightforward and cost-effective.	● Not particularly useful in extreme conditions.	[66]
Arc wire spray	● A protective coating on the internal surface of the engine block ensures resistance against wear and corrosion.	● Limited to utilizing conductive materials and wires for coating purposes.	[67]
Warm spray	● Ideal for substances prone to oxidation when exposed to elevated temperatures or for heat-vulnerable.	● Exceedingly severe settings offer no value.	[65]
Nano-particle growth	● The filler's surface remains undamaged by the process. The high ratio of length to thickness leads to enhanced shear resistance. The performance gets better, and corrosion resistance is increased due to the exfoliated filler.	● The process of filler growth can incur significant costs. Agglomeration of filler material is a potential issue that may arise. The maintenance of a high vacuum poses challenges and can be costly, particularly for certain types of fillers that necessitate surface modification.	[70], [71], [72], [73], [74], [75], [76], [77]

4. COMPOSITE COATING

According to ISO 12944, the most commonly used generic coating systems in marine applications include AK (alkyd), AY (acrylic), ESI (ethyl silicate), EP (epoxy), PUR (polyurethane), PAS (polyaspartic), and PS (polysiloxane) [27]. Single-polymer coating systems are inherently limited in their applications due to certain constraints. To enhance the sliding and strength characteristics and tackle these drawbacks, extra materials like fillers are blended into the coating compositions. However, polymer films exhibit permeability to O_2 and H_2O over time, with instances where the rate of H_2O and O_2 diffusion on layers exceeds the threshold necessary to trigger the corrosion of a metal substrate [78]. Incorporating inorganic fillers is a viable approach to enhancing the anti-corrosion characteristics of organic coatings [79]. Fillers come in various forms, from carbonous to a combination of monomers, ceramics, light metals, silicate minerals, TMS, and nanofillers [80].

Polymer composites incorporate various types of filler materials that serve distinct purposes. There are two primary categories: reinforcing fillers and lubricant fillers. Reinforcing fillers are materials that possess greater strength and modulus in comparison to the plastic base material, thereby enhancing mechanical properties. Fibers and nanofillers have been extensively utilized as reinforcing fillers in various studies. Common examples of conventional reinforcing fibers include carbon fiber, glass fiber, and silica fiber [80]-[81]. Additionally, CNTs have exceptional properties which are highly suitable for enhancing the strength of polymer composite materials, primarily due to their unique one-dimensional structure and remarkable strength [80]-[82]. Montmorillonite, a type of two-dimensional nanoclay, is also widely employed to strengthen the physical properties of polymers. This clay-like substance helps improve the durability and performance of a wide range of plastic-based products [84]. Furthermore, a wide range of nanofillers, such as aluminium oxide, silicon dioxide, zinc oxide, silicon carbide, and copper are suitable for serving as strengthening components in polymer-based composites. Lubricant additives are substances that are designed to reduce the friction between the components in polymer-based materials. Some common examples of these lubricant additives include Teflon, carbon, MoS_2, phosphorene, Au, and Cu. These materials work

by lowering the resistance between the moving parts, which helps to improve the overall performance and efficiency of the composite materials [84-86]. The incorporation of certain reinforcing fillers can enhance the composite performance. This is illustrated by the improved properties of epoxy resin when silicon dioxide and carbon are added [88].

CNTs offer advantages because of their capacity to diminish friction and offer anti-corrosion characteristics, in addition to their pivotal role in diverse tribological applications. Fullerene, graphene, carbon nanotubes, and nanodiamonds are four prominent types of carbon nanomaterials that have been employed in coating applications [88]-[89].

Certain silicon-based minerals, such as montmorillonite and kaolin, possess thin, layered structures with high aspect ratios and substantial interfacial areas. These minerals can be chemically bonded to polymers, enhancing the rigidity and resistance to deformation of the polymer matrix [83],[90]-[91]. Silicon dioxide has been extensively utilized as a filler in various polymer systems, both in synthetic and natural forms. The addition of silica enhances the polymer's stiffness and resistance to deformation, owing to its remarkable stability under temperature changes and its inherent structural strength. However, unlike talc or mica particles, which have a low aspect ratio and form flakes or plates, silica filler particles do not share this characteristic. Consequently, unless the silica particles are minuscule, adding them to the polymer leads to a comparatively small surface coverage to interact. As a result, the reinforcement provided by silica filler is less significant compared to platy fillers. Nevertheless, when the size of the filler particles is reduced to sub-micron dimensions, the composite resin exhibits exceptional and desirable properties. While sub-micron silica and barium sulfate have been employed as nanofillers, organically modified clay-based nanofillers offer the most remarkable properties at a relatively low cost. This is primarily due to their extremely high aspect ratios, which exceed 1000, in contrast to the aspect ratios of common fillers, which are typically 100 or less. This high length-to-diameter ratio of clay particles contributes to improved dimensional stability compared to conventional microfillers. However, a significant challenge arises in the dispersion of nanofiller particles, as their complete dispersion within the polymer matrix during melt processing is difficult or even impossible to achieve. Consequently, the actual properties of nanocomposites may only partially realize their potential or theoretical properties. To overcome this issue, a common approach involves modifying the surface of the clay particles with quats or other. This surface modification process facilitates the desired exfoliation of the clay particles, resulting in the creation of delicate layers with nanometer-scale thickness in the polymer matrix [93].

Ceramic nanoparticles, including SiO_2, Si_3N_4, SiC, TiO_2, and Al_2O_3, demonstrate superior mechanical characteristics under various temperature conditions. Consequently, they are frequently utilized as reinforcing components to improve matrix performance [93]-[97].

The enhancement properties of the composite layer are heavily associated with the filler phase. This is accomplished through various characteristics, including their arrangement, dimensions, form, permeability, and surface modification on the fillers. The bonding between matrix and filler is vital in boosting the protective film. Numerous research approaches have been dedicated to enhancing the performance of resin composites by investigating the correlation between organic resins and inorganic fillers. Typically, fillers in composite materials are treated with chemical agents resulting in strong chemical bonds between separate components and improving water resistance. The hydrophobic or hydrophilic nature of a coating holds significant importance as it allows for the evaluation reaction between surface layers and surroundings. This interaction is vital in improving mechanical properties, wear resistance, and retarding the degradation process. Furthermore, it facilitates the transition of stress from a more flexible organic matrix to a highly rigid inorganic filler [98]-[99].

The filler was modified not only as a linkage and to minimize stress development during polymerization but also to enhance hydrophobic or super hydrophobic properties. Here, the use of various fillers synthesized with a surface modification method is considered. Therefore, this part will recap the development of composite coatings with generic materials commonly applied in marine coatings.

Table 2. Summary effects of filler addition and modification method on corrosion resistance of composite coatings

Generics	Fillers	Modification method	Environment	Achievements	Ref

Epoxy	ZrO_2 particle size 15 nm	Sol-gel with APS (amino propyl trimethoxy silane)	Immersed 3.5wt.% NaCl	The inclusion of 2-3% zirconium dioxide nanoparticles significantly improved the corrosion resistance. This enhancement was due to the improved barrier properties and ionic resistance.	[101]
Epoxy	Mixing ZrO_2 nanoparticle and Cloisite 30B particle size 13 μm	Ternary ammonium salts	Immersed 3.5wt.% NaCl	The addition of zirconium oxide and nanoparticles to the coating systems enhances the coating's anti-corrosion properties. The nanoparticles enhance the coating's barrier and electrical resistance, resulting in better corrosion protection.	[102]
Epoxy	Mixing ZrO_2 particle size 15 nm with Closite 30B particle size 2-13 μm	ZrO_2 with APS, Closite 30B with ternary ammonium salt	Neutral salt spray test	The addition of nano zirconia slightly improves the mechanical properties of the epoxy coating. This is due to the formation of clay clumps that slow down the curing process and reduce the density of polymer crosslinks. The creation of nano-scale voids around the clay buildup also contributes to the enhancement.	[103]
Epoxy	Mixing GO particle size 300 μm with cloisite 15A particle size 13 μm	Nanoclay modified with quaternary alkyl ammonium salt	Immersed 3.5wt.% NaCl	The coating showed very high electrical resistance, over 10^{10} ohm·cm^2, even after being immersion for 18 weeks. This shows the coating is very stable. Other tests like salt spray, pulling, and electrical tests also showed the coating performed better when the clay in it was mixed in better.	[104]
Alkyd	Clay based on MMT particle size of 7-9 μm	Dimethyl dehydrogenated tallow ammonium chloride	Immersed 3wt.% NaCl	The Scanning Electron Microscopy and AFM analysis showed that the nanoclay particles were well-dispersed in the coating. The AFM images confirmed the coating's nanoscale stability, even after prolonged exposure to salt water. This suggests the composite coating had enhanced stability. The Electrochemical Impedance Spectroscopy results also demonstrated that the composite coating provided better corrosion protection compared to other barrier coatings. This improvement is attributed to the flat montmorillonite sheets in the coating, which prevented defects and reduced the transport of water and corrosive substances.	[105]
Epoxy	Mixing bentonite with TiO_2	CTAB (cetyl trimethyl ammonium bromide)	Without corrosion test	The addition of a 5% filler component, at a concentration of 0.1 M CTAB, led to an improvement in the mechanical characteristics of the material. Additionally, the water absorption test demonstrated a direct correlation between the increase in filler content and the material's water absorption capacity.	[106]
Polyurethane	Mixing silica particle size 14 nm with carbon particle size 595 μm	Unmodified	Salt spray test	Increasing the carbon and silica content of a material can improve its corrosion resistance, as demonstrated by various analytical techniques like FTIR, TGA analysis, optical observations, and salt spray testing. These methods have consistently shown that a higher ratio of carbon to silica results in enhanced resistance against corrosion.	[107]

Polyaniline	SiO_2	Unmodified	NaCl 1M	Adding a 10% SiO_2 guarantees the highest corrosion resistance. The initial corrosion rate is 0.00896 mm/year, but it drops to 0.00024408 mm/year after exposure.	[108]
Epoxy	Metalloam	Unmodified	5wt.% NaCl Salt spray test	Metalloam addition did not significantly impact corrosion resistance. However, adding 15% metalloam increased adhesion by 22.5%	[109]
Polyaniline	rGo (reduced graphene oxide)	Unmodified	Potentio dynamic polarization with I^- (iodide) / I_3^- (tri-iodide) based electrolyte	The addition of reduced rGO (graphene oxide) to PANi (polyaniline) coatings significantly reduces the corrosion rate. The PANi/rGO coating with the highest rGO concentration 8wt.% had the lowest corrosion rate at 0.2 mm/year and a protection efficiency of 80.3%. This high performance is due to the passivation effect, which blocks corrosive ions from reaching the substrate surface.	[110]
Epoxy	ZnO particle sizes 910.6 nm and 189.3 nm	Stearic acid	Immersed 3.5wt.% NaCl	9% filler provides optimal results. Modification of the ZnO filler using stearic acid was increase water contact angle. Effect protection coating through barrier effect and hydrophobic effect. Micropores in epoxy composite coatings will be filled by ZnO fillers. Surface modification of the ZnO filler reduces the corrosion rate due to the hydrophobic nature of stearic acid, so the electrolyte tends not to make contact with the modified filler.	[111]
Polyurethane	-	Sol-gel Catecholamine	Immersed 3.5wt.% NaCl	The addition of catecholamines to a sol-gel coating improved its corrosion resistance and adhesion to a waterborne polyurethane layer. The adhesive strength increased from 1.74 MPa to 2.75 MPa. After 120 days of immersion, the coating's resistance to corrosion also improved significantly, as shown by a large increase in the charge transfer resistance from 4.9×10^4 $\Omega \cdot cm^2$ to 1.7×10^7 $\Omega \cdot cm^2$.	[112]
Epoxy	Mixing 2D MXene nanosheets with ZnO QDs (quantum dots)	ATPES (3aminno propyl triethoxy silane)	Immersed 3.5wt.% NaCl	The coating made with a mixture of F-MXene@ZnO and a water-based epoxy polymer is very good at preventing corrosion. When 0.50% of this mixture was added to the water-based epoxy, the coating was able to resist corrosion much better than the neat epoxy. Even after being immersed for 30 days, the coated surface was still 3 times better at preventing corrosion compared to the neat epoxy.	[113]
Epoxy	Nano-alumina	Doped with PB (polybenzopyrrole)	Immersed 3.5wt.% NaCl	The PB/AN@ZE 0.25% film is very good at protecting against corrosion. Tests showed it was able to protect 97.14% of the surface after being submerged for 24 days. The film also stayed strong, with an impedance value of 1.48×10^9 $\Omega.cm^2$ even after 24 hours submerged. This means the film is excellent at preventing corrosion and holding up well in water.	[114]
Epoxy	Graphene oxide	Doped with GPTMS	Salt-mist	The f-GO-epoxy coated samples were tested and showed they are very good at	[115]

				protecting against corrosion. The tests used electrical measurements to check how well the coating resisted corrosion. They also did a pull-off test to see how well the coating stuck to the surface. The results showed the f-GO-epoxy coating was very effective at preventing corrosion.	
Vinyl ester	Two-dimensional MXene nanosheets	MPS (3metha acryloxy propyl trimethoxy silane)	Immersed 3.5wt.% NaCl	The materials in the composite layer work well together. The different parts are connected in a strong way, which makes the layer better at preventing corrosion. The materials are mixed nicely, which makes it harder for harmful things to get through to the surface underneath. This helps the composite layer be more resistant to corrosion.	[116]
Epoxy	Two-dimensional lamellar MXene nanosheets	One-step dopamine-triggered with polyethyleneimine	Immersed 3.5wt.% NaCl	The WEP coating is very good at preventing corrosion. This is because the coating has special fillers that are spread out well, it creates a strong barrier, and it works well with the surface it is on. Even after being submerged for 30 days, the WEP coating with a small amount of MXene was still able to stop corrosion very well. The coating was only about 55 micrometers thick, but it was able to stop corrosion twice as well as the regular WEP coating without the MXene.	[117]
Epoxy	ZIF-67 containing 2-mercatobenzothiazole	PFTS (perfluorooctane trethoxy silane)	Immersed 5wt.% NaCl	The PHBN-ZIF@MBT composite material showed strong barrier properties and the ability to release corrosion inhibitors. After immersion, the coating became much more hydrophobic, with the contact angle increasing from 78.35° to 116.8°. The adhesion strength also improved by 82.6%. Electrochemical Impedance Spectroscopy analysis indicated the composite layer maintained high impedance values even after 28 days submerged, demonstrating effective long-term corrosion protection.	[118]
Epoxy	Micro/nano-sized silica	Sol-gel with ZIF-8 (2-methylimidazole zinc salt)	Immersed 3.5wt.% NaCl	The ZIF-8@SiO2/APTES/EP coating is very good at preventing rust and corrosion. In a saltwater solution, it was able to stop 99.99% of the corrosion. Even after being in the water for 72 hours, it continued to work very well at preventing corrosion. Tests showed that this material formed a thick protective layer on the metal surface. This layer is very resistant to corrosion and is also very stable chemically.	[119]
Epoxy	Basalt	Grafting ZnO	Immersed 3.5wt.% NaCl	The special coating is very good at killing bacteria. This is because the zinc oxide (ZnO) layer in the coating has a very tight structure and sticks very well to the surface. The ZnO layer also makes it harder for the base layer to move around in the resin. This helps the base layer spread out evenly, which makes the coating better at preventing corrosion.	[120]

Vinyl ester-Epoxy	GO (graphene oxide)	Grafting vanillin and silicon	Immersed 3.5wt.% NaCl	The composite material achieved its best performance when 0.1% more of a certain component was added. While the electrical conductivity was still low enough to be considered an insulator, the material saw a 38% increase in breaking strength, a 65.7% increase in contact angle, and 99.03% anti-corrosion efficiency.	[121]
Polyurethane	MMT (montmorillonite)	TA (tannic acid)	Immersed 3.5wt.% NaCl	The coating on this material keeps its strong protection even after being immersed for 50 days. The coating is about 3 times better at protecting the material than the original uncoated material. The coating can also repair small physical damage to itself by using a special chemical reaction when heated. This means the coating is very good at preventing corrosion and lasting a long time.	[122]
Epoxy	Graphene	Solution intercalation technique	Immersed 3.5wt.% NaCl	Adding 1% graphene improves the polymer coating's protective abilities. This is due to the graphene nanoparticles being well-dispersed and distributed. Increasing graphene from 0.5-3% boosts the contact angle and reduces water absorption. But higher concentrations lead to graphene clumping, which decreases corrosion resistance.	[123]
Epoxy	Glass fibers	Modified with 3-Triethoxy silyl propyl amine and grafting with phytic acid and Zn^{2+}	Immersed 3.5wt.% NaCl	The PA-Zn^{2+}-m-GF/WEP coating is very good at stopping wear and corrosion when it has 20% of a special material added to it. After being used for 1000 times, the coating only got about 30% thinner. Even after being immersed for 144 hours, it was still very good at stopping corrosion, with a high electrical resistance.	[124]
Epoxy-PES	CNPs grain size 30nm	Unmodified	NIR laser irradiation testing	The PES/EP-CuS coating exhibited an impressive ability to prevent corrosion and restore the integrity of the material while in use, thus highlighting its resilient self-repairing capacity. This coating demonstrated remarkable efficacy, underscoring its capability to withstand corrosion and repair any resulting damage.	[125]
Epoxy	Hexagonal boron nitride	Triple-functional filler enhances	Immersed 3.5wt.% NaCl and Salt Spray Test	The Ce^{3+}&PANI/h-BN composite coating was found to be very good at preventing corrosion. It was 55.5% and 89.67% effective at stopping corrosion. After being immersed for 40 days and salt spray test, the composite coating was 13 times better at blocking electrical signals than the neat epoxy coating. This shows the composite coating had much better anti-corrosion protection than the neat epoxy coating.	[126]
Polyurethane	Cerium oxide and graphene oxide particle size 0.2–10 µm	Straight forward spraying method	Immersed 3.5wt.% NaCl	Fixes any small holes or problems in the coating, so the metal is fully protected from corrosion. The CeO_2 also releases special ions that create a new layer that protects against corrosion even more. This makes the coating very strong against corrosion.	[127]

				Even after being immersed for 27 days, the coating is still working very well.	
Epoxy	rGO and BTA@HMS	CTAB (cetyl trimethyl ammonium bromide)	Immersed 3.5wt.% NaCl	The coating made of different materials is 4 times better at stopping corrosion than just neat epoxy. BTA@HMS in the coating helps fix any damage to the coating. This makes the coating much better at protecting the surface underneath from corrosion. The protection against corrosion is much stronger, going from 60 $K\Omega \cdot cm^2$ to 3410 $K\Omega \cdot cm^2$.	[128]
Epoxy	Chitin & Chitosan nanoparticle	Unmodified	Immersed 3.5wt.% NaCl	The coating that had 2% chitin nanoparticles in it was stronger and better at sticking to things. Tests also showed that the coating with 2% chitin and chitosan nanoparticles rusted less, was better at holding heavy things, and could hold twice as much weight before breaking.	[129]
Epoxy	Ti_3C_2 MXene 2D materials	Dopamine and loading corrosion inhibitor	Immersed in saline media	The tests showed that coatings with special ingredients to prevent rust and corrosion worked better than regular epoxy coatings without those ingredients. The coatings with the special anti-corrosion ingredients performed better in the tests.	[130]
Epoxy	Nano silicon dioxide	PFDTES via facile spray-coating	Immersed 3.5wt.% NaCl	The self-repairing coating demonstrates remarkable corrosion resistance, as evidenced by an almost eightfold increase in Rct (charge transfer resistance) when compared to untreated Q235 carbon steel substrates. This indicates a significant enhancement in the coating's ability to prevent corrosion. Furthermore, the coating exhibits excellent sustainability in corrosion protection, as it effectively restores its original anti-corrosion ability, ensuring long-lasting protection against corrosion.	[131]
Epoxy	Graphene	MAO coating and spin coating EP	Immersed 3.5wt.% NaCl	The test results showed that the composite layer had a very high corrosion resistance. After being soaked in liquid for 40 days, the layer had a low-frequency modulus of 6.76×10^{10} $\Omega \cdot cm^2$. This is about 100 times higher than the resistance of a normal epoxy coating. This means the composite coating is much better at preventing corrosion compared to a neat coating.	[132]
Alkyd	PANI-Fe_2O_3	Unmodified	Immersed 3.5wt.% NaCl and 1M HCl	The coating made of polyaniline-iron oxide and alkyd resin is better at protecting mild steel from rust compared to just using the neat alkyd. This is because the polyaniline-iron oxide in the coating helps to create a protective layer on the steel and also fills in gaps, making it harder for rust to form. Studies have shown that this special coating is more effective at preventing corrosion than the neat alkyd coating.	[133]
Polyurethane	Graphene	N-Methyl-2-pyrrolidone via ultra sonication	Immersed 3wt.% NaCl and salt spray	The coating made of PU (polyurethane) with 1% graphene flakes had stronger sticking power, about 2.3 MPa, compared to neat PU. The coating with 2% graphene	[134]

			test 5wt.% NaCl	had very good protection against corrosion. After being immersed for 150 days or exposed to salty air for 2500 hours, it still had a high resistance of 2.7 x $10^{\wedge 10}$ Ohm-cm^2, which means it was very good at preventing corrosion.	
Epoxy-Acrylic	Graphene nanoplatelets	HT-PDMS (hydroxyl-terminated polydimethylsiloxane)	Water contact angle and surface adhesion test	The coating with 1% graphene had the highest water contact angle of 99.75 degrees, meaning it was very water-resistant. Adding graphene to the coating made it degrade at a lower temperature. More graphene also meant the coating had less cross-linking, which made it perform a bit worse. This was likely because the graphene particles clumped together in the coating.	[135]
Polysiloxane	Silica nanoparticle and PS-grafted	HDTMS (hexadecyl trimethoxy silane)	Acid and alkali resistance test	Inclusion of silica within the composition of the coating results in heightened surface roughness and a significant enhancement in its hydrophobic properties. Following a rigorous abrasion test consisting of 90 cycles, the water contact angle on the coating can surpass 150°. Moreover, this particular coating demonstrates exceptional durability against the corrosive effects of both acids and alkalis.	[136]
Ethyl silicate	Nickel oxide nanoparticle	Zinc-rich	Immersed 3.5wt.% NaCl	The coating with 3% nickel oxide had much less corrosion and wear compared to the neat ethyl silicate coating. It also was much better at preventing corrosion, going from 3069 to 16482 ohm-square centimeters. This is because the tiny NiO particles in the coating can slow down the dissolving of the zinc and make the coating stronger by filling in small holes and creating complex paths that are hard for corrosion to get through.	[137]
Polysiloxane	SiO_2 and ZnO	PFDTMS (perfluoro decyltrimethoxysilane)	Immersed 3.5wt.% NaCl and Water contact angle test	The incorporation of SiO_2 nanoparticles made the surface of the coating very water-resistant, or "superhydrophobic". The water didn't stick to the surface at all. When measured, the water made a very high angle of 165.3° ± 1.5° on the surface. And the water just rolled off the surface at a very low angle of only 2.2° ± 0.7°. Electrochemical Impedance Spectroscopy tests showed the coating was almost 4 times better at preventing corrosion compared to neat polysiloxane coating. The addition of SiO2 particles made the surface very water-resistant and much better at preventing corrosion.	[138]
Vinyl ester	2D MXene nanosheets	Unmodified	Immersed 3.5 wt.% NaCl	The incorporation of a 0.1wt.% MXene into vinyl ester significantly improved the layer resistance and apparent impedance, with increases reaching 330%. The hydrophobic MXene nanosheets acted as a protective shield, obstructing the penetration of harmful electrolytes and creating a more complex diffusion	[139]

				pathway, thereby enhancing the overall corrosion protection performance.	
Novolac vinyl ester	Silicon nitride particle size <20 µm	DFHMA (dodecafluoro heptyl methacrylat)	Immersed 10 wt.% NaCl	By blending 8wt.% DFHMA with 3wt.% β-Si_3N_4, the resulting nanocomposite coating exhibited effective corrosion protection and desirable hydrophobic characteristics.	[140]
Vinyl ester	Titanium dioxide and graphene	Triggering MEKP and accelerator of cobalt naphthalate	Immersed 3.5 wt.% NaCl	The addition of filler additives to VER films helps disperse cobalt, improves the crystal structure, and boosts corrosion resistance. This is due to the creation of IPNs within the substance. Incorporating a TiO_2 and G hybrid reinforcement into the VER matrix also significantly enhances the corrosion resistance and adhesion properties of the final film.	[141]
PVB-Epoxy	Graphene oxide	Silane coupling agent KH-550	Immersed 3.5 wt.% NaCl	The original PVB/EP coating had a corrosion resistance of 84.03% and a contact angle of 60.43 degrees. After adding 0.89% GO (graphene oxide), the corrosion resistance improved to 92.57% - an 8.54% increase. The contact angle also increased significantly to 114.66 degrees, indicating a major change in the coating's surface properties.	[142]
PDMS	g-C_3N_4 (graphitic carbon nitride)	Tannic acid	Immersed 3.5wt.% NaCl	The composite coating showed excellent corrosion resistance, maintaining very high electrical impedance even after 28 days submerged. This coating also had the ability to self-heal when exposed to light, fully recovering within just 3 hours.	[143]
Polyurethane	Zr and Ni based amorphous alloy powder	Composite metal powder	Immersed 3.5wt.% NaCl	Incorporating amorphous alloys has significantly improved the corrosion resistance of coatings. An analysis found that a 50% Zr-based amorphous alloy composition showed the best performance in reducing corrosion, outperforming the other compositions tested.	[144]
Polyurethane	Graphene oxide	Unmodified	Immersed 3.5 wt.% NaCl and salt spray test	Adding 0.75% graphene oxide to polyurethane coatings significantly improved their anti-corrosion properties. The coatings had very high electrical impedance that didn't decrease even after self-healing from scratches. The coatings also showed excellent corrosion resistance, withstanding a 20-day salt spray test without any visible signs of corrosion.	[145]
Epoxy	Nanoclay MMT	Unmodified	Immersed 0.5M NaCl	Enhanced protection against corrosion can be observed in copper coated with EPMC when subjected to a sodium chloride solution. The incorporation of 5% MMT clay content in the EPMC coating further enhances the level of protection, resulting in the highest level of resistance to corrosion.	[146]
Epoxy	ZrO_2 nanoparticle	APTES (3-amino propyl triethoxy silane)	Immersed 3.5 wt.% NaCl	Epoxy's corrosion resistance can be improved by adding a specific amount of APTES to modify nano ZrO_2. The composite layer with 2% nano ZrO_2 by	[147]

				mass has an impressive impedance of around $1.0 \times 10^{\wedge 5}$ $\Omega.cm^2$, resulting in superior corrosion resistance.	
Epoxy	ZIF-67@DTMS Nanoparticle	DTMS (dodcyltrimethoxysilane)	Immersed 3.5 wt.% NaCl	Adding ZIF-67@DTMS nanoparticles to epoxy coatings improves their corrosion resistance and adhesion. The nanoparticles form strong bonds with the epoxy and fill in any gaps, creating a better barrier against harmful substances. This enhances the overall anti-corrosion performance of the coating.	[148]
Epoxy	ZIF-8	PPy (conductive polypyrrole)	Immersed 3.5 wt.% NaCl and salt spray test	The addition of fillers significantly enhances the corrosion resistance of epoxy coatings. This improved protection comes from the combined effects of passive and active corrosion-fighting mechanisms. The PPy@ZIF-8 particles act as passive nanofillers that shield the surface, plus they can self-heal by generating a protective iron oxide and zinc hydroxide layer on the steel.	[149]
Epoxy	Fluorinated graphene	ZIF-8 and Triton X-100	Immersed 3.5 wt.% NaCl	The coating modified with FG had better mechanical properties, more resistance to wear, and longer-lasting protection against corrosion compared to the unmodified EP coating. However, the limited compatibility between FG and the resins made it difficult to significantly improve the corrosion resistance.	[150]
Epoxy	Graphene oxide	Maleic acid diamine	Immersed 3.5 wt.% NaCl	The addition of 0.3% M-GO into a water-based epoxy coating provided excellent anti-corrosion properties. After being submerged for 96 hours, the composite coating showed very high impedance, extremely low corrosion current, and nearly 99.9% protection efficiency against corrosion	[151]
Epoxy	h-BN and DA	Dual self-healing effect BTA and PDA	Immersed 3.5 wt.% NaCl	The addition of BPCT nanosheets to waterborne EP coatings improves the coatings' ability to block harmful substances and self-heal any defects. This results in exceptional corrosion resistance for the coated materials.	[152]

5. CONCLUSION

Marine environments exhibit unique characteristics that differentiate them from other natural conditions. These environments are known to possess elevated levels of corrosive elements, such as extreme humidity and aggressive atmospheres. This makes alloys susceptible to localized corrosion. The Society for Protective Coatings provides valuable recommendations on coating selection and application.

The traditional marine coating approach involves a layer-by-layer application of primer, intermediate, and top coatings. The selection of these coatings is determined by the desired thickness required for the marine structures. For atmospheric protection, a common practice is to apply single or double layers of epoxy. For enhanced performance, a more expensive system using zinc-rich primer, epoxy, and polyurethane can be used. Coating systems specifically designed for atmospheric conditions are generally utilized in intertidal and splash zones. Submerged areas are typically coated with single, double, or triple-layer solid epoxy.

The limitations of using single polymers as generic coatings have led to the widespread adoption of incorporating fillers to enhance their characteristics and transform them into composites. In the realm of marine coatings, the options for fillers are currently restricted to glass flakes and powders. The primary concern regarding heavy-duty marine coatings is their adhesive properties. Even the best coating materials are useless if they don't stick well to the surface. That's why it's crucial to carefully formulate the entire coating system to ensure strong adhesion. In the production of composite coatings, the filler material must be uniformly dispersed into the matrix. Insufficient dispersion of fillers can result in agglomeration, impeding the matrix from fully bonding with other fillers and consequently diminishing the adhesion properties. The remedy for this predicament lies in modifying the filler with a coupling agent. For instance, the inclusion of 2D fillers like nanoclay can enhance the barrier effect and mechanical properties of polymers. However, a limitation associated with nanoclay is its layered silica structure, which requires modification with quaternary ammonium compounds or other coupling agents to achieve intercalated or exfoliated nanocomposites.

The incorporation of fillers into polymers serves a pivotal role in augmenting their characteristics, particularly with respect to corrosion resistance, in comparison to unfilled polymers. However, it is paramount to meticulously evaluate the filler type, particle size, and composition. Certain fillers may necessitate surface modification prior to incorporation. By reducing the filler particle size to the submicron range, the composite material can exhibit enhanced and distinctive properties. Conversely, an excessive filler composition could result in agglomeration issues before the polymer is fully cured.

This review provides a thorough and critical examination of the development of composite coatings and their potential use for marine applications. The purpose of this concise review is to contribute to exploring new filler materials and surface modification techniques that could improve the performance of composite coatings.

REFERENCES

[1] H. Kurnia, Sudarmono, A. Wahyuni, N. Adistyani, and A. Sulaeman, "Penggunaan material logam di berbagai industri manufaktur Indonesia: Sistematik kajian literatur," *Industry Xplore*, vol. 8, pp. 220-228, 2023. Doi: 10.36805/teknikindustri.v8i1.5098.

[2] S. Chandrasekaran and A. Jain, "Materials for ocean structures," *Ocean Structures*, CRC Press, pp. 129-194, 2016. Doi: 10.1201/9781315366692-4.

[3] H. Hastuti, A. Muhidu, R. Rastin, and E. Mokodompit, "Indonesia's marine economic potential as a maritime country: Marine economy," *International Journal of Science, Technology & Management*, vol. 4, pp. 813-825, 2023. Doi: 10.46729/ijstm.v4i4.897.

[4] D. Caesaron, Y. Maimury, and B. Peminatan, "Evaluasi dan usulan pengembangan energi terbarukan untuk keberlangsungan energi nasional," *Journal of Industrial Engineering and Management Systems*, vol. 7, no. 2, 2014. Doi: 10.30813/jiems.v7i2.116.

[5] O. Sarhan and M. Raslan, "Offshore petroleum rigs/platforms: An overview of analysis, design, construction, and installation," *International Journal of Advanced Engineering, Sciences and Applications*, vol. 2, no. 1, pp. 7-12, 2021. Doi: 10.47346/ijaesa.v2i1.58.

[6] B. Isecke, M. Schütze, and H.-H. Strehblow, "Corrosion," in *Springer Handbook of Metrology and Testing*, H. Czichos, T. Saito, and L. Smith, Eds., Berlin, Heidelberg:

DOI : 10.55981/metalurgi.2024.746

Metalurgi is Sinta 2 Journal (https://sinta.kemdikbud.go.id/journals/profile/3708) accredited by Ministry of Education, Culture, Research, and Technology, Republic Indonesia

Springer Berlin Heidelberg, 2011, pp. 667-741. Doi: 10.1007/978-3-642-16641-9_12.
[7] M. Hayatdavoodi, "Dhanak and xiros (Eds.): Springer handbook of ocean engineering," *J Ocean Eng Mar Energy*, vol. 3, no. 3, pp. 293-295, 2017. Doi: 10.1007/s40722-017-0083-9.
[8] R. W. Revie and H. H. Uhlig, "Frontmatter," in *Corrosion and Corrosion Control*, Wiley, 2008. Doi: 10.1002/9780470277270.fmatter.
[9] L. L. Shreir, R. A. Jarman, and G. T. Burstein, Eds., "L.L. SHREIR, OBE 1914-1992," in *Corrosion (Third Edition)*, Oxford: Butterworth-Heinemann, 1994, pp. xiv–xv. Doi: 10.1016/B978-0-08-052351-4.50003-0.
[10] G. A. Cragnolino, "2 - Corrosion fundamentals and characterization techniques," in *Techniques for Corrosion Monitoring (Second Edition)*, L. Yang, Ed., Woodhead Publishing, 2021, pp. 7-42. Doi: 10.1016/B978-0-08-103003-5.00002-3.
[11] U. Wahyuningsih, H. Rusjdi, and E. Sulistiyo, "Penanggulangan korosi pada pipa gas dengan metode catodic protection (anoda korban)" *Jurnal Power Plant*, vol. 5, no. 1, 2017.
[12] A. L. Ortega, R. Bayón, and J. L. Arana, "Evaluation of protective coatings for offshore applications. Corrosion and tribo-corrosion behavior in synthetic seawater," *Surf Coat Technol*, vol. 349, pp. 1083-1097, 2018. Doi: 10.1016/j.surfcoat.2018.06.089.
[13] M. F. Montemor, "Functional and smart coatings for corrosion protection: A review of recent advances," *Surf Coat Technol*, vol. 258, pp. 17-37, 2014. Doi: 10.1016/j.surfcoat.2014.06.031.
[14] H. Tamura, "The role of rusts in corrosion and corrosion protection of iron and steel," *Corros Sci*, vol. 50, no. 7, pp. 1872-1883, 2008. Doi: 10.1016/j.corsci.2008.03.008.
[15] A. H. Al-Moubaraki and I. B. Obot, "Corrosion challenges in petroleum refinery operations: Sources, mechanisms, mitigation, and future outlook," *Journal of Saudi Chemical Society*, vol. 25, no. 12, pp. 101370, 2021. Doi: 10.1016/j.jscs.2021.101370.
[16] Z. Tian, H. Yu, L. Wang, M. Saleem, F. Ren, P. Ren, Y. Chen, R. Sun, Y. Sun, and L. Huang, "Recent progress in the preparation of polyaniline nanostructures and their applications in anticorrosive coatings," *RSC Advances*, vol. 4, no. 54. Royal Society of Chemistry, pp. 28195-28208, 2014. Doi: 10.1039/c4ra03146f.
[17] I. S. Cole and D. Marney, "The science of pipe corrosion: A review of the literature on the corrosion of ferrous metals in soils," *Corros Sci*, vol. 56, pp. 5-16, 2012. Doi: 10.1016/j.corsci.2011.12.001.
[18] M. Yasir, F. Ahmad, P. Megat-Yusoff, S. Ullah, and M. Jimenez, "Latest trends for structural steel protection by using intumescent fire protective coatings: a review," *Surface Engineering*, vol. 36, pp. 1-30, 2019. Doi: 10.1080/02670844.2019.1636536.
[19] M. A. Malik, M. A. Hashim, F. Nabi, S. A. AL-Thabaiti, and Z. Khan, "Anti-corrosion Ability of Surfactants: A Review," Int J Electrochem Sci, vol. 6, no. 6, pp. 1927–1948, 2011. Ddoi: 10.1016/S1452-3981(23)18157-0.
[20] K. L. Mercer and W. F. Langelier, "The analytical control of anti-corrosion water treatment," *J Am Water Works Assoc*, vol. 110, 1936. [Online]. Available: https://api.semanticscholar.org/CorpusID:107825312
[21] J. B. Wachtman and R. A. Haber, "Ceramic films and coatings," *Materials and Corrosion*, 1993. [Online]. Available: https://api.semanticscholar.org/CorpusID:109813803
[22] A. Stankiewicz, I. Szczygieł, and B. Szczygieł, "Self-healing coatings in anti-corrosion applications," *J Mater Sci*, vol. 48, pp. 8041-8051, 2013, [Online]. Available: https://api.semanticscholar.org/CorpusID:59451802
[23] M. R. Thakare, J. A. Wharton, R. J. K. Wood, and C. Menger, "Exposure effects of alkaline drilling fluid on the microscale abrasion-corrosion of WC-based hard metals," *Wear*, vol. 263, no. 1, pp. 125-136, 2007. Doi: 10.1016/j.wear.2006.12.047.
[24] V. Sharma, S. Kumar, M. Kumar, and D. Deepak, "High-temperature oxidation performance of Ni-Cr-Ti and Ni-5Al coatings," *Mater Today Proc*, vol. 26, pp. 3397-3406, 2020. Doi: 10.1016/j.matpr.2019.11.048.
[25] E. G. Kocheemoolayil and M. Andy, "Marine Corrosion and its Management." *International Journal of Science Technology and Management*, vol. 4, special issue no. 01, 2015.
[26] J. Zhang, W. Qin, W. Chen, Z. Feng, D. Wu, L. Liu, and Y. Wang, "Integration of antifouling and anti-cavitation coatings on propellers: a review," *Coatings*, vol. 13, no. 9, 2023. Doi: 10.3390/coatings13091619.
[27] A. Wang, K. De Silva, M. Jones, P. Robinson, G. Larribe, and W. Gao, "Anticorrosive coating systems for marine propellers," *Prog*

Org Coat, vol. 183, pp. 107768, 2023. Doi: 10.1016/j.porgcoat.2023.107768.
[28] ISO 12944-5, *Paints and varnishes - Corrosion protection of steel structures by protective paint systems*, 3rd ed. Switzerland: ISO, 2018.
[29] B. N. Popov, "Chapter 13 - Organic Coatings," in *Corrosion Engineering*, B. N. Popov, Ed., Amsterdam: Elsevier, 2015, pp. 557-579. Doi: 10.1016/B978-0-444-62722-3.00013-6.
[30] SSPC: The Society for Protective Coatings, "Use of coatings to control corrosion of maritime structures" Port Technology International 63 Mooring and Berthing, 2019.
[31] "The Power of Powder Coating," Northpoint Ltd. [Online]. Available: https://www.northpoint.ltd.uk/2024/02/26/the-power-of-powder-coating/. [Accessed: Aug. 31, 2024].
[32] A. Palanisamy, N. V Salim, J. Parameswaranpillai, and N. Hameed, "Water sorption and solvent sorption of epoxy/block-copolymer and epoxy/thermoplastic blends," *Handbook of Epoxy Blends*, J. Parameswaranpillai, N. Hameed, J. Pionteck, and E. M. Woo, Eds., Cham: Springer International Publishing, 2017, pp. 1097-1111. Doi: 10.1007/978-3-319-40043-3_40.
[33] M. Liu, X. Mao, H. Zhu, A. Lin, and D. Wang, "Water and corrosion resistance of epoxy–acrylic–amine waterborne coatings: Effects of resin molecular weight, polar group, and hydrophobic segment," *Corros Sci*, vol. 75, pp. 106-113, 2013. Doi: 10.1016/j.corsci.2013.05.020.
[34] L. H. Sharpe, *Adhesion International 1993*, 1st Edition. London: Taylor & Francis Group, 1996.
[35] A. Mirmohseni and S. Zavareh, "Preparation and characterization of an epoxy nanocomposite toughened by a combination of thermoplastic, layered and particulate nano-fillers," *Mater Des*, vol. 31, no. 6, pp. 2699-2706, 2010. Doi: 10.1016/j.matdes.2010.01.035.
[36] A. M. Madhusudhana, K. N. S. Mohana, M. B. Hegde, S. R. Nayak, K. Rajitha, and N. K. Swamy, "Functionalized graphene oxide-epoxy phenolic novolac nanocomposite: an efficient anticorrosion coating on mild steel in saline medium," *Adv Compos Hybrid Mater*, vol. 3, no. 2, pp. 141-155, 2020. Doi: 10.1007/s42114-020-00142-8.
[37] G. Xiong, P. Kang, J. Zhang, B. Li, J. Yang, G. Chen, Z. Zhou, and Q. Li, "Improved adhesion, heat resistance, anticorrosion properties of epoxy resins/POSS/methyl phenyl silicone coatings," *Prog Org Coat*, vol. 135, pp. 454-464, 2019. Doi: 10.1016/j.porgcoat.2019.06.017.
[38] H. Zhao, J. Ding, P. Liu, and H. Yu, "Boron nitride-epoxy inverse 'nacre-like' nanocomposite coatings with superior anticorrosion performance," *Corros Sci*, vol. 183, pp. 109333, 2021. Doi: 10.1016/j.corsci.2021.109333.
[39] J. Ding, H. Zhao, M. Zhou, P. Liu, and H. Yu, "Super-anticorrosive inverse nacre-like graphene-epoxy composite coating," *Carbon N Y*, vol. 181, pp. 204-211, 2021. Doi: 10.1016/j.carbon.2021.05.017.
[40] F.-L. Jin, X. Li, and S.-J. Park, "Synthesis and application of epoxy resins: A review," *Journal of Industrial and Engineering Chemistry*, vol. 29, pp. 1-11, 2015. Doi: 10.1016/j.jiec.2015.03.026.
[41] J. Zhu, C. Abeykoon, and N. Karim, "Investigation into the effects of fillers in polymer processing," *International Journal of Lightweight Materials and Manufacture*, vol. 4, no. 3, pp. 370-382, 2021. Doi: 10.1016/j.ijlmm.2021.04.003.
[42] R. Muraliraja, T. R. Tamilarasan, S. Udayakumar, and C. K. Arvinda Pandian, "The Effect of Fillers on the Tribological Properties of Composites," *Tribological Applications of Composite Materials*, Springer Singapore, 2021, pp. 243–266. Doi: 10.1007/978-981-15-9635-3_9.
[43] Y. Ren, L. Zhang, G. Xie, Z. Li, H. Chen, H. Gong, W. Xu, D. Guo, and J. Luo, "A review on tribology of polymer composite coatings," *Friction*, vol. 9, no. 3. Tsinghua University, pp. 429-470, 2021. Doi: 10.1007/s40544-020-0446-4.
[44] C. Su, F. Xue, T. Li, Y. Xin, and M. Wang, "Study on the tribological properties of carbon fabric/polyimide composites filled with SiC nanoparticles," *Journal of Macromolecular Science, Part B*, vol. 55, no. 6, pp. 627-641, 2016. Doi: 10.1080/00222348.2016.1179248.
[45] A. S. H. Makhlouf, "1 - Current and advanced coating technologies for industrial applications," in *Nanocoatings and Ultra-Thin Films*, A. S. H. Makhlouf and I. Tiginyanu, Eds., Woodhead Publishing, 2011, pp. 3-23. Doi: 10.1533/9780857094902.1.3.
[46] Q. Zhang, D. Sando, and V. Nagarajan, "Chemical route derived bismuth ferrite thin films and nanomaterials," *J Mater Chem C*

Mater, vol. 4, no. 19, pp. 4092-4124, 2016. Doi: 10.1039/C6TC00243A.

[47] H. G. Prengel, W. R. Pfouts, and A. T. Santhanam, "State of the art in hard coatings for carbide cutting tools," *Surf Coat Technol*, vol. 102, no. 3, pp. 183-190, 1998. Doi: 10.1016/S0257-8972(96)03061-7.

[48] P. P. Luff and M. White, "The structure and properties of evaporated polyethylene thin films," *Thin Solid Films*, vol. 6, no. 3, pp. 175-195, 1970. Doi: 10.1016/0040-6090(70)90038-6.

[49] J.-O. Carlsson and P. M. Martin, "Chapter 7 - Chemical Vapor Deposition," in *Handbook of Deposition Technologies for Films and Coatings (Third Edition)*, P. M. Martin, Ed., Boston: William Andrew Publishing, 2010, pp. 314-363. Doi: 10.1016/B978-0-8155-2031-3.00007-7.

[50] V. Khanna, K. Singh, S. Kumar, S. A. Bansal, M. Channegowda, I. Kong, M. Khalid, and V. Chaudhary, "Engineering electrical and thermal attributes of two-dimensional graphene reinforced copper/aluminium metal matrix composites for smart electronics," *ECS Journal of Solid State Science and Technology*, vol. 11, no. 12, pp. 127001, 2022. Doi: 10.1149/2162-8777/aca933.

[51] T. Maruyama and T. Kanagawa, "Electrochromic properties of niobium oxide thin films prepared by chemical vapor deposition," *J Electrochem Soc*, vol. 141, no. 10, pp. 2868, 1994. Doi: 10.1149/1.2059247.

[52] K.-H. Dahmen, "Chemical Vapor Deposition," in *Encyclopedia of Physical Science and Technology (Third Edition)*, R. A. Meyers, Ed., New York: Academic Press, 2003, pp. 787-808. Doi: 10.1016/B0-12-227410-5/00102-2.

[53] B. Fotovvati, S. F. Wayne, G. Lewis, and E. Asadi, "A review on melt-pool characteristics in laser welding of metals," *Advances in Materials Science and Engineering*, vol. 2018, pp. 4920718, 2018. Doi: 10.1155/2018/4920718.

[54] D. Sreekanth and N. Rameshbabu, "Development and characterization of MgO/hydroxyapatite composite coating on AZ31 magnesium alloy by plasma electrolytic oxidation coupled with electrophoretic deposition," *Mater Lett*, vol. 68, pp. 439-442, 2012. Doi: 10.1016/j.matlet.2011.11.025.

[55] S. P. Sah, Y. Tatsuno, Y. Aoki, and H. Habazaki, "Dielectric breakdown and healing of anodic oxide films on aluminum under single pulse anodizing," *Corros Sci*, vol. 53, no. 5, pp. 1838-1844, 2011. Doi: 10.1016/j.corsci.2011.02.001.

[56] M. Dziaduszewska, M. Shimabukuro, T. Seramak, A. Zieliński, and T. Hanawa, "Effects of micro-arc oxidation process parameters on characteristics of calcium-phosphate containing oxide layers on the selective laser melted Ti13Zr13Nb Alloy," *Coatings*, 2020. [Online]. Available: https://api.semanticscholar.org/CorpusID:225445191

[57] W. Shang, B. Chen, X. Shi, Y. Chen, and X. Xiao, "Electrochemical corrosion behavior of composite MAO/sol-gel coatings on magnesium alloy AZ91D using combined micro-arc oxidation and sol-gel technique," *J Alloys Compd*, vol. 474, no. 1, pp. 541-545, 2009. Doi: 10.1016/j.jallcom.2008.06.135.

[58] M. R. Bayati, A. Z. Moshfegh, and F. Golestani-Fard, "Micro-arc oxidized S-TiO2 nanoporous layers: Cationic or anionic doping?" *Mater Lett*, vol. 64, pp. 2215-2218, 2010. [Online]. Available: https://api.semanticscholar.org/CorpusID:97620342

[59] D. Sreekanth, N. Rameshbabu, and K. Venkateswarlu, "Effect of various additives on morphology and corrosion behavior of ceramic coatings developed on AZ31 magnesium alloy by plasma electrolytic oxidation," *Ceram Int*, vol. 38, no. 6, pp. 4607-4615, 2012. Doi: 10.1016/j.ceramint.2012.02.040.

[60] L. R. Krishna, K. R. C. Somaraju, and G. Sundararajan, "The tribological performance of ultra-hard ceramic composite coatings obtained through micro-arc oxidation," *Surf Coat Technol*, vol. 163-164, pp. 484-490, 2003. Doi: 10.1016/S0257-8972(02)00646-1.

[61] D. Venkateswarlu, N. Rameshbabu, S. D, A. C. Bose, V. Muthupandi, and S. Subramanian, "Fabrication and characterization of micro-arc oxidized fluoride containing titania films on Cp Ti," *Ceram Int*, vol. 39, p. 801, 2013. Doi: 10.1016/j.ceramint.2012.07.001.

[62] S. Sampath, V. Alagan, bullet Venkateswarlu, N. Rameshbabu, and N. Parthasarathi, "Enhanced visible light photocatalytic activity of P-block elements (C, N and F) doped porous TiO2 coatings on Cp-Ti by micro-arc oxidation," *Journal of Porous Materials*, vol. 22, pp. 545-557, 2015.

[63] E. Linga Reddy, J. Karuppiah, H. C. Lee, and D. H. Kim, "Steam reforming of methanol over copper loaded anodized aluminum oxide (AAO) prepared through electrodeposition," *J Power Sources*, vol. 268, pp. 88-95, 2014. Doi: 10.1016/j.jpowsour.2014.05.082.

[64] Y. Sasikumar, K. Indira, and N. Rajendran, "Surface modification methods for titanium and its alloys and their corrosion behavior in biological environment: A review," *J Bio Tribocorros*, vol. 5, no. 2, p. 36, 2019. Doi: 10.1007/s40735-019-0229-5.

[65] S. Kumar, A. Handa, V. Chawla, N. K. Grover, and R. Kumar, "Performance of thermal-sprayed coatings to combat hot corrosion of coal-fired boiler tube and effect of process parameters and post-coating heat treatment on coating performance: a review," *Surface Engineering*, vol. 37, no. 7. Taylor and Francis Ltd., pp. 833-860, 2021. Doi: 10.1080/02670844.2021.1924506.

[66] S. Kumar, M. Kumar, and N. Jindal, "Overview of cold spray coatings applications and comparisons: a critical review," *World Journal of Engineering*, vol. 17, no. 1, pp. 27-51, 2020. Doi: 10.1108/WJE-01-2019-0021.

[67] E. Sadeghi, N. Markocsan, and S. V Joshi, "Advances in corrosion-resistant Thermal spray coatings for renewable energy power plants. Part I: effect of composition and microstructure," *Journal of Thermal Spray Technology*, vol. 28, pp. 1749-1788, 2019. [Online]. Available: https://api.semanticscholar.org/CorpusID:207990369

[68] V. Petri, "Thermal spray coating processes", *Comprehensive materials processing*, 1st edition Volume 4: Coatings and films. Elsevier. 2014. p. 229-276

[69] R. Goyal, B. Sidhu, and V. Chawla, "Hot corrosion performance of plasma-sprayed multiwalled carbon nanotube–Al_2O_3 composite coatings in a coal-fired boiler at 900 °C," *J Mater Eng Perform*, vol. 29, pp. 1-12, 2020. Doi: 10.1007/s11665-020-05070-8.

[70] S. Kongparakul, S. Kornprasert, P. Suriya, D. Le, C. Samart, N. Chantarasiri, P. Prasassarakich, and G. Guan, "Self-healing hybrid nanocomposite anticorrosive coating from epoxy/modified nanosilica/perfluorooctyl triethoxysilane," *Prog Org Coat*, vol. 104, pp. 173-179, 2017. Doi: 10.1016/j.porgcoat.2016.12.020.

[71] S. M. Shang and W. Zeng, "4 - Conductive nanofibres and nanocoatings for smart textiles," in *Multidisciplinary Know-How for Smart-Textiles Developers*, T. Kirstein, Ed., Woodhead Publishing, 2013, pp. 92-128. Doi: 10.1533/9780857093530.1.92.

[72] N. Raghavendra, H.N. Narasimha Murthy, K. R. V. Mahesh, M. Mylarappa, K.P. Ashik, D. M. K. Siddeswara, and M. Krishna, "Effect of Nanoclays on the performance of Mechanical, Thermal and Flammability of Vinylester based nanocomposites," *Mater Today Proc*, vol. 4, pp. 12109-12117, 2017. Doi: 10.1016/j.matpr.2017.09.138.

[73] M. Alsaadi, M. Bulut, A. Erklig, and A. Jabbar, "Nano-silica inclusion effects on mechanical and dynamic behavior of fiber reinforced carbon/Kevlar with epoxy resin hybrid composites," *Compos B Eng*, vol. 152, 2018, Doi: 10.1016/j.compositesb.2018.07.015.

[74] M. Behzadnasab, M. Mirabedini, and K. Kabiri, "Effect of various combinations of zirconia and organoclay nanoparticles on mechanical and thermal properties of an epoxy nanocomposite coating," *Compos Part A Appl Sci Manuf*, vol. 43, pp. 2095, 2012. Doi: 10.1016/j.compositesa.2012.07.002.

[75] M. Behzadnasab, M. Mirabedini, and M. Esfandeh, "Corrosion protection of steel by epoxy nanocomposite coatings containing various combinations of clay and nanoparticulate zirconia," *Corros Sci*, vol. 75, 2013. Doi: 10.1016/j.corsci.2013.05.024.

[76] M. Bagci, M. Demirci, E. Şükür, and H. Kaybal, "The effect of nanoclay particles on the incubation period in solid particle erosion of glass fibre/epoxy nanocomposites," *Wear*, vol. 444-445, pp. 203159, 2019. Doi: 10.1016/j.wear.2019.203159.

[77] A. M. Kumar, A. Khan, R. Suleiman, M. Qamar, S. Saravanan, and H. Dafalla, "Bifunctional CuO/TiO_2 nanocomposite as nanofiller for improved corrosion resistance and antibacterial protection," *Prog Org Coat*, vol. 114, pp. 9-18, 2018. Doi: 10.1016/j.porgcoat.2017.09.013.

[78] J. E. O. Mayne, "The mechanism of the protection of iron and steel by paint," *Anti-Corrosion Methods and Materials*, vol. 20, no. 10, pp. 3-8, 1973. Doi: 10.1108/eb006930.

[79] Z. W. Wicks, F. N. Jones, S. P. Pappas, and D. A. Wicks, "Organic Coatings: Science and Technology" John Wiley & Sons, 2007. DOI:10.1002/047007907X

[80] Y. Ren, L. Zhang, G. Xie, Z. Li, H. Chen, H. Gong, W. Xu, D. Guo, and J. Luo, "A review on tribology of polymer composite coatings," *Friction*, vol. 9, no. 3, pp. 429-470, 2021. Doi: 10.1007/s40544-020-0446-4.

[81] G. Wang, D. Yu, A. D. Kelkar, and L. Zhang, "Electrospun nanofiber: Emerging reinforcing filler in polymer matrix composite materials," *Prog Polym Sci*, vol. 75, pp. 73-107, 2017. Doi: 10.1016/j.progpolymsci.2017.08.002.

[82] M. G. Segatelli, I. V. P. Yoshida, and M. do C. Gonçalves, "Natural silica fiber as reinforcing filler of nylon 6," *Compos B Eng*, vol. 41, no.

1, pp. 98-105, 2010. Doi: 10.1016/j.compositesb.2009.05.006.
[83] J. N. Coleman, U. Khan, and Y. K. Gun'ko, "Mechanical Reinforcement of Polymers Using Carbon Nanotubes," *Advanced Materials*, vol. 18, no. 6, pp. 689-706, 2006. Doi: 10.1002/adma.200501851.
[84] P. Podsiadlo, A. K. Kaushik, E. M. Arruda, A. M. Waas, B. S. Shim, J. Xu, H. Nandivada, B. G. Pumplin, J. Lahann, A. Ramamoorthy, and N. A. Kotov, "Ultrastrong and stiff layered polymer nanocomposites," *Science (1979)*, vol. 318, no. 5847, pp. 80-83, 2007. Doi: 10.1126/science.1143176.
[85] S. V Panin, D. A. Nguyen, L. A. Kornienko, L. R. Ivanova, and B. B. Ovechkin, "Comparison on the efficiency of solid-lubricant fillers for polyetheretherketone-based composites," *AIP Conf Proc*, vol. 2051, no. 1, pp. 020232, 2018. Doi: 10.1063/1.5083475.
[86] P. Cai, T. Wang, and Q. Wang, "Effect of several solid lubricants on the mechanical and tribological properties of phenolic resin-based composites," *Polym Compos*, vol. 36, no. 12, pp. 2203-2211, 2015. Doi: 10.1002/pc.23132.
[87] M. Zalaznik, M. Kalin, S. Novak, and G. Jakša, "Effect of the type, size, and concentration of solid lubricants on the tribological properties of the polymer PEEK," *Wear*, vol. 364-365, pp. 31-39, 2016. Doi: 10.1016/j.wear.2016.06.013.
[88] Q. B. Guo, M. Z. Rong, G. L. Jia, K. T. Lau, and M. Q. Zhang, "Sliding wear performance of nano-SiO2/short carbon fiber/epoxy hybrid composites," *Wear*, vol. 266, no. 7, pp. 658-665, 2009. Doi: 10.1016/j.wear.2008.08.005.
[89] W. Zhai, N. Srikanth, L. B. Kong, and K. Zhou, "Carbon nanomaterials in tribology," *Carbon N Y*, vol. 119, pp. 150-171, 2017. Doi: 10.1016/j.carbon.2017.04.027.
[90] W. Zhai and K. Zhou, "Nanomaterials in superlubricity," *Adv Funct Mater*, vol. 29, no. 28, pp. 1806395, 2019. Doi: 10.1002/adfm.201806395.
[91] T. Agag, T. Koga, and T. Takeichi, "Studies on thermal and mechanical properties of polyimide–clay nanocomposites," *Polymer (Guildf)*, vol. 42, no. 8, pp. 3399-3408, 2001. Doi: 10.1016/S0032-3861(00)00824-7.
[92] H. Wang, C. Zeng, M. D. Elkovitch, L. J. Lee, and K. W. Koelling, "Processing and properties of polymeric nano-composites," *Polym Eng Sci*, vol. 41, pp. 2036-2046, 2001. [Online]. Available: https://api.semanticscholar.org/CorpusID:137568665
[93] M. Tolinski, "Overview of fillers and fibers," *Additives for Polyolefins*, Elsevier, 2009, pp. 93-119. Doi: 10.1016/b978-0-8155-2051-1.00007-8.
[94] H.-J. Song and Z.-Z. Zhang, "Investigation of the tribological properties of polyfluo wax/polyurethane composite coating filled with nano-SiC or nano-ZrO2," *Materials Science and Engineering: A*, vol. 426, no. 1, pp. 59-65, 2006. Doi: 10.1016/j.msea.2006.03.104.
[95] Y. Chen, S. Zhou, H. Yang, and L. Wu, "Structure and properties of polyurethane/nanosilica composites," *J Appl Polym Sci*, vol. 95, pp. 1032-1039, 2005. Doi: 10.1002/app.21180.
[96] G. Zhang, A. K. Schlarb, S. Tria, and O. Elkedim, "Tensile and tribological behaviors of PEEK/nano-SiO2 composites compounded using a ball milling technique," *Compos Sci Technol*, vol. 68, no. 15, pp. 3073-3080, 2008. Doi: 10.1016/j.compscitech.2008.06.027.
[97] S. S. Vaisakh, A. A. Peer Mohammed, M. Hassanzadeh, J. F. Tortorici, R. Metz, and S. Ananthakumar, "Effect of nano-modified SiO2/Al2O3 mixed-matrix micro-composite fillers on thermal, mechanical, and tribological properties of epoxy polymers," *Polym Adv Technol*, vol. 27, no. 7, pp. 905-914, 2016. Doi: 10.1002/pat.3747.
[98] H.-J. Song, Z.-Z. Zhang, and X.-H. Men, "The tribological behaviors of the polyurethane coating filled with nano-SiO2 under different lubrication conditions," *Compos Part A Appl Sci Manuf*, vol. 39, no. 2, pp. 188-194, 2008. Doi: 10.1016/j.compositesa.2007.11.003.
[99] I. D. Sideridou and M. M. Karabela, "Effect of the amount of 3-methacyloxypropyltrimethoxysilane coupling agent on physical properties of dental resin nanocomposites," *Dental Materials*, vol. 25, no. 11, pp. 1315-1324, 2009. Doi: 10.1016/j.dental.2009.03.016.
[100] J. Antonucci, S. Dickens, B. Fowler, H. Xu, and W. McDonough, "Chemistry of silanes interfaces in dental polymers and composites," 2005. [Online]. Available: https://tsapps.nist.gov/publication/get_pdf.cfm?pub_id=854442
[101] M. Behzadnasab, S. M. Mirabedini, K. Kabiri, and S. Jamali, "Corrosion performance of epoxy coatings containing silane treated ZrO_2 nanoparticles on mild steel in 3.5% NaCl solution," *Corros Sci*, vol. 53, no. 1, pp. 89-98, 2011. Doi: 10.1016/j.corsci.2010.09.026.
[102] M. Behzadnasab, S. M. Mirabedini, and M. Esfandeh, "Corrosion protection of steel by

epoxy nanocomposite coatings containing various combinations of clay and nanoparticulate zirconia," *Corros Sci*, vol. 75, pp. 134-141, 2013. Doi: 10.1016/j.corsci.2013.05.024.

[103] S. M. Mirabedini, M. Behzadnasab, and K. Kabiri, "Effect of various combinations of zirconia and organoclay nanoparticles on mechanical and thermal properties of an epoxy nanocomposite coating," *Compos Part A Appl Sci Manuf*, vol. 43, no. 11, pp. 2095-2106, 2012. Doi: 10.1016/j.compositesa.2012.07.002.

[104] M. G. Sari, M. Abdolmaleki, M. Rostami, and B. Ramezanzadeh, "Nanoclay dispersion and colloidal stability improvement in phenol novolac epoxy composite via graphene oxide for the achievement of superior corrosion protection performance," *Corros Sci*, vol. 173, 2020. Doi: 10.1016/j.corsci.2020.108799.

[105] J. Li, L. Ecco, M. Fedel, V. Ermini, G. Delmas, and J. Pan, "In-situ Atomic Force Microscopy and EIS study of a solvent-borne alkyd coating with nanoclay for corrosion protection of carbon steel," *Prog Org Coat*, vol. 87, pp. 179-188, 2015. Doi: 10.1016/j.porgcoat.2015.06.003.

[106] Alvian, Kenrick, and I. Iskandinata, "Pengaruh penambahan bentonit termodifikasi sebagai pengisi terhadap sifat mekanik dan penyerapan air komposit epoksi," *Jurnal Teknik Kimia USU*, vol. 5, pp. 39-4, 2017. Doi: 10.32734/jtk.v5i4.1553.

[107] B. Soegijono, F. Susetyo, and H. Notonegoro, "Perilaku ketahanan korosi komposit coating poliuretan/silika/ karbon pada baja karbon rendah," *FLYWHEEL : Jurnal Teknik Mesin Untirta*, pp. 57, 2019. Doi: 10.36055/fwl.v0i0.4775.

[108] H. Ummah and Munasir, "Studi sifat anti-korosi material coating CAT-PANi/SiO2 dengan metode polarisasi linear," *Jurnal Inovasi Fisika Indonesia,* vol. 04 no. 03, pp 133-137, 2015.

[109] G. Mahfuzh, "Pengaruh penambahan metalloam terhadap ketahanan korosi dan daya lekat pelapisan dengan cat epoksi primer yang diaplikasikan pada substrat baja karbon rendah," Skripsi S1, Departemen Teknik Metalurgi dan Material, Universitas Indonesia, Depok, Indonesia, 2010.

[110] R. A. Nugraha, "Karakteristik material komposit nano polyaniline (PANi) dan oksida grafena tereduksi (rGO) sebagai pelapis proteksi korosi dan katalis pada katoda DSSC dengan substrat baja karbon AISI 1086," Tesis S2, Departemen Teknik Metalurgi dan Material, Universitas Indonesia, Depok, Indonesia, 2018.

[111] Arham, "Performa ketahanan korosi baja ST-37 dilapisi komposit epoksi - ZnO dengan modifikasi permukaan melalui metode electrochemical impedance spectroscopy," Tesis S2, Departemen Teknik Metalurgi dan Material, Universitas Indonesia, Depok, Indonesia, 2022.

[112] J. Li, L. Wang, H. Bai, C. Chen, L. Liu, H. Guo, B. Lei, G. Meng, Z. Yang, and Z. Feng, "Development of an eco-friendly waterborne polyurethane/catecholamine/ sol-gel composite coating for achieving long-lasting corrosion protection on Mg alloy AZ31," *Prog Org Coat*, vol. 183, 2023. Doi: 10.1016/j.porgcoat.2023.107732.

[113] Y. Li, Y. Zhan, Y. Chen, H. Jia, X. Chen, F. Zhu, and X. Yang, "Waterborne epoxy composite coating with long-term corrosion resistance through synergy of MXene nanosheets and ZnO quantum dots," *Colloids Surf A Physicochem Eng Asp*, vol. 681, pp. 132707, 2024. Doi: 10.1016/j.colsurfa.2023.132707.

[114] M. Thakran and S. Lata, "Polybenzopyrrole/nano-alumina composite blend with zirconium silicate reinforced epoxy as protective coating to subside corrosion of carbon steel within a dilute NaCl solution," *J Mol Struct*, vol. 1298, pp. 137068, 2024. Doi: 10.1016/j.molstruc.2023.137068.

[115] L. Xie, W. Zhou, B. Zhou, S. Bi, P. Zhang, Q. Tian, and Z. Yu, "Exploring salt-mist corrosion resistance of GPTMS functionalized graphene oxide reinforced epoxy resin composite coating on shot-peened Ti-15333 titanium alloy," *Surfaces and Interfaces*, vol. 44, p. 103675, 2024, doi: https://doi.org/10.1016/j.surfin.2023.103675.

[116] W. Chen, Z. Wu, X. He, Y. Su, G. Zheng, S. K. Oh, and C. Mei, "Achieving superior anti-corrosion properties of vinyl ester resin coatings via compositing with 3-methacryloxy propyl trimethoxysilane functionalized MXene nanosheets," *Polym Test*, vol. 127, p. 108203, 2023. Doi: 10.1016/j.polymertesting.2023.108203.

[117] Y. Chen, Y. Zhan, H. Dong, Y. Li, X. Yang, A. Sun, X. Chen, F. Zhu, and H. Jia, "Two-dimensional lamellar MXene nanosheets/waterborne epoxy composite coating: Dopamine triggered surface modification and long-term anticorrosion performance," *Colloids Surf A Physicochem Eng Asp*, vol. 674, p. 131865, 2023. Doi: 10.1016/j.colsurfa.2023.131865.

[118] B. Peng, Z. Yu, H. Chen, K. Liao, Y. Guo, J. Tang, and H. Wen, "Boron nitride and ZIF-67 composite material to improve the long term corrosion resistance of epoxy resin coating," *Diam Relat Mater*, vol. 139, 2023. Doi: 10.1016/j.diamond.2023.110299.

[119] Y. Teng, X. Wei, B. Wu, Y. Liu, N. Fan, Y. Ma, F. Wang, X. Dou, X. Yang, and W. Zhang, "Superhydrophobic and corrosion-resistant of 2-methylimidazolezincsalt-based coating enhanced with silane modification," *Colloids Surf A Physicochem Eng Asp*, vol. 683, p. 132940, 2024. Doi: 10.1016/j.colsurfa.2023.132940.

[120] Y. Liu, F. Meng, F. Wang, and L. Liu, "Dual-action epoxy coating with anti-corrosion and antibacterial properties based on well-dispersed ZnO/basalt composite," *Composites Communications*, vol. 42, 2023. Doi: 10.1016/j.coco.2023.101674.

[121] C. A. Xu, Z. Chu, X. Li, H. Fang, W. Zhou, Y. Hu, X. Chen, and Z. Yang, "Vanillin and organosilicon functionalized graphene oxide modified ester resin composite coatings with excellent anti-corrosion properties," *Prog Org Coat*, vol. 183, 2023. Doi: 10.1016/j.porgcoat.2023.107804.

[122] S. Li, Y. Xu, F. Xiang, P. Liu, H. Wang, W. Wei, and S. Dong, "Enhanced corrosion resistance of self-healing waterborne polyurethane coating based on tannic acid modified cerium-montmorillonites composite fillers," *Prog Org Coat*, vol. 178, pp. 107454, 2023. Doi: 10.1016/j.porgcoat.2023.107454.

[123] S. S. Ashok Kumar, I. A. Wonnie Ma, K. Ramesh, and S. Ramesh, "Development of graphene incorporated acrylic-epoxy composite hybrid anti-corrosion coatings for corrosion protection," *Mater Chem Phys*, vol. 303, pp. 127731, 2023. Doi: 10.1016/j.matchemphys.2023.127731.

[124] J. Zhang, W. G. Lu, H. Yan, Z. B. Zhao, L. Xu, J. H. Ye, and W. Li, "Improvement of wear-resistance and anti-corrosion of waterborne epoxy coating by synergistic modification of glass flake with phytic acid and Zn2+," *Ceram Int*, vol. 49, no. 11, Part A, pp. 17910-17920, 2023. Doi: 10.1016/j.ceramint.2023.02.158.

[125] J. Wei, T. Shen, W. Cao, L. Jiang, Y. He, and W. Li, "Colorable photothermal-induced self-repairing anti-corrosion coating based on confined solid-liquid transition," *J Mater Sci Technol*, 2024. Doi: 10.1016/j.jmst.2024.02.052.

[126] N. Shi, Z. Li, X. Li, H. Luo, J. Jin, S. Dong, and H. Li, "H-BN base triple-functional filler enhances the anti-corrosion performance of epoxy coating," *Polymer (Guildf)*, pp. 126975, 2024. Doi: 10.1016/j.polymer.2024.126975.

[127] C. Xie, P. Zhang, M. Xue, Z. Yin, Y. Luo, Z. Hong, W. Li, and Z. Zhang, "Long-lasting anti-corrosion of superhydrophobic coating by synergistic modification of graphene oxide with polydopamine and cerium oxide," *Constr Build Mater*, vol. 418, pp. 135283, 2024. Doi: 10.1016/j.conbuildmat.2024.135283.

[128] Z. Yang, S. Yu, W. Sun, Z. Xing, W. Gao, L. Wang, X. Nie, W. Li, and G, "High-efficiency graphene/epoxy composite coatings with outstanding thermal conductive and anti-corrosion performance," *Compos Part A Appl Sci Manuf*, vol. 181, pp. 108152, 2024. Doi: 10.1016/j.compositesa.2024.108152.

[129] M. Esmailzadeh, E. Tammari, T. Safarpour, S. M. Razavian, and L. Pezzato, "Anti-corrosion effect of chitin and chitosan nanoparticles in epoxy coatings," *Mater Chem Phys*, vol. 317, pp. 129097, 2024. Doi: 10.1016/j.matchemphys.2024.129097.

[130] G. Khorgami, S. Arash Haddadi, M. Okati, T. H. Mekonnen, and B. Ramezanzadeh, "In situ-polymerized and nano-hybridized Ti3C2-MXene with PDA and Zn-MOF carrying phosphate/glutamate molecules; toward the development of pH-stimuli smart anti-corrosion coating," *Chemical Engineering Journal*, vol. 484, pp. 149630, 2024. Doi: 10.1016/j.cej.2024.149630.

[131] J. Sun, J. Wang, W. Xu, and B. Zhang, "A mechanically robust superhydrophobic corrosion resistant coating with self-healing capability," *Mater Des*, vol. 240, pp. 112881, 2024. Doi: 10.1016/j.matdes.2024.112881.

[132] P. S. Sui, C. B. Liu, A. M. Zhang, C. Sun, L. Y. Cui, and R. C. Zeng, "Superior corrosion resistance and thermal/electro properties of graphene-epoxy composite coating on Mg alloy with biomimetic interface and orientation," *Transactions of Nonferrous Metals Society of China (English Edition)*, vol. 34, no. 1, pp. 157-170, 2024. Doi: 10.1016/S1003-6326(23)66388-5.

[133] V. S. Sumi, S. R. Arunima, M. J. Deepa, M. A. Sha, A. H. Riyas, M. S. Meera, V. S. Saji, and S. M. A. Shibli, "PANI-Fe2O3 composite for enhancement of active life of alkyd resin coating for corrosion protection of steel," *Mater Chem Phys*, vol. 247, pp. 122881, 2020. Doi: 10.1016/j.matchemphys.2020.122881.

[134] G. V. Pham, D. L. Pham, T. D. Nguyen, H. H. Do, K. N. Hui, G. K. Pham, and D. A. Dinh, "Solution blending preparation of polyurethane/graphene composite: Improving the mechanical and anti-corrosive properties of the coating on aluminum surface," *Mater Lett*, vol. 359, pp. 135905, 2024. Doi: 10.1016/j.matlet.2024.135905.

[135] S. S. Ashok Kumar, I. A. Wonnie Ma, K. Ramesh, and S. Ramesh, "The synergistic effects of graphene on the physical, hydrophobic, surface, and thermal properties of acrylic-epoxy-polydimethylsiloxane composite coatings," *Int J Adhes Adhes*, vol. 128, pp. 103546, 2024. Doi: 10.1016/j.ijadhadh.2023.103546.

[136] J. Wang, L. Zhang, and C. Li, "Superhydrophobic and mechanically robust polysiloxane composite coatings containing modified silica nanoparticles and PS-grafted halloysite nanotubes," *Chin J Chem Eng*, vol. 52, pp. 56-65, 2022. Doi: 10.1016/j.cjche.2021.12.017.

[137] H. Salehinasab, R. Majidi, I. Danaee, L. Vrsalović, S. Saliminasab, and D. Zarei, "Engineering a zinc-rich ethyl silicate coating based on nickel oxide nanoparticles for improving anticorrosion performance," *Hybrid Advances*, vol. 5, pp. 100132, 2024. Doi: 10.1016/j.hybadv.2023.100132.

[138] Y. Ouyang, Z. Huang, R. Fang, L. Wu, Q. Yong, and Z.-H. Xie, "Silica nanoparticles enhanced polysiloxane-modified nickel-based coatings on Mg alloy for robust superhydrophobicity and high corrosion resistance," *Surf Coat Technol*, vol. 450, pp. 128995, 2022. Doi: 10.1016/j.surfcoat.2022.128995.

[139] H. Fang, Y. Dai, Z. Lu, Z. Yang, and Y. Wei, "Enhancement of barrier and corrosion protection performance of vinyl ester resin coating via incorporation of MXene nanosheets," *Results in Engineering*, vol. 19, pp. 101330, 2023. Doi: 10.1016/j.rineng.2023.101330.

[140] P. Gong, Y. Li, and G. Zhang, "Enhancing anti-corrosion property of novolac vinyl ester coatings on mild steel through introduction of fluoric acrylic monomer and β-Si3N4 nanoparticles," *Colloids Surf A Physicochem Eng Asp*, vol. 635, p. 128075, 2022. Doi: 10.1016/j.colsurfa.2021.128075.

[141] E. Khamme, A. Sakulkalavek, and R. Sakdanuphab, "Anti-corrosion performance of vinyl ester resin films with titanium dioxide and graphene hybrid reinforcement," *Mater Today Commun*, vol. 33, pp. 104888, 2022. Doi: 10.1016/j.mtcomm.2022.104888.

[142] L. Chen, X. Ni, Y. Shen, Z. Liu, and C. Liu, "Experimental and simulation investigation on hydrophobicity and corrosion resistance of graphene oxide reinforced composite coating," *Appl Surf Sci*, vol. 648, pp. 159072, 2024. Doi: 10.1016/j.apsusc.2023.159072.

[143] S. Zhang, Y. Shen, J. Lu, Z. Chen, L. Li, F. Guo, and W. Shi, "Tannic acid-modified g-C3N4 nanosheets /polydimethylsiloxane as a photothermal-responsive self-healing composite coating for smart corrosion protection," *Chemical Engineering Journal*, vol. 483, pp. 149232, 2024. Doi: 10.1016/j.cej.2024.149232.

[144] Z. Ma, C. Xia, T. Yang, N. Liu, H. Wang, C. Liang, G. Wang, and Q. Li, "Effects of Zr-based and Ni-based amorphous alloy powders on the wear resistance and corrosion behavior of polyurethane composite coatings on aluminum alloys," *Colloids Surf A Physicochem Eng Asp*, vol. 685, pp. 133178, 2024. Doi: 10.1016/j.colsurfa.2024.133178.

[145] W. Pang, H. Jiang, S. Wang, T. He, H. Chen, T. Yan, M. Cheng, S. Sun, and C. Li, "Graphene oxides enhanced polyurethane-based composite coating with long term corrosion resistance and self-healing property," *Eur Polym J*, vol. 207, pp. 112825, 2024. Doi: 10.1016/j.eurpolymj.2024.112825.

[146] V. Kumar, N. K. Arya, A. V. Ullas, and G. Ji, "Coating of epoxy resin and MMT clay nano-composite on copper and examination of their corrosion behaviors in NaCl," *Mater Today Proc*, 2023. Doi: 10.1016/j.matpr.2023.02.172.

[147] J. Wu, G. Ji, and Q. Wu, "Preparation of epoxy/ZrO2 composite coating on the Q235 surface by electrostatic spraying and its corrosion resistance in 3.5% NaCl solution," *RSC Adv*, vol. 12, no. 17, pp. 10625-10633, 2022. Doi: 10.1039/d2ra01220k.

[148] Y. Lei, Z. N. Jiang, X. Q. Zeng, Y. Y. Li, X. Wang, H. F. Liu, and G. A. Zhang, "Preparation of ZIF-67@DTMS NPs/Epoxy composite coating and its anti-corrosion performance for Q235 carbon steel in 3.5 wt.% NaCl solution," *Colloids Surf A Physicochem Eng Asp*, vol. 656, pp. 130370, 2023. Doi: 10.1016/j.colsurfa.2022.130370.

[149] Z. He, H. Lin, X. Zhang, Y. Chen, W. Bai, Y. Lin, R. Jian, and Y. Xu, "Self-healing epoxy composite coating based on polypyrrole@MOF nanoparticles for the long-efficiency corrosion protection on

steels," *Colloids Surf A Physicochem Eng Asp*, vol. 657, pp. 130601, 2023. Doi: 10.1016/j.colsurfa.2022.130601.
[150] S. Duan, X. Lin, B. Dou, H. Yang, Y. Zhang, W. Emori, X. Gao, and Z. Fang, "Triton X-100 assisted composite of fluorinated graphene and ZIF-8 for epoxy coatings with high corrosion and wear resistance on carbon steel," *Prog Org Coat*, vol. 171, pp. 107047, 2022. Doi: 10.1016/j.porgcoat.2022.107047.
[151] L. Zhou, P. Zhang, L. Shen, L. Chu, J. Wu, Y. Ding, B. Zhong, X. Zhang, and N. Bao, "Modified graphene oxide/waterborne epoxy composite coating with enhanced corrosion resistance," *Prog Org Coat*, vol. 172, pp. 107100, 2022. Doi: 10.1016/j.porgcoat.2022.107100.
[152] R. Zou, G. Xiao, C. Chen, C. Chen, Z. Yang, F. Zhong, M. Wang, and Y. Li, "High barrier and durable self-healing composite coating: Boron nitride combined with cyclodextrin for enhancing the corrosion protection properties of waterborne epoxy coating," *Colloids Surf A Physicochem Eng Asp*, vol. 653, pp. 129896, 2022. Doi: 10.1016/j.colsurfa.2022.129896.

Metalurgi (2024) 1: 37 – 48

METALURGI
Majalah Ilmu dan Teknologi
p-ISSN 0126-3188 | e-ISSN 2443-3926
ejurnalmaterialmetalurgi.lipi.go.id

GREEN APPROACHES TO EXTRACTIVE METALLURGY: A NOVEL SYNTHESIS OF SUSTAINABLE PRACTICES

Rahadian Nopriantoko*
Mechanical Engineering, Krisnadwipayana University
Kampus UNKRIS Jatiwaringin, Jakarta, Indonesia 13077
*E-mail: rahadiann@unkris.ac.id

Received: 27-02-2024, Revised: 14-05-2024, Accepted: 22-05-2024

Abstract

The realm of extractive metallurgy, a cornerstone for diverse industrial applications, has traditionally grappled with environmental challenges stemming from conventional extraction methods. This thorough literature review delves into the realm of innovative green approaches within extractive metallurgy, with the overarching goal of synthesizing sustainable practices. The introduction casts a spotlight on the environmental quandaries associated with traditional metallurgical practices, underscoring the imperative for ecologically friendly alternatives. The research methodology meticulously entails a comprehensive review of peer-reviewed literature, applying stringent criteria to handpick studies that delve into sustainable metallurgical practices. The results and discussion section intricately categorizes and dissects an array of green approaches in metal extraction, including bioleaching, ionic liquids, supercritical fluid extraction, green hydrometallurgy, electrochemical methods, and hybrid processes, providing nuanced insights into their efficacy and sustainability. Through the lens of case studies, the study sheds light on recent strides made by industries that have wholeheartedly embraced these sustainable practices, with a keen focus on unraveling their consequential environmental and economic impacts. Moreover, the study conscientiously addresses the challenges encountered in the adoption of green metallurgy and adeptly identifies latent opportunities for further development in this transformative field. The findings resonate with a resounding call for the widespread adoption of sustainable practices within extractive metallurgy, emphasizing their profound implications for both industrial application and the trajectory of future research endeavors. This expanded exploration underscores the pivotal role of environmentally conscious approaches in reshaping the landscape of extractive metallurgy, paving the way for a more sustainable and responsible future.

Keywords: *Green, extraction, metallurgy, eco-friendly, sustainability*

1. INTRODUCTION

The extraction of metals, a crucial process in various industries, has historically relied on methods with significant environmental challenges. Conventional techniques like pyrometallurgy and hydrometallurgy involve hazardous chemicals, high energy consumption, and substantial waste generation, contributing to environmental degradation. The escalating concerns about the ecological footprint of extractive metallurgy have led to a paradigm shift towards green approaches. Green metallurgy, integrating sustainable practices, aims to minimize the environmental impact of metal extraction while remaining economically viable [1].

The primary objective of this study is to systematically explore and evaluate innovative green approaches within the domain of extractive metallurgy. The specific aims are as follows: To assess and delineate the environmental challenges associated with conventional methods of metal extraction, including the ecological impact on soil, water, and air quality. To conduct a comprehensive review of peer-reviewed literature, focusing on recent advancements and emerging practices in green metallurgy. To categorize and analyze various green approaches

DOI : 10.55981/metalurgi.2024.748

Metalurgi is Sinta 2 Journal (https://sinta.kemdikbud.go.id/journals/profile/3708) accredited by Ministry of Education, Culture, Research, and Technology, Republic Indonesia

in metal extraction, evaluating their effectiveness in terms of metal recovery and sustainability in mitigating environmental impact. To present and analyze case studies of industries that have successfully adopted green metallurgical practices, emphasizing both environmental and economic outcomes. To identify and discuss challenges encountered in implementing green approaches and to explore opportunities for further development and optimization of sustainable metallurgical practices. To contribute insights to the academic and industrial communities by synthesizing current knowledge on green approaches in extractive metallurgy, and to propose avenues for future research and innovation in the field. By achieving these objectives, this research aims to provide a comprehensive understanding of the current state of green metallurgy, emphasizing its potential to revolutionize extractive metallurgical practices toward sustainability.

The literature review addresses the environmental drawbacks of traditional extractive metallurgy methods, emphasizing the need for sustainable practices aligned with green energy and thermal engineering principles [2]. It aims to provide valuable insights to both academic and industrial communities by reviewing recent advancements, exploring environmentally friendly approaches, and suggesting future research and innovation opportunities in the field. The conceptual framework is grounded in dimensions such as understanding environmental challenges, embracing green principles, exploring alternative solvents, assessing energy efficiency, considering economic viability, examining case studies, and addressing implementation challenges. Through these dimensions, the study seeks to provide a comprehensive understanding of the current state of green metallurgy and contribute to the development of novel, sustainable practices in extractive metallurgy [3].

2. MATERIALS AND METHODS

The research design involves a systematic literature review to investigate and synthesize green approaches in extractive metallurgy. Key components include a thorough search of databases, inclusion criteria focusing on sustainability, data extraction, quality evaluation, categorization based on themes, and thematic synthesis. The design also includes an in-depth analysis of case studies, considering both environmental and economic perspectives. The findings will be comprehensively discussed, leading to conclusions and implications for industry and future research. The research design prioritizes recent, peer-reviewed literature, diverse methodologies, innovative practices, and a global perspective to compile a reliable body of knowledge on sustainable practices in extractive metallurgy.

A comprehensive discussion of the findings, including the effectiveness and challenges of green approaches in extractive metallurgy. Formulation of conclusions based on the synthesized knowledge, highlighting implications for industry and future research directions. The research design is structured to provide a robust foundation for understanding and evaluating the current landscape of sustainable practices in extractive metallurgy, with a focus on innovative and green methodologies. Inclusion of literature directly related to green approaches in extractive metallurgy, focusing on sustainable practices, environmentally friendly methodologies, and innovations aimed at reducing the ecological footprint of metal extraction.

3. RESULTS AND DISCUSSION

3.1 Eco-Friendly Metal Extraction Methods

The exploration of eco-friendly metal extraction methods represents a pivotal shift in the field of extractive metallurgy, addressing the ecological concerns associated with conventional techniques. Several innovative approaches have emerged, each aiming to minimize environmental impact while ensuring efficient metal recovery.

Bioleaching involves the use of microorganisms to extract metals from ores [4]-[7]. The flow diagrams for bioleaching as shown in Fig. 1, is environmentally friendly as it eliminates the need for harsh chemicals traditionally used in metallurgical processes. Microorganisms, such as bacteria and fungi, catalyze the dissolution of metals, offering a sustainable alternative with lower energy requirements. Bioleaching has proven effective in extracting metals from various ores, especially for low-grade deposits. The use of microbial activity reduces the need for harsh chemicals, making it an eco-friendly alternative. The bioleaching reactors use acidophilic bacteria or fungi that oxidize the mineral sulfides and help solubilize the metals into the leaching solution. This is an environmentally friendly alternative to conventional acid leaching. Bioleaching demonstrates sustainability by promoting the use of natural processes and minimizing the environmental impact associated with traditional leaching methods. However, challenges include

the specificity of microbial strains and the need for optimization in large-scale applications.

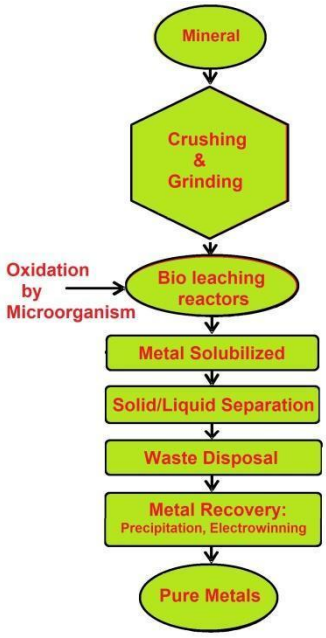

Figure 1. Bioleaching flow diagrams

The use of ionic liquids as alternative solvents in metal extraction has gained prominence [8]-[11], as shown in Fig. 2. Ionic liquids are molten salts at low temperatures and exhibit unique properties, including low volatility and high thermal stability.

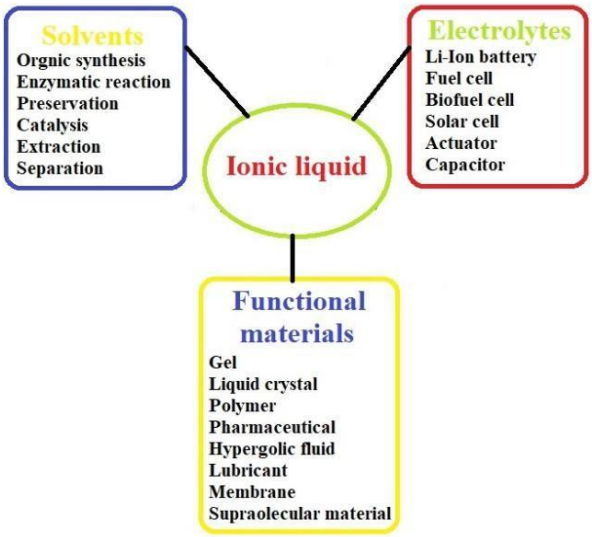

Figure 2. Ionic liquids in metal extraction

Their application in metal extraction reduces the environmental impact associated with conventional solvents, contributing to a greener approach. Ionic liquids exhibit high metal solubility and selectivity, making them effective in extracting metals. Their unique properties contribute to improved efficiency compared to conventional solvents. While ionic liquids offer a greener alternative to traditional solvents, concerns related to toxicity and recyclability need to be addressed. Ongoing research focuses on developing more sustainable ionic liquid formulations.

Supercritical fluid extraction, as shown in Fig. 3, involves the use of supercritical fluids to extract metals from ores. Operating under specific temperature and pressure conditions, supercritical fluids offer enhanced metal selectivity and reduced environmental footprint compared to conventional extraction methods that use organic solvents [12]-[16]. Supercritical fluid extraction enhances metal selectivity and offers advantages in terms of reduced solvent usage. The method is effective for certain metal types and is especially promising for applications requiring high purity. The use of supercritical fluids aligns with green principles, but challenges include high operating pressures and the energy-intensive nature of the process. Continued research aims to improve energy efficiency and reduce environmental impact.

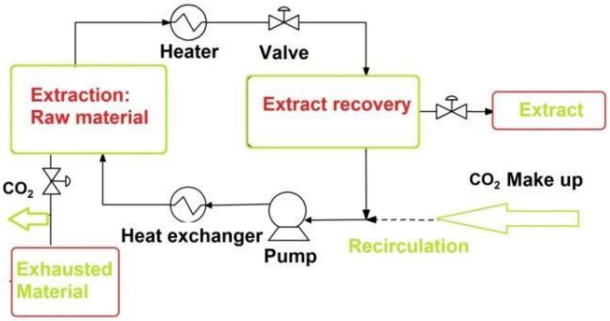

Figure 3. Supercritical extraction

Green hydrometallurgical processes as shown in Fig. 4, utilize environmentally benign leaching agents, such as water and organic acids, to extract metals [17]-[20]. These processes avoid the use of toxic reagents, minimizing environmental contamination in the leaching process uses H_2SO_4 (sulfuric acid) and HCl (hydrochloric acid) as reagents, resulting in the formation of sulfate and chloride salts as separation products. The separation products from using organic acid leachants would typically be metal salts of those organic acids, such as metal citrates or oxalates, rather than metal sulfates or chlorides produced from mineral acids. Additionally, the recovery of valuable metals from electronic waste through hydrometallurgical routes contributes to sustainable resource management. Green hydrometallurgical processes, utilizing benign leaching agents, effectively extract metals from ores and electronic waste. These processes often achieve comparable or improved metal recovery rates. By avoiding toxic reagents,

hydrometallurgical processes contribute to sustainability. However, considerations include the need for process optimization, water usage, and the management of leachate solutions to minimize environmental impact.

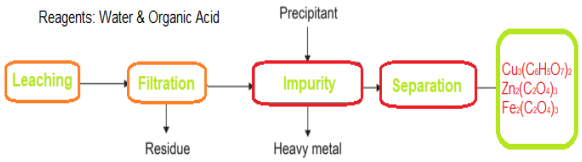

Figure 4. Green hydrometallurgical processes

Electrochemical methods as shown in Fig. 5, such as electro-winning and electro-deposition, provide energy-efficient alternatives for metal recovery [21]-[24]. The electrowinning process involves feeding a metal-bearing solution into an electrowinning cell, where an inert anode and an electrolyte solution facilitate the flow of ions. At the cathode, metal ions from the solution are reduced and plated onto the cathode surface. The plated metal is then periodically stripped from the cathode, yielding pure metal products.

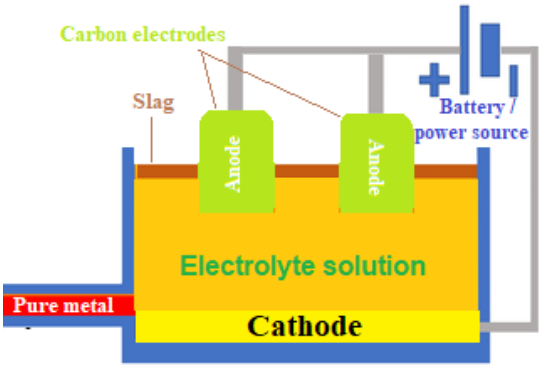

Figure 5. Electrochemical method

These processes often require lower temperatures and can be powered by renewable energy sources, aligning with the principles of green chemistry and reducing the overall carbon footprint of metallurgical operations. Electrochemical methods provide energy-efficient metal recovery with high purity. These methods are effective for certain metals and can be integrated into existing processes. The energy efficiency of electrochemical methods aligns with sustainability goals. However, challenges include the selection of suitable electrode materials and addressing the environmental impact of electrode position waste.

Hybrid processes as shown in Fig. 6 combine multiple environmentally friendly techniques to optimize metal extraction [25]-[28]. For example, integrating bioleaching with ion exchange or coupling ionic liquids with supercritical fluid extraction can enhance metal recovery rates and reduce the overall environmental impact. While these methods exhibit promise in terms of environmental sustainability, their practical implementation faces challenges. Issues such as scalability, economic feasibility, and process optimization need further exploration. However, the reviewed methods collectively represent a paradigm shift toward greener practices in extractive metallurgy, providing a foundation for more sustainable and responsible metal production. Hybrid processes that combine multiple green approaches often lead to improved metal recovery rates and process efficiency. Synergies between different methods contribute to improved overall effectiveness. The sustainability of hybrid processes depends on the specific combination of methods employed. Challenges include optimizing the integration of different processes and addressing potential trade-offs in terms of environmental impact.

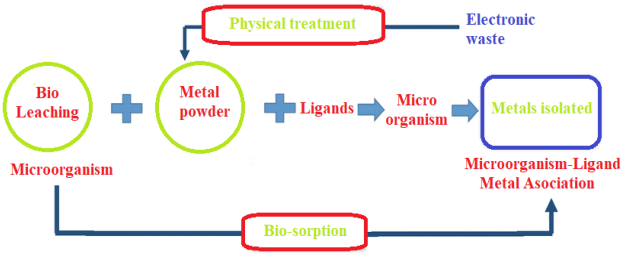

Figure 6. Hybrid processes

Each green metallurgical approach demonstrates varying degrees of effectiveness and sustainability. The choice of method should consider factors such as metal type, ore characteristics, and process scalability. Further research and innovation are essential to address challenges and enhance the overall sustainability of these green approaches in extractive metallurgy.

3.2 Conventional Extraction Processes and Transitioning to Green Extraction Processes

Multitudes of different traditional metal extraction processes have been implemented on an industrial scale. Pyrometallurgy and hydrometallurgy have been most commonly used in industrial-scale metal recovery due to them being effective and well-established. However, these methods are often associated with the use of hazardous reagents, substantial energy consumption and waste generation, and other significant environmental issues.

Pyrometallurgical processes, which involve high-temperature treatment of ores or ore concentrations, are high-energy-consuming and produce large amounts of greenhouse gases. In addition, significant amounts of sulfur dioxide and particulate matter can be emitted into the atmosphere.

While hydrometallurgical processes work with lower temperatures, they often include harmful chemicals such as cyanide, acids, and organic solvents. If not properly managed, such chemicals get into water bodies, negatively impacting human health and the environments. The application of conventional extraction processes also has a detrimental impact on the environment outside the operational stages. The disposal of tailings and waste streams results in soil and water pollution, destruction of habitats, and loss of biodiversity.

To mitigate the environmental impact of metal extraction, a paradigm shift towards green approaches is essential. Green extraction processes prioritize the principles of green chemistry, such as atom economy, waste minimization, and the use of environmentally benign substances. The following sections will discuss various green approaches in metal extraction, highlighting their advantages over conventional processes and providing data to support their environmental and economic benefits.

Energy Efficiency Comparison

One of the key advantages of green extraction processes is their potential for energy savings compared to conventional methods. Figure 7 illustrates a comparison of energy requirements between a conventional pyrometallurgical process and a green bioleaching process for copper extraction. As shown in the figure, the green bioleaching process exhibits significantly lower energy requirements compared to the conventional pyrometallurgical process across various levels of copper extraction [29]. This energy efficiency can translate into reduced greenhouse gas emissions and operational costs, contributing to environmental sustainability and economic viability. It is important to note that the energy savings and environmental benefits of green extraction processes may vary depending on the specific metal, ore characteristics, and process parameters. However, the general trend suggests that green approaches offer a promising avenue for mitigating the environmental impact of metal extraction while maintaining economic feasibility.

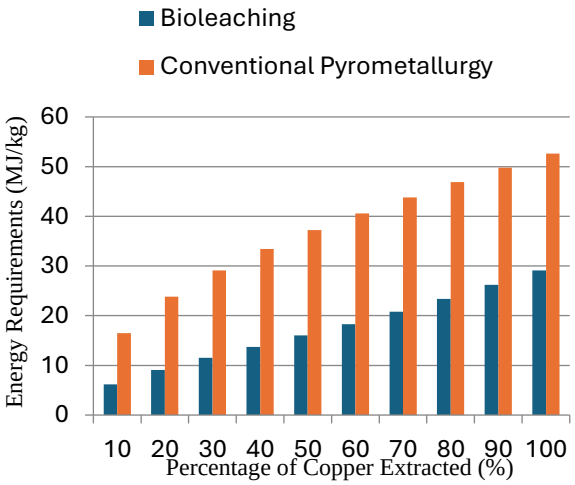

Figure 7. Energy requirements efficiency comparison

In addition to energy efficiency, green extraction processes often involve the use of environmentally benign substances and generate less hazardous waste compared to conventional methods. Table 1 provides a comparison of chemical usage and waste generation between a conventional hydrometallurgical process and a green ionic liquid-based extraction process for the REEs (recovery of rare earth elements). As shown in the table, the green ionic liquid-based extraction process avoids the use of hazardous acids and organic solvents, instead utilizing ionic liquids, which are generally less toxic and can be recycled [30]. Consequently, this green approach generates significantly less hazardous waste compared to the conventional hydrometallurgical process. These examples illustrate the potential advantages of green extraction processes in terms of energy efficiency, chemical usage, and waste minimization. However, it is crucial to conduct comprehensive life cycle assessments and techno-economic analyses to evaluate the overall sustainability and economic viability of these approaches for specific applications.

Table 1. Comparison of chemical usage and waste generation

Process	Chemical usage	Hazardous waste generated
Conventional hydrometallurgy	Acids, organic solvents	High (acidic and organic waste streams)
Green ionic liquid extraction	Ionic liquids	Low (ionic liquids can be recycled)

3.3 Research and Innovation Findings

Recent research in extractive metallurgy emphasizes green approaches for sustainable metal extraction [31], including innovations in alloy production to reduce carbon emissions and closed-loop recycling systems [32]-[33] for efficient metal recovery. Biomimicry-inspired metallurgical processes [34]-[35] and the adoption of circular economy models are gaining traction, emphasizing resource efficiency, waste reduction, and energy-efficient smelting technologies. Urban mining initiatives focus on recovering valuable metals from electronic waste, utilizing advanced separation and extraction technologies to contribute to resource conservation and waste reduction. The development and application of green solvents, such as ionic liquids and bio-based alternatives [36]-[37], mark a significant innovation in replacing environmentally harmful chemicals in metallurgical processes. A holistic approach to sustainability involves engaging with local communities, collaborative efforts, and transparent metallurgical practices [38], [39], demonstrating a paradigm shift towards greener practices. Green metallurgical practices substantially reduce the environmental footprint of metal extraction, contributing to a sustainable resource management model. These practices also lead to cost savings, market competitiveness, and positive stakeholder relations [40]. Implementing green approaches demonstrates social responsibility, positively impacting stakeholder relations, enhancing industry reputation, and fostering long-term partnerships. Green practices contribute to both environmental preservation and economic viability, establishing a resilient foundation for the metallurgical industry.

Advanced research explores nanotechnology applications for more efficient and selective metal extraction, minimizing the need for harmful reagents [41]-[42]. Integration of machine learning algorithms optimizes extractive processes, enhancing efficiency, reducing energy consumption, and improving overall performance. The implementation of sensor technologies enables real-time monitoring, allowing for immediate adjustments to minimize environmental incidents or suboptimal performance. The development of hybrid extraction systems synergistically combines multiple green approaches [43], enhancing metal recovery rates and overall process efficiency. The adoption of cradle-to-cradle design principles focuses on designing fully recyclable products and processes, contributing to a circular economy. Advanced alloy design using 3D printing technologies enables precise control of alloy composition, optimizing mechanical properties with reduced environmental impact. Electrochemical recovery from industrial effluents minimizes waste and efficiently extracts trace metals from dilute solutions.

The application of blockchain technology enhances supply chain transparency, tracking metal sources and providing verifiable information about origin and environmental footprint. Future research may explore advanced nanomaterials, AI and big data analytics for process optimization, closed-loop systems, novel green solvents, expanded electrochemical technologies, enhanced life cycle assessment methodologies, green additives in metallurgical processes, collaborative initiatives for supportive policies, and integration of smart manufacturing principles and Industry 4.0 technologies [44]-[48]. The evolving landscape of extractive metallurgy offers exciting opportunities for future research and technological advancements, aiming for a more sustainable, efficient, and environmentally friendly metallurgical sector.

3.4 Impact, Challenges and Opportunities

The adoption of green approaches in extractive metallurgy positively impacts customer perception, brand differentiation, and market share [49]. Environmentally conscious consumers increasingly value and prefer companies committed to sustainability. Green practices contribute to brand differentiation, providing a competitive edge in a market where sustainability is a key differentiator [50]. Metallurgical companies prioritizing green initiatives stand out, attracting environmentally aware consumers and securing loyalty. Embracing green approaches opens avenues for market expansion and diversification. Companies positioning themselves as leaders in sustainable metallurgy attract a broader consumer base and gain access to markets prioritizing eco-friendly practices.

Adhering to green practices aligns with regulatory standards and certifications, enhancing credibility and consumer trust [51]. Compliance with environmental regulations not only meets legal requirements but also resonates positively with environmentally conscious customers. Green approaches provide opportunities for consumer education and engagement. Transparent communication fosters a sense of shared values, increasing customer loyalty. Ethical and sustainable practices attract

socially responsible investors, improving access to capital for expansion and innovation. Strong sustainability profiles enhance investor confidence. Sustainable marketing involves transparent communication, leveraging certifications, crafting compelling narratives, transparent product labeling, collaborations with environmental organizations, and creating avenues for consumer engagement. Positioning products as premium offerings with enhanced environmental credentials and regularly sharing updates on environmental impact metrics contribute to a transparent marketing strategy. Sustainable practices lead to increased customer trust, loyalty, and advocacy. Customers prefer products or services aligned with their environmental values, contributing to a positive brand perception.

The journey towards green approaches in extractive metallurgy faces challenges such as initial costs, resistance to change, and evolving regulations [52]-[54]. Reliable sourcing of green materials is crucial, and advancements in energy-efficient technologies present significant potential [55]-[57]. Smart sensor networks, biomimicry, sustainable alloy design, and circular economy principles offer opportunities for further development. Overcoming challenges requires collaborative efforts, proactive adaptation to regulations, and addressing uncertainties. Challenges include technological gaps, initial costs, resistance to change, evolving regulations, and sourcing green materials. Scaling up sustainable practices, providing adequate training, managing public perception, and optimizing infrastructure are additional challenges. Overcoming limitations requires collaborative efforts, addressing uncertainties, and aligning with sustainable practices. A successful shift to cyanide-free extraction methods reduced environmental impact and operational costs [58]-[62]. Transition to energy-efficient smelting technologies led to reduced emissions, improved resource efficiency, and economic benefit [63]-[64]. Implementation of closed-loop systems reduced water consumption, minimized environmental impact, and resulted in cost savings. Adoption of sustainable alloy design contributed to market differentiation, premium positioning, increased market share, and brand loyalty. Urban mining initiatives: Recovery of precious metals from electronic waste minimized environmental impact and demonstrated economic viability. These case studies showcase the successful adoption of green metallurgical practices, emphasizing environmental benefits alongside substantial economic gains, providing valuable models for other sectors in the industry.

3.5 Contribution and Future Research Directions

The synthesis of current knowledge on green approaches in extractive metallurgy is valuable for academic and industrial communities, offering insights for widespread implementation. Key contributions include a systematic review that facilitates the identification and adoption of best practices in green metallurgy for academic and industrial stakeholders. Synthesizing knowledge enables a comprehensive environmental impact assessment of green metallurgical practices, influencing policy formulation and corporate strategies [65]-[67]. The nuanced understanding of the economic viability of green practices aids industrial stakeholders and policymakers in making informed decisions and conducting cost-benefit analyses. The synthesis serves as a platform for technology transfer and collaboration between academia and industry, fostering a smoother transition toward green approaches. Consolidated knowledge forms the foundation for developing educational resources and training programs, enriching curricula, and preparing future metallurgists for sustainable practices.

Looking ahead, future research and innovation should concentrate on developing eco-friendly alternatives to improve extraction efficiency while minimizing the environmental impact. Researching ways to further minimize waste, promote recycling, and extend the life cycle of materials for improved resource efficiency [68]-[69]. Exploring how artificial intelligence and machine learning can enhance process control, predictive maintenance, and overall operational efficiency. Delving into biomimicry to develop sustainable extraction methods, materials, and processes inspired by the efficiency of ecosystems. Conducting comprehensive assessments to understand the full environmental impact of metallurgical processes and improve supply chain resilience. Prioritizing research on efficient and scalable methods for extracting valuable metals from electronic devices, reducing the demand for traditional mining [70]-[72]. Encouraging collaboration between metallurgy, chemistry, environmental science, and engineering for holistic solutions. Investigating the social impact of green metallurgical practices on local communities, including community perceptions and engagement strategies. The synthesis provides a foundation for future advancements, allowing

academic and industrial communities to collectively contribute to the evolution of sustainable practices in the metallurgical industry.

Future research could explore collaborative initiatives between industries and governments to create supportive policies for sustainable practices. This involves establishing frameworks for incentive programs, regulatory standards, and industry certifications that promote and reward environmentally responsible metallurgical practices. Integration of smart manufacturing principles and Industry 4.0 technologies can further optimize the efficiency of metallurgical operations. IoT (Internet of Things) devices, sensors, and real-time data analytics can be employed to enhance process monitoring, control, and overall resource management. Conducting comprehensive techno-economic analyses can provide valuable insights into the economic feasibility of green practices. Future research may refine and expand these analyses to include a broader range of factors, such as market dynamics, policy impacts, and societal benefits. These potential future research directions and technological developments hold the promise of advancing the field of green approaches in extractive metallurgy. By exploring these avenues, researchers and industry stakeholders can contribute to the ongoing transformation of metallurgical practices toward greater sustainability.

4. CONCLUSION

The exploration of green approaches in extractive metallurgy signifies a transformative shift towards sustainability and environmental responsibility. The synthesis of current knowledge and case studies highlights progress, challenges, and innovation within the metallurgical industry, leading to several key conclusions. The review shows a notable industry shift towards sustainability, with practices evolving to minimize environmental impact and promote responsible resource management, including eco-friendly extraction methods and circular economy integration. Successful case studies demonstrate the feasibility of balancing environmental stewardship with economic viability. Industries adopting green practices achieve cost savings, improved efficiency, and enhanced market competitiveness. The synthesis emphasizes the importance of integrating both environmental and economic considerations in the pursuit of sustainability. Challenges in implementing green approaches, such as technological barriers and resistance to change, are acknowledged as catalysts for innovation. Collaboration, technological advancements, and strategic management are identified as means to overcome these challenges. The synthesis highlights the resilience of the metallurgical sector in navigating obstacles and driving positive change.

While significant strides have been made, the synthesis underscores the need for continued research and collaboration. Future exploration areas include advanced green solvents, digital technologies, and nature-inspired design. Cross-disciplinary collaboration, community engagement, and a focus on social impact emerge as crucial elements in steering the metallurgical industry towards a sustainable future. The progress, challenges, and untapped potential in green extractive metallurgy contribute to academic understanding and offer actionable insights for industry stakeholders. As the metallurgical sector embraces green approaches, the synthesis serves as a call to action for ongoing research, innovation, and collaborative efforts to ensure a harmonious coexistence between industrial processes and environmental preservation.

ACKNOWLEDGMENT

The author would like to express gratitude to the family and institutions for supporting this work.

REFERENCES

[1] R. Pell, L Tijsseling, K. Goodenough, "Towards sustainable extraction of technology materials through integrated approaches," *Nat. Rev. Earth Environ.*, vol. 2, no. 10, pp. 665-679, 2021. Doi: 10.1038/s43017-021-00211-6.

[2] R. Nopriantoko, *Rekayasa Sistem Termal dan Energi*. CV Jejak (Jejak Publisher), 2024.

[3] G. Chauhan, P. R. Jadhao, K. K. Pant, and K. D. P. Nigam, "Novel technologies and conventional processes for recovery of metals from waste electrical and electronic equipment: challenges & opportunities-a review," *J. Environ. Chem. Eng.*, vol. 6, no. 1, pp. 1288-1304, 2018. Doi:10.1016/j.jece.2018.01.032.

[4] W. Sajjad, G. Zheng, G. Din, X. Ma, M. Rafiq, and W. Xu, "Metals extraction from sulfide ores with microorganisms: the bioleaching technology and recent developments," *Trans. Indian Inst. Met.*, vol. 72, pp. 559-579, 2019. Doi: 10.1007/s12666-018-1516-4.

[5] C. L. Brierley and J. A. Brierley,

"Progress in bioleaching: part B: applications of microbial processes by the minerals industries," *Appl. Microbiol. Biotechnol.*, vol. 97, no. 17, pp. 7543-7552, 2013. Doi: 10.1007/s00253-013-5095-3.

[6] D. B. Johnson, "Biomining-biotechnologies for extracting and recovering metals from ores and waste materials," *Curr. Opin. Biotechnol.*, vol. 30, pp. 24-31, 2014. Doi: 10.1016/j.copbio.2014.04.008.

[7] S. Mahajan, A. Gupta, and R. Sharma, "Bioleaching and biomining," *Princ. Appl. Environ. Biotechnol. a Sustain. Futur.*, pp. 393-423, 2017. Doi: 10.1007/978-981-10-1866-4_13.

[8] M. R. Asrami, N. N. Tran, K. D. P. Nigam, and V. Hessel, "Solvent extraction of metals: role of ionic liquids and microfluidics," *Sep. Purif. Technol.*, vol. 262, pp. 118289, 2021. Doi: 10.1016/j.seppur.2020.118289.

[9] S. Prusty, S. Pradhan, and S. Mishra, "Ionic liquid as an emerging alternative for the separation and recovery of Nd, Sm, and Eu using solvent extraction technique-A review," *Sustain. Chem. Pharm.*, vol. 21, pp. 100434, 2021. Doi: 10.1016/j.scp.2021.100434.

[10] A. J. Greer, J. Jacquemin, and C. Hardacre, "Industrial applications of ionic liquids," *Molecules*, vol. 25, no. 21, pp. 5207, 2020. Doi: 10.3390/molecules25215207.

[11] W. Vereycken, S. Riaño, T. Van Gerven, and K. Binnemans, "Extraction behavior and separation of precious and base metals from chloride, bromide, and iodide media using undiluted halide ionic liquids," *ACS Sustain. Chem. Eng.*, vol. 8, no. 22, pp. 8223-8234, 2020. Doi: 10.1021/acssuschemeng.0c01181.

[12] F. Lin, D. Liu, S. Maiti Das, N. Prempeh, Y. Hua, and J. Lu, "Recent progress in heavy metal extraction by supercritical CO2 fluids," *Ind. Eng. Chem. Res.*, vol. 53, no. 5, pp. 1866-1877, 2014. Doi: 10.1021/ie4035708.

[13] S. M. Fayaz, M. A. Abdoli, M. Baghdadi, and A. Karbasi, "Ag removal from e-waste using supercritical fluid: improving efficiency and selectivity," *Int. J. Environ. Stud.*, vol. 78, no. 3, pp. 459-473, 2021. Doi: 10.1080/00207233.2020.1834305.

[14] Ž. Knez, M. Pantić, D. Cör, Z. Novak, and M. K. Hrnčič, "Are supercritical fluids solvents for the future?," *Chem. Eng. Process. Intensif.*, vol. 141, pp. 107532, 2019. Doi: 10.1016/j.cep.2019.107532.

[15] J. Torzewski, K. Grzelak, M. Wachowski, and R. Kosturek, "Microstructure and low cycle fatigue properties of AA5083 H111 friction stir welded joint," *Materials (Basel).*, vol. 13, no. 10, pp. 2381, 2020. Doi: 10.3390/ma13102381.

[16] J. Płotka-Wasylka, M. Rutkowska, K. Owczarek, M. Tobiszewski, and J. Namieśnik, "Extraction with environmentally friendly solvents," *TrAC Trends Anal. Chem.*, vol. 91, pp. 12-25, 2017. Doi: 10.1016/j.trac.2017.03.006.

[17] Y. Yao, M. Zhu, Z. Zhao, B. Tong, Y. Fan, and Z. Hua, "Hydrometallurgical processes for recycling spent lithium-ion batteries: a critical review," *ACS Sustain. Chem. Eng.*, vol. 6, no. 11, pp. 13611-13627, 2018. Doi: 10.1021/acssuschemeng.8b03545.

[18] M. N. Le and M. S. Lee, "A review on hydrometallurgical processes for the recovery of valuable metals from spent catalysts and life cycle analysis perspective," *Miner. Process. Extr. Metall. Rev.*, vol. 42, no. 5, pp. 335-354, 2021. Doi: 10.1080/08827508.2020.1726914.

[19] X. Li, Q. Gao, S. Jiang, C. Nie, X. Zhu, and T. Jiao, "Review on the gentle hydrometallurgical treatment of WPCBs: Sustainable and selective gradient process for multiple valuable metals recovery," *J. Environ. Manage.*, vol. 348, pp. 119288, 2023. Doi: 10.1016/j.jenvman.2023.119288.

[20] V. Gunarathne, A. U. Rajapaksha, M. Vithanage, D. Alessi, R. Selvasembian, M. Naushad, "Hydrometallurgical processes for heavy metals recovery from industrial sludges," *Crit. Rev. Environ. Sci. Technol.*, vol. 52, no. 6, pp. 1022-1062, 2022. Doi: 10.1080/10643389.2020.1847949.

[21] Y. Xue and Y. Wang, "Green electrochemical redox mediation for valuable metal extraction and recycling from industrial waste," *Green Chem.*, vol. 22, no. 19, pp. 6288-6309, 2020. Doi: 10.1039/D0GC02028A.

[22] H. Wang, Z. Lei, X. Zhang, B. Zhou, and J. Peng, "A review of deep learning for renewable energy forecasting," *Energy Convers. Manag.*, vol. 198, pp. 111799, 2019. Doi:

10.1016/j.enconman.2019.111799.
[23] L. Yang, W. Hu, Z. Chang, Tian L., D. Fang, P. Shao, H. Shi, X. Luo, "Electrochemical recovery and high value-added reutilization of heavy metal ions from wastewater: Recent advances and future trends," *Environ. Int.*, vol. 152, pp. 106512, 2021. Doi: 10.1016/j.envint.2021.106512.
[24] Y. Li, S. Liu, Y. Ming Chen, "Electro-deposition behavior in methanesulfonic-acid-based lead electro-refining," *J. Sustain. Metall.*, vol. 7, pp. 1910-1916, 2021. Doi: 10.1007/s40831-021-00467-8.
[25] D. Pant, D. Joshi, M. K. Upreti, and R. K. Kotnala, "Chemical and biological extraction of metals present in E-waste: a hybrid technology," *Waste Manag.*, vol. 32, no. 5, pp. 979-990, 2012. Doi: 10.1016/j.wasman.2011.12.002.
[26] S. Frioui, R. Oumeddour, and S. Lacour, "Highly selective extraction of metal ions from dilute solutions by hybrid electrodialysis technology," *Sep. Purif. Technol.*, vol. 174, pp. 264-274, 2017. Doi: 10.1016/j.seppur.2016.10.028.
[27] S. Radi, Y. Toubi, M. El-Massaoudi, M. Bacquet, S. Degoutin, and Y. N. Mabkhot, "Efficient extraction of heavy metals from aqueous solution by novel hybrid material based on silica particles bearing new Schiff base receptor," *J. Mol. Liq.*, vol. 223, pp. 112-118, 2016. Doi: 10.1016/j.molliq.2016.08.024.
[28] C. Lin, S. Lirio, Y. Chen, C. Lin, and H. Huang, "A novel hybrid metal-organic framework-polymeric monolith for solid-phase microextraction," *Chem. Eur. J.*, vol. 20, no. 12, pp. 3317-3321, 2014. Doi: 10.1002/chem.201304458.
[29] H. R. Watling, "The bioleaching of sulfide minerals with emphasis on copper sulfides-a review," *Hydrometallurgy*, vol. 84, no. 1-2, pp. 81-108, 2006. Doi: 10.1016/j.hydromet.2006.05.001.
[30] Z. Zhu, Y. Pranolo, and C. Y. Cheng, "Separation of uranium and thorium from rare earth for rare earth production - A review," *Miner. Eng.*, vol. 77, pp. 185-196, 2015. Doi: 10.1016/j.mineng.2015.03.012.
[31] K. Binnemans and P. T. Jones, "Ionic liquids and deep-eutectic solvents in extractive metallurgy: Mismatch between academic research and industrial applicability," *J. Sustain. Metall.*, vol. 9, no. 2, pp. 423-438, 2023. Doi: 10.1007/s40831-023-00681-6.
[32] A. Gupta and B. Basu, "Sustainable primary aluminum production: technology status and future opportunities," *Trans. Indian Inst. Met.*, vol. 72, pp. 2135-2150, 2019. Doi: 10.1007/s12666-019-01699-9.
[33] S. Gupta, K. K. Pant, and G. Corder, "An environmentally benign closed-loop process for the selective recovery of valuable metals from industrial end-of-life lithium-ion batteries," *Chem. Eng. J.*, vol. 446, pp. 137397, 2022. Doi: 10.1016/j.cej.2022.137397.
[34] S. Santosa, P. Livotov, A. P. Chandra Sekaran, and L. Rubianto, "Nature-Inspired Principles for Sustainable Process Design in Chemical Engineering," in *Creative Solutions for a Sustainable Development: 21st International TRIZ Future Conference, TFC 2021, Bolzano, Italy, Proceedings 21*, Springer, pp. 30-41, 2021. Doi: 10.1007/978-3-030-86614-3_3.
[35] B. Zhang, H. Gao, X. Tong, S. Liu, L. Gan, and Y. Chen, "Pressure retarded osmosis and reverse electrodialysis as power generation membrane systems," in *Current Trends and Future Developments on (Bio-) Membranes*, Elsevier, 2019, pp. 133-152. Doi: 10.1016/B978-0-12-813545-7.00006-4.
[36] J. Cao and E. Su, "Hydrophobic deep eutectic solvents: The new generation of green solvents for diversified and colorful applications in green chemistry," *J. Clean. Prod.*, vol. 314, pp. 127965, 2021. Doi: 10.1016/j.jclepro.2021.127965.
[37] L. Lajoie, A.-S. Fabiano-Tixier, and F. Chemat, "Water as green solvent: methods of solubilization and extraction of natural products-past, present and future solutions," *Pharmaceuticals*, vol. 15, no. 12, pp. 1507, 2022. Doi: 10.3390/ph15121507.
[38] A. Ivanković, A. Dronjić, A. M. Bevanda, and S. Talić, "Review of 12 principles of green chemistry in practice," *Int. J. Sustain. Green Energy*, vol. 6, no. 3, pp. 39-48, 2017. Doi: 10.11648/j.ijrse.20170603.12.
[39] L. Mammino, "Green chemistry: Chemistry working for sustainability," in *Green Chemistry and Computational Chemistry*, Elsevier, 2022, pp. 41-54. Doi: 10.1016/B978-0-12-819879-7.00011-8.
[40] B. Bridgens, K. Hobson, D. Lilley, J. Lee,

J. L. Scott, and G. T. Wilson, "Closing the loop on E-waste: A multidisciplinary perspective," *J. Ind. Ecol.*, vol. 23, no. 1, pp. 169-181, 2019. Doi: 10.1111/jiec.12645.

[41] A. Pugazhendhi, S. Shobana, D. Nguyen, R. Banu, P. Siva, S. W. Chang, V. Kumar, G. Kumar, "Application of nanotechnology (nanoparticles) in dark fermentative hydrogen production," *Int. J. Hydrogen Energy*, vol. 44, no. 3, pp. 1431-1440, 2019. Doi: 10.1016/j.ijhydene.2018.11.114.

[42] P. Kasinathan, R. Pugaz, R. M. Elasavaran, V. K. Ramachandara, V. Ramanathan, S. Subram, S. Kumar, K. Nandaghopai, R. Vijaya, Sankar R. R. Devandiran, M. Alsharif, "Realization of sustainable development goals with disruptive technologies by integrating industry 5.0, society 5.0, smart cities and villages," *Sustainability*, vol. 14, no. 22, pp. 15258, 2022. Doi: 10.3390/su142215258.

[43] W. Yu, W. Peng, Y. Shu, Q. Zeng, and M. Jiang, "Experimental evidence extraction system in data science with hybrid table features and ensemble learning," in *Proceedings of The Web Conference 2020*, pp. 951-961, 2020. Doi: 10.1145/3366423.3380174.

[44] M. Wu, W. Cao, X. Chen, and J. She, *Intelligent optimization and control of complex metallurgical processes*, vol. 3. Springer, 2020. Doi: 10.1007/978-981-15-1145-5.

[45] T. Verevka, A. Mirolyubov, and J. Makio, "Opportunities and barriers to using big data technologies in the metallurgical industry," in *International Scientific Conference on Innovations in Digital Economy*, Springer, 2020, pp. 86-102. Doi: 10.1007/978-3-030-84845-3_6.

[46] M. A. Camilleri, "The circular economy's closed loop and product service systems for sustainable development: A review and appraisal," *Sustain. Dev.*, vol. 27, no. 3, pp. 530-536, 2019. Doi: 10.1002/sd.1909.

[47] S. H. Farjana, N. Huda, M. A. P. Mahmud, and R. Saidur, "A review on the impact of mining and mineral processing industries through life cycle assessment," *J. Clean. Prod.*, vol. 231, pp. 1200-1217, 2019. Doi: 10.1016/j.jclepro.2019.05.264.

[48] H. Liu, Q. Li, G. Li, and R. Ding, "Life cycle assessment of the environmental impact of the steelmaking process," *Complexity*, vol. 2020, 2020. Doi: 10.1155/2020/8863941.

[49] M. Hofmann, H. Hofmann, C. Hagelüken, and A. Hool, "Critical raw materials: A perspective from the materials science community," *Sustain. Mater. Technol.*, vol. 17, p. e00074, 2018. Doi: 10.1016/j.susmat.2018.e00074.

[50] M. Trippl, S. Baumgartinger-Seiringer, A. Frangenheim, A. Isaksen, and J. O. Rypestøl, "Unravelling green regional industrial path development: Regional preconditions, asset modification, and agency," *Geoforum*, vol. 111, pp. 189-197, 2020. Doi: 10.1016/j.geoforum.2020.02.016.

[51] J. Rybak, A. Adigamov, C. Kongar-Syuryun, M. Khayrutdinov, and Y. Tyulyaeva, "Renewable-resource technologies in mining and metallurgical enterprises providing environmental safety," *Minerals*, vol. 11, no. 10, p. 1145, 2021. Doi: 10.3390/min11101145.

[52] N. Mariotti, "Recent advances in eco-friendly and cost-effective materials towards sustainable dye-sensitized solar cells," *Green Chem.*, vol. 22, no. 21, pp. 7168–7218, 2020. Doi: 10.1039/D0GC01148G.

[53] K. Moustakas, M. Loizidou, M. Rehan, and A. S. Nizami, "A review of recent developments in renewable and sustainable energy systems: Key challenges and future perspective," *Renewable and Sustainable Energy Reviews*, vol. 119. Elsevier, pp. 109418, 2020. Doi: 10.1016/j.rser.2019.109418.

[54] S. S. de Jesus and R. Maciel Filho, "Are ionic liquids eco-friendly?" *Renew. Sustain. Energy Rev.*, vol. 157, pp. 112039, 2022. Doi: 10.1016/j.rser.2021.112039.

[55] C. D. Hills, N. Tripathi, and P. J. Carey, "Mineralization technology for carbon capture, utilization, and storage," *Front. Energy Res.*, vol. 8, pp. 142, 2020. Doi: 10.3389/fenrg.2020.00142.

[56] P. Cavaliere and P. Cavaliere, "Carbon capture and storage: Most efficient technologies for greenhouse emissions abatement," *Clean Ironmak. Steelmak. Process. Effic. Technol. Green. Emiss. Abat.*, pp. 485-553, 2019. Doi: 10.1007/978-3-030-21209-4_9.

[57] M. Gautam, B. Pandey, and M. Agrawal, "Carbon footprint of aluminum

production: emissions and mitigation," in *Environmental carbon footprints*, Elsevier, 2018, pp. 197-228. Doi: 10.1016/B978-0-12-812849-7.00008-8.

[58] A. N. Manzila, T. Moyo, and J. Petersen, "A study on the applicability of Agitated cyanide leaching and thiosulphate leaching for gold extraction in artisanal and small-scale gold mining," *Minerals*, vol. 12, no. 10, pp. 1291, 2022. Doi: 10.3390/min12101291.

[59] J. McNeice, H. Mahandra, and A. Ghahreman, "Application of biogenic thiosulfate produced by methylophaga sulfidovorans for sustainable gold extraction," *ACS Sustain. Chem. Eng.*, vol. 10, no. 30, pp. 10034–10046, 2022. Doi: 10.1021/acssuschemeng.2c02872.

[60] M. Soleymani Naeini, "Electrochemical study of gold thiosulfate extraction process." Queen University Thesis, 2022.

[61] P. Torkaman, "Study of unconventional techniques to eliminate mercury use from artisanal gold mining operations." University of British Columbia, 2023.

[62] E. Jorjani and H. A. Sabzkoohi, "Gold leaching from ores using biogenic lixiviants: A review," *Curr. Res. Biotechnol.*, vol. 4, pp. 10-20, 2022. Doi: 10.1016/j.crbiot.2021.12.003.

[63] A. P. Ratvik, R. Mollaabbasi, and H. Alamdari, "Aluminium production process: from Hall–Héroult to modern smelters," *ChemTexts*, vol. 8, no. 2, p. 10, 2022. Doi: 10.1007/s40828-022-00162-5.

[64] Y. He, K. Zhou, Y. Zhang, H. Xiong, and L. Zhang, "Recent progress of inert anodes for carbon-free aluminum electrolysis: a review and outlook," *J. Mater. Chem. A*, vol. 9, no. 45, pp. 25272-25285, 2021. Doi: 10.1039/D1TA07198J.

[65] W. Wu, S. An, C.-H. Wu, S.-B. Tsai, and K. Yang, "An empirical study on green environmental system certification affects financing cost of high energy consumption enterprises-taking metallurgical enterprises as an example," *J. Clean. Prod.*, vol. 244, pp. 118848, 2020. Doi: 10.1016/j.jclepro.2019.118848.

[66] E. Matinde, G. S. Simate, and S. Ndlovu, "Mining and metallurgical wastes: a review of recycling and re-use practices," *J. South. African Inst. Min. Metall.*, vol. 118, no. 8, pp. 825-844, 2018. Doi: 10.17159/2411-9717/2018/v118n8a5.

[67] B. Debnath, R. Chowdhury, and S. K. Ghosh, "Sustainability of metal recovery from E-waste," *Front. Environ. Sci. Eng.*, vol. 12, pp. 1-12, 2018. Doi: 10.1007/s11783-018-1044-9.

[68] L. A. Cisternas, J. I. Ordóñez, R. I. Jeldres, and R. Serna-Guerrero, "Toward the implementation of circular economy strategies: An overview of the current situation in mineral processing," *Miner. Process. Extr. Metall. Rev.*, vol. 43, no. 6, pp. 775-797, 2022. Doi: 10.1080/08827508.2021.1946690.

[69] L. Holappa, M. Kekkonen, A. Jokilaakso, and J. Koskinen, "A review of circular economy prospects for stainless steelmaking slags," *J. Sustain. Metall.*, vol. 7, no. 3, pp. 806-817, 2021. Doi: 10.1007/s40831-021-00392-w.

[70] L. H. Xavier, M. Ottoni, and L. P. P. Abreu, "A comprehensive review of urban mining and the value recovery from e-waste materials," *Resour. Conserv. Recycl.*, vol. 190, pp. 106840, 2023. Doi: 10.1016/j.resconrec.2022.106840.

[71] A. Lukowiak, L. Zur, R. Tomala, T. N. Lamtran, A. Bouajaj, W. Strek, G. C. Righini, M. Wickleder, M. Ferrari, "Rare earth elements and urban mines: Critical strategies for sustainable development," *Ceram. Int.*, vol. 46, no. 16, pp. 26247-26250, 2020. Doi: 10.1016/j.ceramint.2020.03.067.

[72] A. P. Paiva and C. A. Nogueira, "Ionic liquids in the extraction and recycling of critical metals from urban mines," *Waste and Biomass Valorization*, vol. 12, pp. 1725-1747, 2021. Doi: 10.1007/s12649-020-01115-0.

Metalurgi (2024) 1: 49 - 62

METALURGI
Majalah Ilmu dan Teknologi
p-ISSN 0126-3188 | e-ISSN 2443-3926
ejurnalmaterialmetalurgi.lipi.go.id

MICROSTRUCTURAL STABILITY AND HIGH-TEMPERATURE OXIDATION BEHAVIOR OF $Al_{0.25}$CoCrCuFeNi HIGH ENTROPY ALLOY

Fadhli Muhammad[a,*], Ernyta Mei Lestari[a], Tria Laksana Achmad[a], Akhmad Ardian Korda[a], Budi Prawara[b], Djoko Hadi Prajitno[c], Bagus Hayatul Jihad[d], Muhamad Hananuputra Setianto[d], and Eddy Agus Basuki[a]

[a]Department of Metallurgical Engineering, Institut Teknologi Bandung
Jl. Ganesha No. 10, Bandung, Indonesia 40132
[b]Research Centre for Advanced Materials, National Research and Innovation Agency
Jl. Sangkuriang, Bandung, Indonesia 40135
[c]Research Organization for Nuclear Technology, National Research and Innovation Agency
Jl. Tamansari No. 71, Bandung, Indonesia 40132
[d]Research Center for Rocket Technology, National Research and Innovation Agency
Jalan Raya Lapan, Parungpanjang, Kabupaten Bogor, Indonesia 16350
*E-mail: fadhlim_08@itb.ac.id

Received: 26-01-2024, Revised: 23-08-2024, Accepted: 12-09-2024

Abstract

$Al_{0.25}$CoCrCuFeNi is a high-entropy alloy composed of transition metals, specifically designed for high-temperature applications owing to its favorable mechanical properties, high melting point, and excellent high-temperature resistance. This alloy has been identified as a promising material for space exploration, particularly in the fabrication of combustion chambers and rocket nozzles by the National Aeronautics and Space Agency. Ongoing alloy development involves modifying the elemental composition. This study reduced aluminum content in the equiatomic AlCoCrCuFeNi alloy to $Al_{0.25}$CoCrCuFeNi, followed by isothermal oxidation treatments at 800, 900, and 1000°C. A series of experiments were conducted to investigate the microstructure stability and oxidation behavior of the $Al_{0.25}$CoCrCuFeNi alloy. The alloying elements were melted using a single DC electric arc furnace, followed by homogenization at 1100°C for 10 hours in an inert atmosphere. Subsequently, samples were cut into coupons for isothermal oxidation testing at the desired temperatures for 2, 16, 40, and 168 hours. The oxidized samples were characterized using XRD (x-ray diffraction), SEM (scanning electron microscopy) equipped with EDS (energy-dispersive X-ray spectroscopy), optical microscopy, and Vickers hardness testing. The as-homogenized alloy consisted of two constituent phases: an FCC (face-centered cubic) phase in the dendritic region and a copper-rich FCC phase in the inter-dendritic region. The oxides formed during the oxidation process included Al_2O_3, Cr_2O_3, Fe_3O_4, CoO, CuO, NiO, and spinel oxides $(Co, Ni, Cu)(Al, Cr, Fe)_2O_4$), with distinct formation mechanisms at each temperature.

Keywords: *High-entropy alloy, isothermal oxidation, FCC structure, high temperature, phase stability*

1. INTRODUCTION

Equipment and machinery employed in high-temperature applications, including rocket nozzles, nuclear reactor piping systems, aircraft and power plant gas turbine blades, power plant boilers, steam turbines, and combustion engine exhaust facilities, necessitate materials capable of enduring elevated temperatures. These components demand properties essential for operation in environments characterized by high temperatures, stresses, pressures, and exposure to oxidative and corrosive conditions.

Nickel-based superalloys were traditionally considered the most suitable materials for high-temperature applications [1]-[3]. However, these alloys have now reached their operational temperature limits. A γ'-Ni_3Al is an ordered, coherent precipitate that significantly strengthens nickel-based superalloys. When the temperature exceeds their γ-NiAl/γ'-Ni_3Al equilibrium solvus temperature, complete dissolution of the γ'

DOI : 10.55981/metalurgi.2024.745

Metalurgi is Sinta 2 Journal (https://sinta.kemdikbud.go.id/journals/profile/3708) accredited by Ministry of Education, Culture, Research, and Technology, Republic Indonesia

precipitate occurs, leading to a relatively weak γ solid solution matrix [4]-[5].

Among numerous potential materials, HEAs (high entropy alloys) offer a promising solution to the challenge of balancing high-temperature strength with oxidation and corrosion resistance. HEAs differ from conventional alloys by having equal molar concentrations of each constituent element [6]. These alloys exhibit four primary effects: high entropy, lattice distortion, sluggish diffusion, and the cocktail effect. The cocktail effect allows for tailoring alloy properties through adjustments in elemental composition [7].

HEAs also referred to as multi-component alloys, have been developed specifically for high-temperature applications. This category includes refractory high entropy alloys (RHEAs) and transition metal high entropy alloys (TM-HEAs). RHEAs, such as VNbMoTaW, MoNbTaW, and CrMoTaNb, are renowned for their exceptional mechanical properties [8]. However, they can be brittle and costly due to the use of refractory elements. TM-HEAs are composed of more affordable elements, including Fe, Al, Co, Ni, Cu, Ti, and Cr [9]. Some elements, such as FeNi, Cu, and Al, have also been produced in Indonesia.
HEA composed of transition metals, such as AlCoCrFeNi, AlCoCrCuFeNi, and CoCrFeNiTi [6], have been extensively studied. Lu et al. [10] observed that a decreased diffusion rate of aluminum in AlCoCrFeNi alloys leads to a lower oxidation rate, thereby improving their oxidation resistance. Butler et al. [11]-[12] evaluated the influence of aluminum content on the oxidation behavior of as-cast AlxCoCrFeNi at 1050°C. They determined that alloys with relatively low aluminum levels developed discontinuous chromium oxide (Cr2O3) layers on the outer surface and internal aluminum oxide (Al_2O_3) scales. Conversely, alloys with higher aluminum concentrations developed a continuous Al_2O_3 layer. However, due to its high aluminum content, the equiatomic AlCoCrCuFeNi often exhibits brittle behavior. The study sought to reduce the aluminum content of the equiatomic AlCoCrCuFeNialloy to $Al_{0.25}$CoCrCuFeNi. The objective was to evaluate the impact of this reduction on the alloy's isothermal oxidation resistance, microstructure stability, and hardness.

2. MATERIALS AND METHODS

A vacuum arc furnace produced the high entropy alloy with a nominal composition of Al0.25CoCrCuFeNi under an argon atmosphere on a water-cooled copper mold. The purity of each element metal was more than 99.7 wt.%. The ingots were flipped and re-melted at least five times to ensure the homogeneous composition obtained. The homogenization was further carried out using a horizontal tube furnace under an argon atmosphere with a flow of 10 mL/min for 10 h at 1100 °C. Specimens with dimensions of approximately 7.5 mm x 4 mm x 2 mm were extracted from the ingots for the oxidation test. The specimens were oxidized at 800, 900, and 1000 °C in laboratory air, with 2, 16, and 40 h exposure times for each temperature. An extended oxidation test for 168 h was conducted at 1000 °C to observe oxidation behavior further. Isothermal oxidation tests were performed in a horizontal tube furnace in which both ends of the tube opened and can achieve a maximum working temperature of around 1200 °C.

During oxidation tests, specimens were placed in alumina boats and positioned in the heating zone once the target temperature was reached. They were then removed from the furnace and allowed to cool in the air once the oxidation tests were completed. One specimen was used for each oxidation test. After each oxidation test, the sample was weighed using an analytical balance with an accuracy of 0.1 mg.
The phase constitution of the oxidized sample and oxidation product were characterized by XRD (x-ray diffraction) SmartLab, Rigaku using Cu-Kα radiation (λ=0.154 nm) functioning at 40 kV. Microstructure and chemical composition were studied using an optical microscope and SEM (scanning electron microscope) JCM-7000 NeoScope™, JEOL equipped with an EDS (energy dispersive spectrometer).The cross-section surface was subject to mechanical polishing but not etching. The Vickers hardness test was conducted on a polished cross-sectional surface using a diamond pyramid indentation undera 98.07 N load applied for 20 s. Five indentations were measured to obtain an average value of each sample.

3. RESULTS AND DISCUSSION

3.1 Microstructure Analysis and Hardness of $Al_{0.25}$CoCrCuFeNi

Previous studies [13]-[14] have reported that the $Al_{0.3}$CoCrCuFeNi alloy consists of a DR (dendritic region) with an FCC (face-centered cubic) microstructure and an inter-dendritic region (ID) with Cu-rich FCC microstructure. Butler, et al. [11] also investigated the oxidation behavior of $Al_x(CoCrFeNi)_{100-x}$ alloy (x = 8, 10, 12, 15, 20, 30 at.%) and confirmed that the microstructure of high entropy alloy with low Al content is FCC, whereas those with high Al

content exhibit a BCC (body-centered cubic) structure.

According to the phase diagram constructed by Turchi et al. [1], the $Al_{0.25}CoCrCuFeNi$ alloy exists in equilibrium with the FCC phase and a Cu-rich FCC phase at 800, 900, and 1000 ℃. To predict the crystal structure of the alloy, the VEC (valence electron concentration) was calculated. A VEC of 8.52 for $Al_{0.25}CoCrCuFeNi$ indicates the stability of the FCC structure [13]. Other thermodynamic parameters, including the entropy of mixing (ΔS_{mix}), enthalpy of mixing (ΔH_{mix}), atomic size mismatch (δ), and mixing parameter (Ω), were also calculated and found to be 14.34 $JK^{-1}mol^{-1}$, 0.62 $kJmol^{-1}$, 3.18%, and 40.19, respectively.

As illustrated in Fig. 1, the microstructure reveals that the dark-colored inter-dendritic region exhibits a Cu-rich FCC structure, while the bright-colored dendritic region possesses an FCC structure. According to Table 1, the inter-dendritic section contains the highest concentration of copper at 63.91 at.% as determined by EDS. The segregation of copper in the inter-dendritic regions can be attributed to the bonding energy between copper and other elements. Copper exhibits a positive enthalpy of mixing with cobalt, chromium, iron, and nickel, which are 6, 12, 13, and 4 kJ/mol, respectively [14].

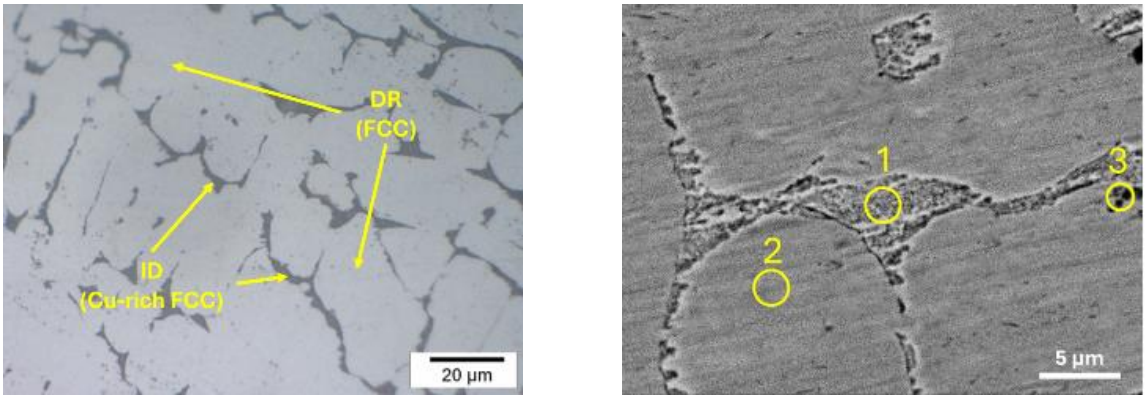

(a) (b)

Figure 1. Microstructure of *as-homogenized* $Al_{0.25}CoCrCuFeNi$alloy. (a) Optical microscope showing dendritic and inter-dendritic areas at high magnification, (b) Backscattered electron image showing dendritic and inter-dendritic areas. Point 1-3 indicate EDS point analysis

This suggests that copper tends to avoid bonding preferentially with the dendrite part, which is enriched in cobalt, chromium, iron, and nickel. Table 1 further demonstrates that the inter-dendritic region exhibits a higher aluminum content than the initial composition, while the copper in the dendritic region displays a lower concentration of approximately 9.89% compared to the initial composition of 19.05%.

Table 1. Chemical composition of *as-homogenized*$Al_{0.25}CoCrCuFeNi$ obtained from EDS point analysis

Point	Elements (at.%)					
	Al	Co	Cr	Cu	Fe	Ni
1	10.56	3.19	1.51	63.91	2.76	18.07
2	5.69	22.56	21.54	9.89	21.34	20.34
3	16.30	21.20	18.50	11.83	17.57	17.78

Figure 2 illustrates the average hardness values of the *as-homogenized* $Al_{0.25}CoCrCuFeNi$. The hardness test results indicate a general trend of decreasing hardness with increasing exposure time.

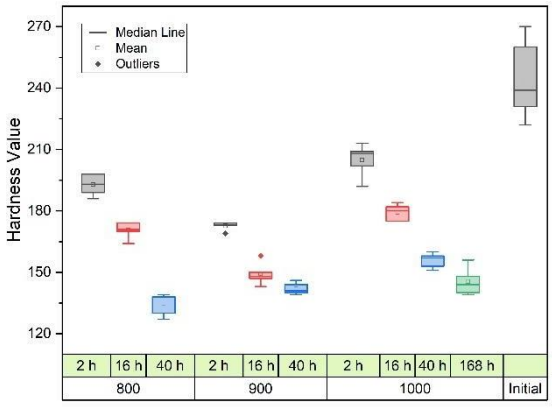

Figure 2. The hardness value of the $Al_{0.25}CoCrCuFeNi$ alloy at various temperatures as a function of exposure time. (Initial means *as-homogenized* alloy)

This decrease in hardness is attributed to the reduced Al content, which becomes concentrated at the substrate due to the diffusion of Al atoms to the metal/oxide interface to form a protective Al_2O_3 layer. During oxidation, Al is consumed to

create this protective layer, resulting in a concentration gradient that drives the diffusion of Al atoms from the substrate to the surface. Aluminum has a larger atomic radius (143 pm) than the other alloying elements (ranging from 124 to 128 pm). Consequently, a decrease in Al content leads to a reduction in lattice distortion within the alloy [15].

3.2 Oxidation Kinetic

Figure 3 presents the specific weight gain of the $Al_{0.25}CoCrCuFeNi$ alloy during isothermal oxidation testing within the 800-1000 °C temperature range. At 800 and 900 °C, no substantial weight gain was observed, and the oxidation profile exhibited steady growth. However, at 1000 °C, a significant increase in weight gain was noted after 40 h of oxidation, suggesting a rapid oxidation rate.

During the initial stages of oxidation, an astable oxide scale was observed for up to 16 hat all oxidation temperatures. However, the alloy demonstrated a sudden increase in oxidation rate after prolonged exposure at 1000 °C, resulting in rapid oxidation. To gain further insights into its oxidation behavior, the oxidation test was extended to 168 h, revealing a semi-parabolic oxidation profile.

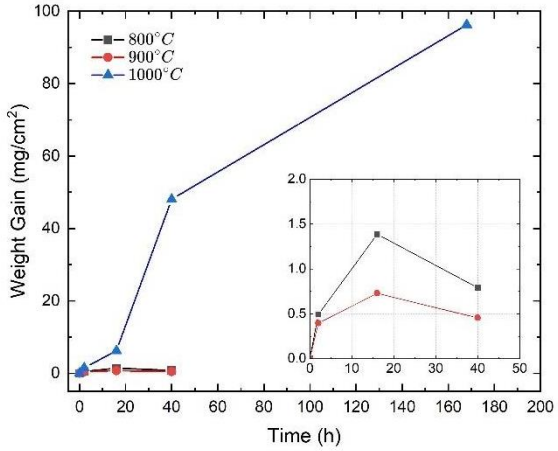

Figure 3. Oxidation weight gain of the $Al_{0.25}CoCrCuFeNi$ alloy at 800-1000 °C

In summary, the oxidation resistance of the $Al_{0.25}CoCrCuFeNi$ is strongly influenced by temperature and time. However, the primary objective of this study is to elucidate the oxidation mechanism and morphology of the formed oxides, rather than delving into detailed information on oxidation kinetics, such as the oxidation rate.

3.3 Oxide Scale Morphology

Figure 4 presents the XRD diffractogram of the alloy at 800-1000 °C. The diffractogram patterns indicate the formation of Al_2O_3, Cr_2O_3, NiO, CoO, Fe_3O_4, CuO, and spinel. All types ofAl_2O_3formed were transient oxides, with variations such as γ-Al_2O_3, δ-Al_2O_3, and θ-Al_2O_3 at 800, 900, and 1000°C, respectively. However, these transient oxides exhibit poor oxidation resistance [16]. Additionally, an alloy substrate consisting of FCC and Cu-rich FCC phases was detected at all temperature ranges.

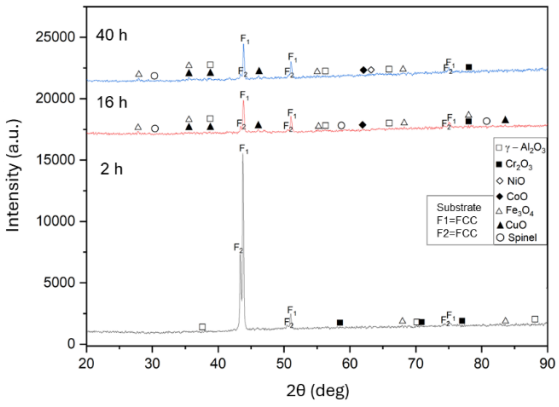

(a)

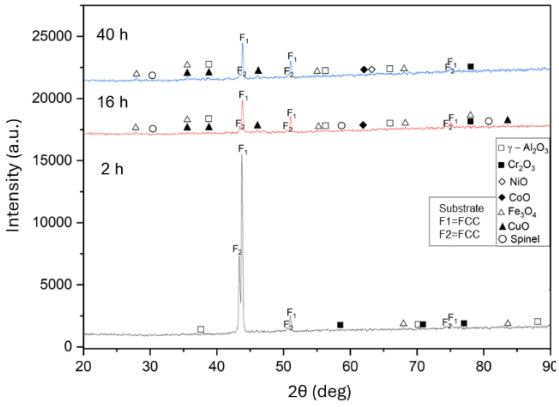

(b)

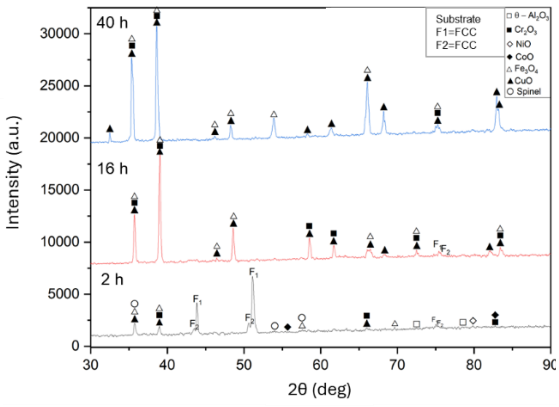

(c)

Figure 4. The XRD diffractogram of the $Al_{0.25}CoCrCuFeNi$ alloy at (a) 800 °C, (b) 900 °C, (c) 1000 °C

Figures 5-7 illustrate the morphology of the oxide layer formed on the surface of $Al_{0.25}CoCuCrFeNi$ for samples held at 800, 900, and 1000 °C for 40 h, as well as samples held at

1000 ℃ for 168 h in Fig. 8. The composition of the formed oxides in Fig. 5(a), as presented in Table 2, is predominantly composed of Cu and Cr, with respective compositions of 23.03 at% and 14.38 at.%.

Figure 5(b) depicts the oxide morphology, which is dominated by Al, followed by Cr with a composition of 33.83 at.% and 8.12 at.%, respectively. In Figure 5(c), the morphological image reveals a small plate-like shape of a spinel oxide composed of Al-Cr-Cu-Fe.

Table 2. Chemical composition of oxidized sample at 800 °C for 40 h according to EDS point analysis in Figure 5

Point	Elements (at.%)						
	Al	Co	Cr	Cu	Fe	Ni	O
1	1.56	4.22	14.38	23.03	2.15	1.58	53.07
2	33.83	2.44	8.12	2.11	3.24	2.44	48.29
3	17.23	3.40	13.00	9.08	10.34	2.69	44.27

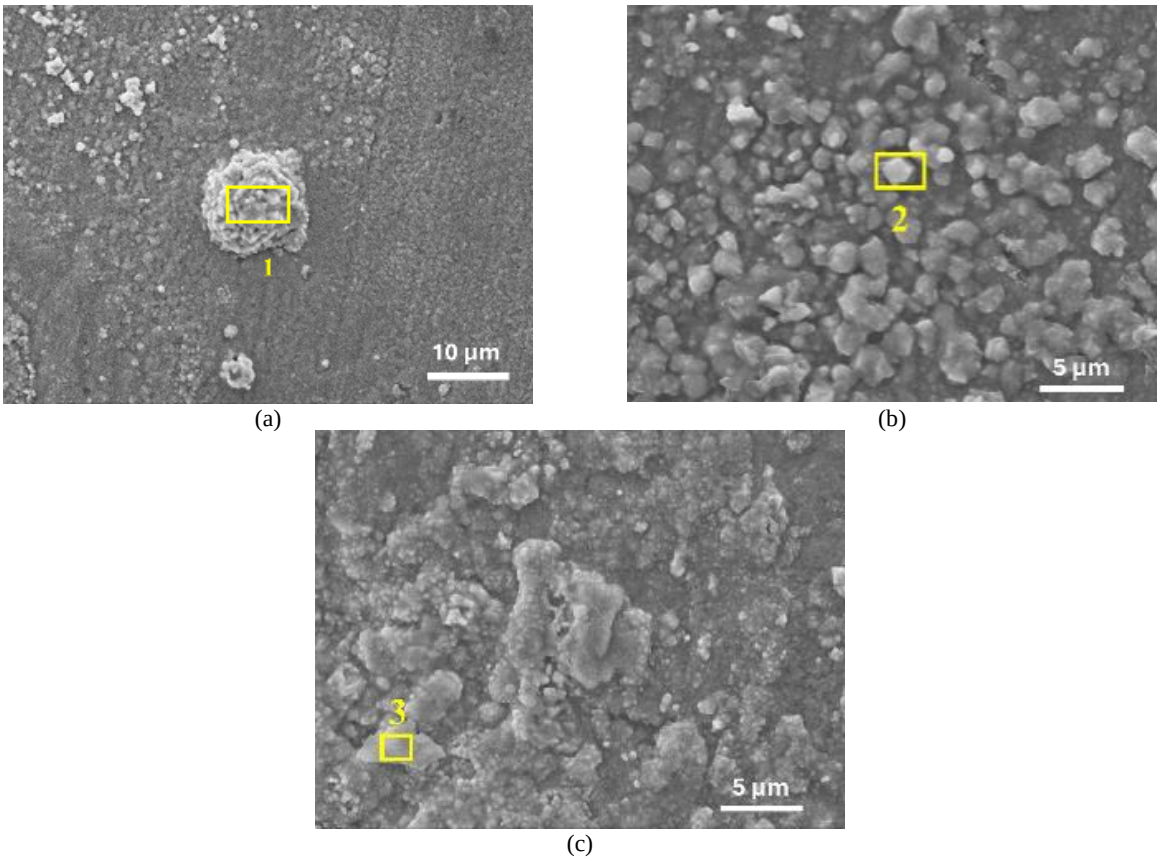

(a) (b) (c)

Figure 5. Surface morphology of sample at 800 °C for 40 h

In the sample oxidized at 900 ℃ for 40 h, a thin oxide layer formed on the surface. SEM analysis revealed that certain portions of the oxide had peeled off, as illustrated in Figs. 6(a) and 6(c).

The composition of these peeled-off sections corresponds to $Al_{0.25}CoCrCuFeNi$, except Cu (see Table 3). Figure 6(b) depicts a thin plate-like structure with Al as the dominant element, indicating the formation of Al_2O_3 oxide.

Table 3. Chemical composition of oxidized sample at 900 °C for 40 h according to EDS point analysis in Figure 6

Point	Elements (at.%)						
	Al	Co	Cr	Cu	Fe	Ni	O
1	31.72	0.48	1.59	1.06	0.35	0.43	64.37
2	4.20	21.79	21.99	5.26	21.48	19.78	5.50

The outermost oxide layer formed on the surface of the samples oxidized at 1000 ℃ for 40 h and 168h is predominantly composed of Cu.

Table 4. Chemical composition of oxidized sample at 1000 °C for 40 h according to EDS point analysis in Figure 7

Point	Elements (at.%)						
	Al	Co	Cr	Cu	Fe	Ni	O
1	2.29	0.50	0.56	39.78	0.28	0.87	55.72
2	0.70	1.15	-	54.51	0.04	0.04	43.56
3	0.15	1.31	0.08	49.64	0.08	0.64	48.10

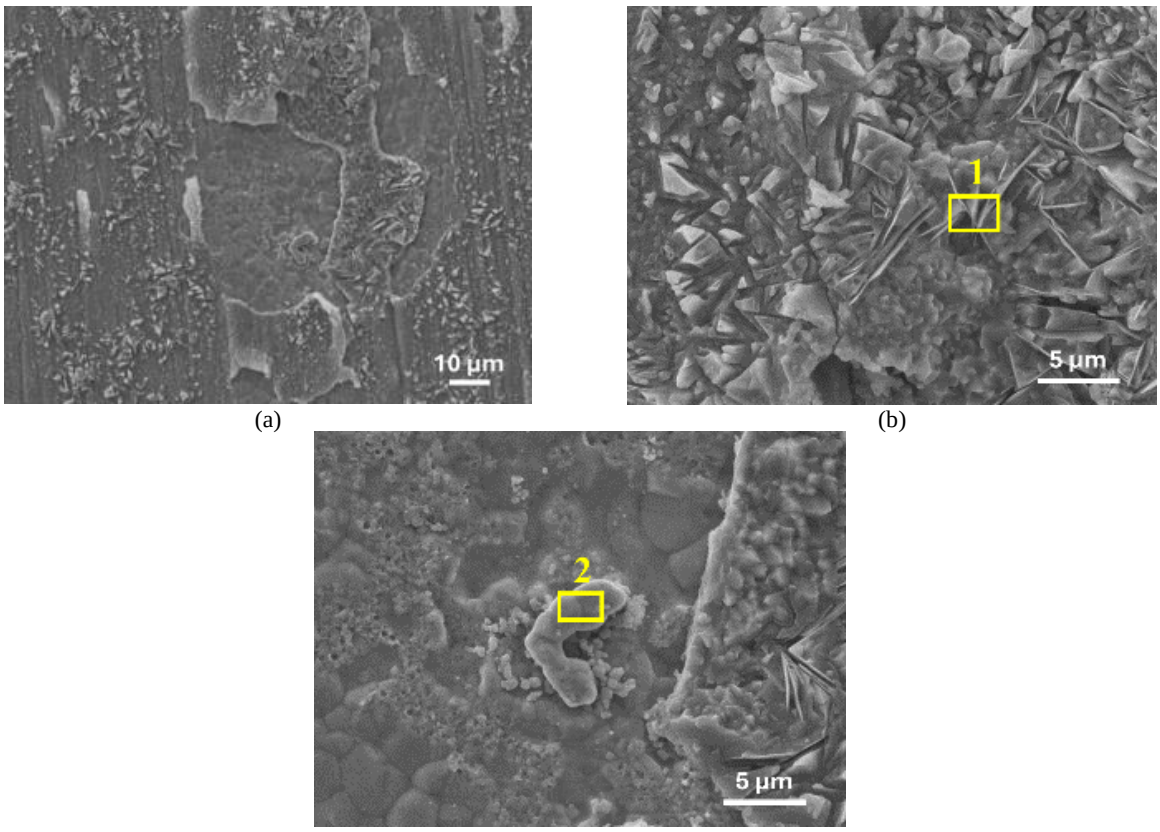

(a) (b) (c)

Figure 6. Surface morphology of sample at 900 °C for 40 h

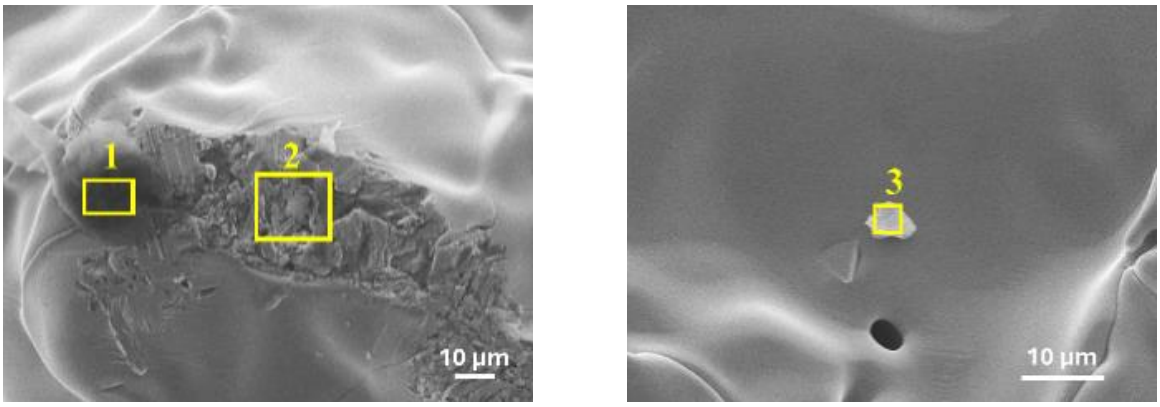

(a) (b)

Figure 7. Surface morphology of sample at 1000 °C for 40 h

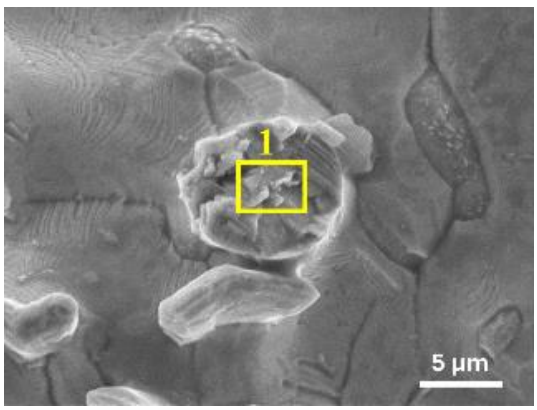

Figure 8. Surface morphology of sample at 1000 °C for 168 h

EDS point analysis of Figs. 7 and 8 indicate that the outermost oxide layer is dominated by Cu, as shown in Tables 4 and 5. The resulting CuO oxide layer exhibits a dense and non-porous structure.

Table 5. Chemical composition of oxidized sample at 1000 °C for 168 h according to EDS point analysis in Figure 8

Point	Elements (at.%)						
	Al	Co	Cr	Cu	Fe	Ni	O
1	0.05	2.35	-	42.08	0.13	1.61	53.78

3.4 Cross-section Analysis

Figures 9-11 depict the X-ray mapping of the alloy cross section after oxidation testing at 800, 900, and 1000 ℃ for 2 h. At 800 ℃, a thin oxide layer dominated by Al and Cr formed on the sample surface, as shown in Fig. 9. Meanwhile, the oxide layer at 900 ℃ is composed of a mixture of elements, including Al, Co, Cr, Cu, Fe, and Ni. Internal oxidation occurred due to the formation of transient oxides during the initial oxidation period. These lower oxides allow anions to diffuse faster than cations, resulting in the formation of a mixed oxide layer with a predominance of Al and Cr along the inter-dendritic phase.

Figure 11 illustrates the oxide layer formed at 1000 ℃, which consists of a mixture of Al, Co, Cr, Cu, Fe, and Ni. The order of oxide layer formation aligns with the stability of oxide compounds as depicted in the Ellingham-Richardson diagram. Each layer is dominated by a particular oxide, with the order from lowest to highest stability being Al_2O_3, Cr_2O_3, spinel ((Co, Ni, Cu)(Al, Cr, Fe)$_2O_4$), a mixture of simple oxides (Fe_3O_4, CoO, NiO), and CuO. The Al_2O_3 layer was only partially formed due to Al depletion near the surface. Consequently, other elements are more likely to form oxides at a faster rate. At 1000 ℃, CuO formed in the upper layer due to the dominant presence of Cu in the inter-dendritic region. In contrast, Y. Y. Liu et al. [15] investigated the oxidation of $Al_xCoCrCuFeNi$ alloy at 1000 ℃ for 100 h and found that CuO oxide did not form in the outer layer of the oxide layer due to the poor adhesion properties of Cr_2O_3 oxide, which led to excessive exfoliation.

3.5 Oxidation Mechanism

The oxidation of the alloy can lead to the formation of a mixed oxide compound. When considering oxide formation, it is essential to account for the stability of the oxide-forming elements within the alloy. Several factors influence the kinetics of alloy oxidation, including the diffusivity of oxygen and the propensity of the alloying elements to react with oxygen. As a result, the oxides formed will exhibit varying growth rates, and the composition of the oxide at the metal/oxide interface will gradually change. The oxide with the highest concentration will ultimately dominate the growth of the oxide layer in that region.

Figure 12 illustrates the oxidation mechanism of the alloy at 800 and 900 ℃. The oxidation process begins with the interaction of oxygen with the substrate surface, where oxygen ions (anions) react with metal ions (cations) on the substrate. In the early stages of oxidation, a thin oxide layer or transient oxides, such as FeO, CoO, CuO, NiO, and spinel ((Co,Ni,Cu)(Al,Cr,Fe)$_2O_4$), forms on the metal surface. During exposure, oxygen diffuses through the transient oxide layer. According to the Ellingham-Richardson diagram, Cr and Al are the elements most likely to react under these conditions. This reaction leads to the formation of a Cr_2O_3 layer, which reduces the pO_2 within the substrate, facilitating the subsequent formation of an Al_2O_3 layer. The Al_2O_3 layer exhibits more stable properties at low oxygen activity. Both Cr_2O_3 and Al_2O_3 layers will thicken, further reducing the oxygen activity in the substrate.

As oxidation exposure time increases, an Al_2O_3 layer is anticipated to form uniformly and protectively on the alloy surface. However, the Al_2O_3 formed is a transient alumina (γ-Al_2O_3, δ-Al_2O_3, θ-Al_2O_3) that is less protective compared to α-Al_2O_3. This less protective nature allows for the diffusion of oxygen ions into the substrate through the oxide layer. If the oxygen content within the alloy exceeds its solubility limit, internal oxidation will occur beneath the oxide layer.

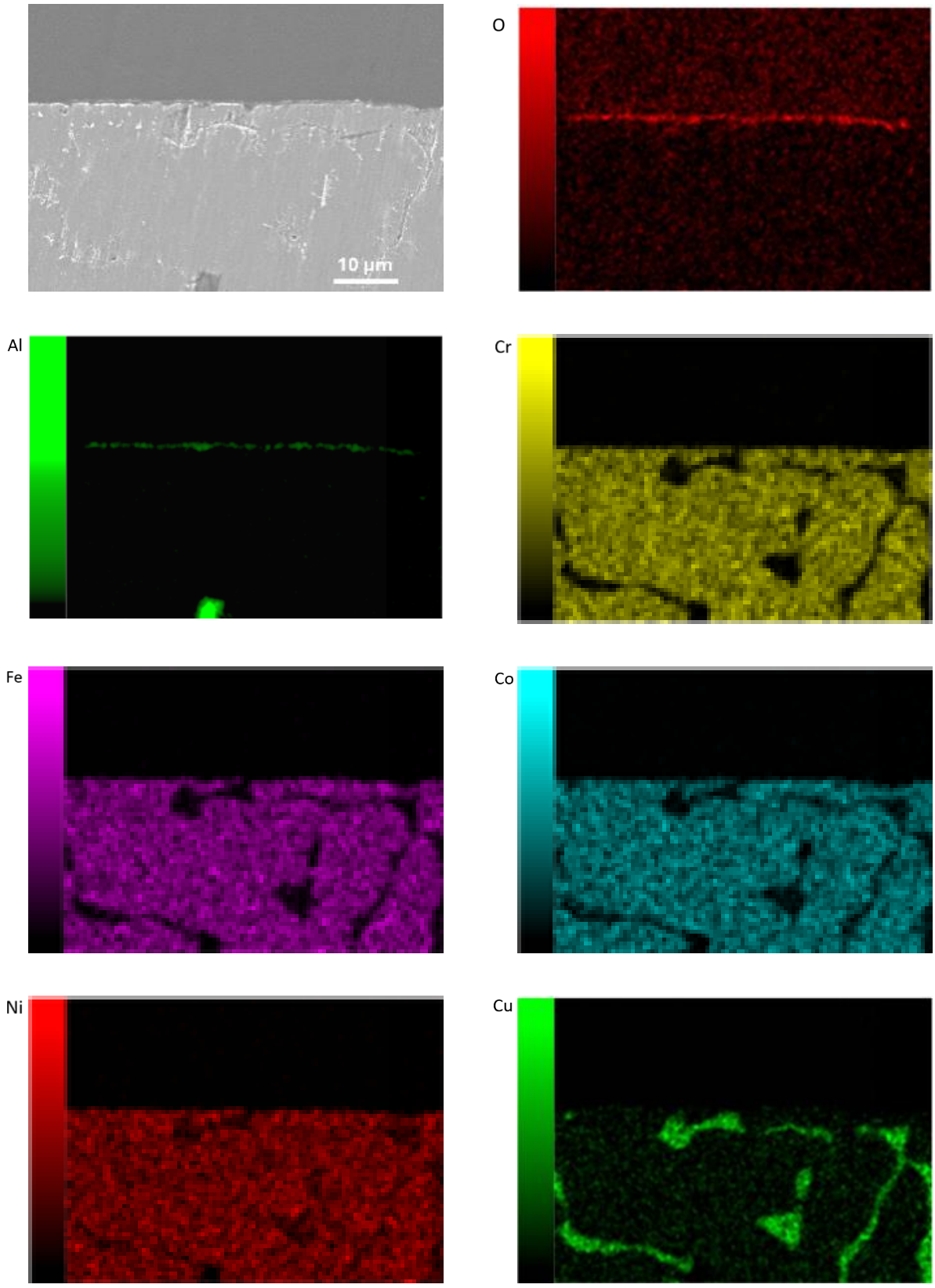

Figure 9. EDS mapping of cross-section sample at 800 °C for 2 h

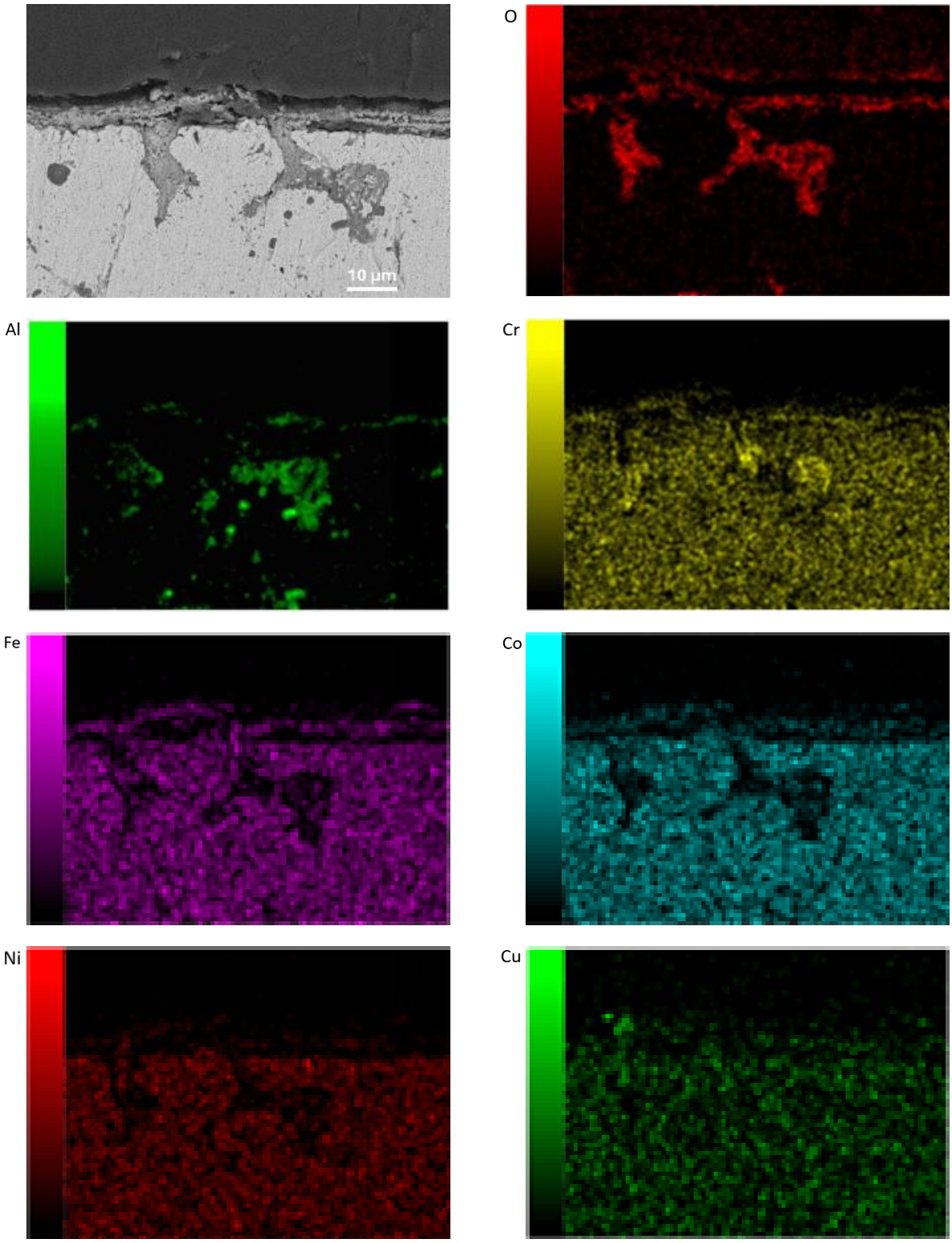

Figure 10. EDS mapping of cross-section sample at 900 °C for 2 h

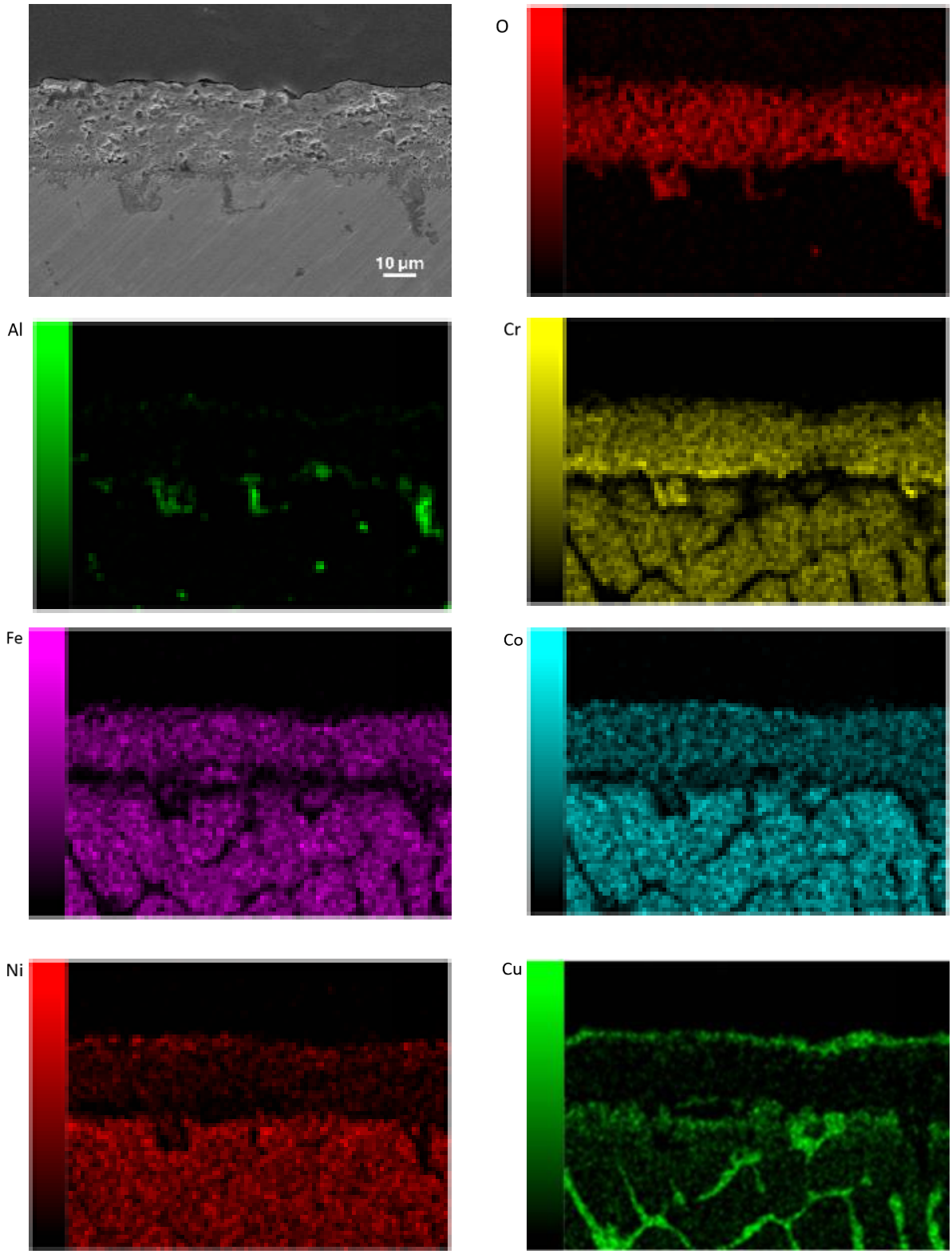

Figure 11. EDS mapping of cross-section sample at 1000 °C for 2 h

In this alloy, internal oxidation predominantly occurs along the inter-dendritic region, resulting in the formation of Al_2O_3 along with small amounts of Cr_2O_3 and CuO. Other elements will also form oxides, such as Fe_3O_4, CoO, CuO, NiO, and spinel ($(Co,Ni,Cu)(Al,Cr,Fe)_2O_4$). CuO oxide is formed on the surface of the oxide layer parallel to the inter-dendritic area due to the high Cu content in that region.

The oxidation mechanism of the $Al_{0.25}CoCrCuFeNi$ alloy at 1000 °C deviates from the previous mechanism due to the absence of a continuous Al_2O_3 layer, rendering it non-protective.

Initially, Cr_2O_3 forms during oxidation, followed by the formation of non-continuous Al_2O_3 due to Al depletion near the oxide/substrate interface.

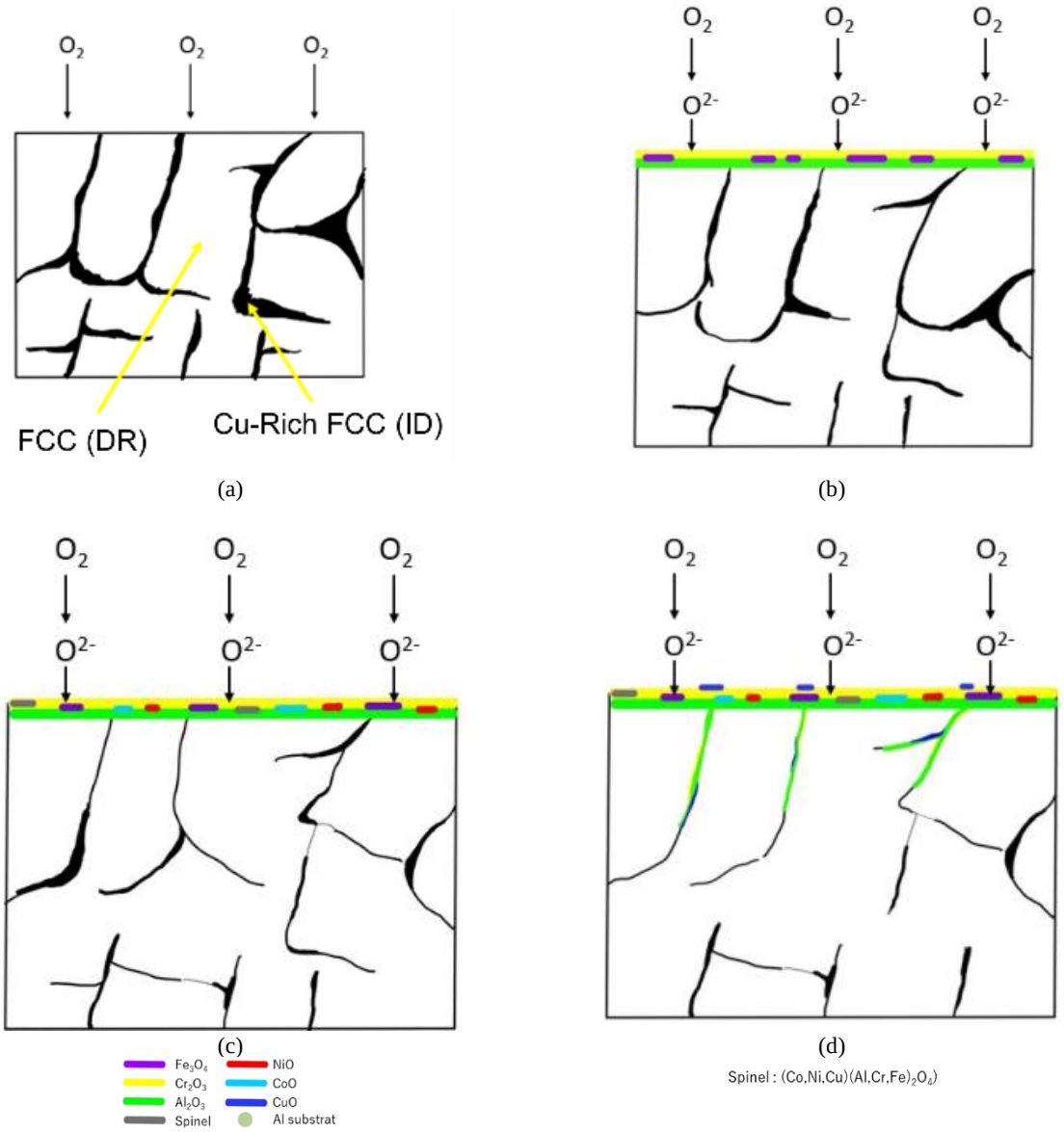

Figure 12. Illustration of oxidation mechanism of $Al_{0.25}CoCrCuFeNi$ alloy at 800 and 900 °C. (a) → (b) → (c) → (d)

This depletion is attributed to the slower diffusion rate of Al compared to other elements. The order of diffusion speed for elements from the lowest is as follows: Al, Cr, Ni, Co, and Fe. This sequence results in the formation of oxide layers such as Cr_2O_3, Fe_3O_4, CoO, NiO, and CuO, as well as spinel ($(Co,Ni,Cu)(Al,Cr,Fe)_2O_4$), on the outermost layer of the oxide scale.

CuO is formed in the outermost layer of the oxide layer in Cu-rich inter-dendritic areas. Consequently, the diffusion of Cu will occur extensively in multiple directions as illustrated in Fig. 13.

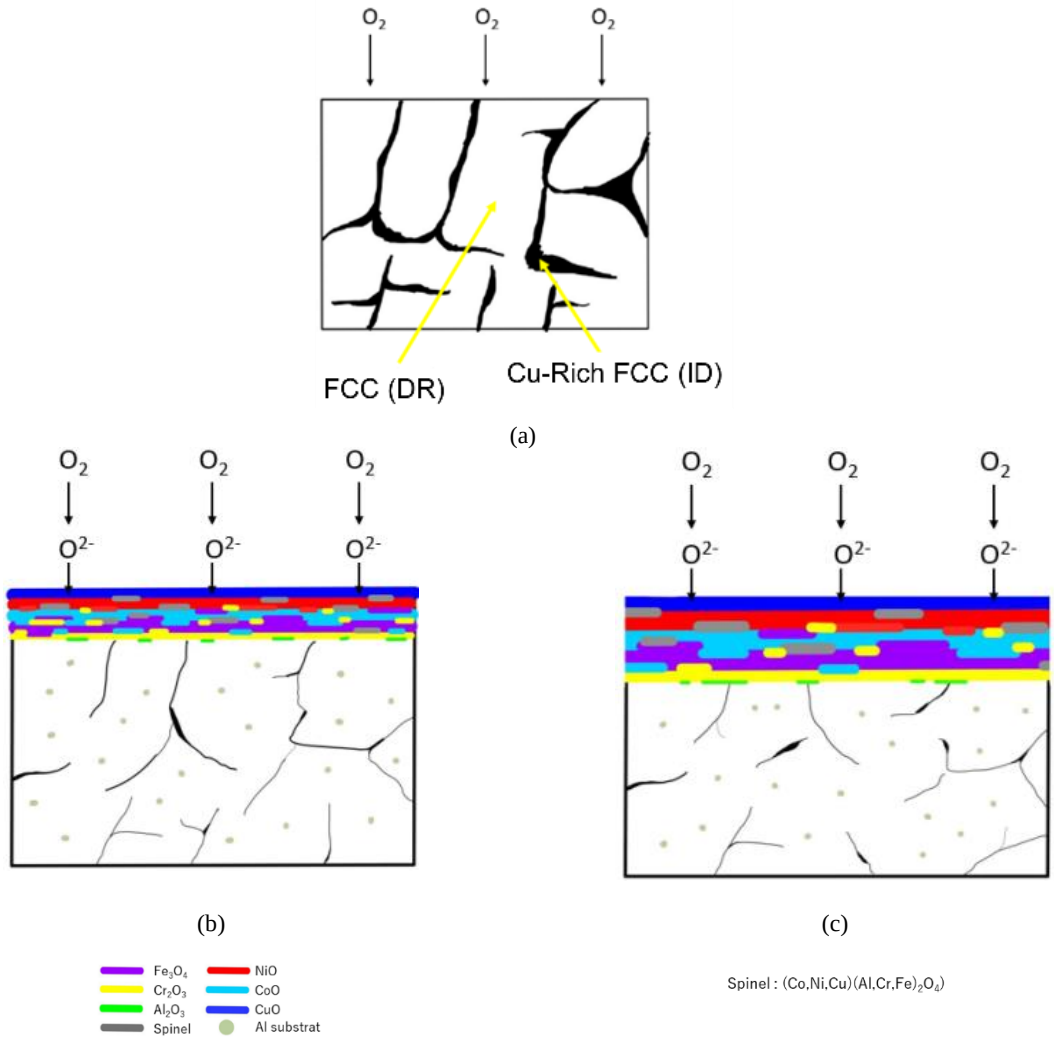

Figure 13. Illustration of oxidation mechanism of $Al_{0.25}CoCrCuFeNi$ alloy at 1000 °C. (a) → (b) → (c)

4. CONCLUSION

The oxidation behavior and microstructural evolution of the $Al_{0.25}CoCrCuFeNi$ HEA were examined at 800, 900, and 1000 °C for 2, 16, and 40 h. SEM-EDS confirmed that this alloy consists of an FCC phase in the dendritic region and a Cu-rich FCC phase in the inter-dendritic regions, consistent with the Hume Rothery rules and valence electron concentration value. The oxides formed during the oxidation process include Al_2O_3, Cr_2O_3, Fe_3O_4, CoO, CuO, NiO, and spinel oxides $(Co,Ni,Cu)(Al,Cr,Fe)_2O_4$), with distinct formation mechanisms at a temperature below 900 °C compared to those at or above 1000 °C. All types of Al_2O_3 formed were transient oxides, with variations such as γ-Al_2O_3, δ-Al_2O_3, and θ-Al_2O_3 at 800, 900, and 1000 °C, respectively.

ACKNOWLEDGMENT

This research was funded by the Program Riset dan Inovasi untuk Indonesia Maju (RIIM) Gelombang 2 the National Research and Innovation Agency (BRIN) and Educational Fund Management Institution (LPDP), grant number 78/IV/KS/11/2022 and 834/IT1.B07/KS.00/2022 which is greatly acknowledge.

REFERENCES

[1] A. Turchi, D. Bianchi, F. Nasuti, and M. Onofri, "A numerical approach for the study of the gas–surface interaction in carbon–phenolic solid rocket nozzles," *Aerosp Sci Technol*, vol. 27, no. 1, pp. 25-31, 2013. Doi: 10.1016/j.ast.2012.06.003.

[2] C. Katsarelis, P. Chen, P. Gradl, C. Protz, Z. Jones, D. Ellis, and L. Evans, "Additive manufacturing of NASA HR-1 material for liquid rocket engine component applications," *JANNAF Dec*, p. https://ntrs.nasa.gov/search.jsp?R=20200001007, 2019. [Online]. Available: https://ntrs.nasa.gov/api/citations/20200001007/downloads/20200001007.pdf%0Ahttps://ntrs.nasa.gov/search.jsp?R=20200001007

[3] Md. Shahwaz, P. Nath, and I. Sen, "A critical review on the microstructure and mechanical properties correlation of additively manufactured nickel-based superalloys," *J Alloys Compd*, vol. 907, pp. 164530, 2022. Doi: 10.1016/j.jallcom.2022.164530.

[4] T. M. Pollock and S. Tin, "Nickel-based superalloys for advanced turbine engines: Chemistry, microstructure and properties," *J Propuls Power*, vol. 22, no. 2, pp. 361-374, 2006. Doi: 10.2514/1.18239.

[5] W. Xia, X. Zhao, L. Yue, and Z. Zhang, "A review of composition evolution in Ni-based single crystal superalloys," *J Mater Sci Technol*, vol. 44, pp. 76-95, 2020. Doi: 10.1016/j.jmst.2020.01.026.

[6] Y. Zhang, T. T. Zuo, Z. Tang, M. C. Gao, K. A. Dahmen, P. K. Liaw, and Z. P. Lu, "Microstructures and properties of high-entropy alloys," *Prog Mater Sci*, vol. 61, pp. 1-93, 2014. Doi: 10.1016/J.PMATSCI.2013.10.001.

[7] J. W. Yeh, "Recent progress in high-entropy alloys," *Annales de Chimie: Science des Materiaux*, vol. 31, no. 6, pp. 633-648, 2006. Doi: 10.3166/acsm.31.633-648.

[8] T. Wang, W. Jiang, X. Wang, B. Jiang, C. Rong, Y. Wang, J. Yang, and D. Zhu, "Microstructure and properties of Al0.5NbTi3VxZr2 refractory high entropy alloys combined with high strength and ductility," *Journal of Materials Research and Technology*, vol. 24, pp. 1733-1743, 2023. Doi: 10.1016/J.JMRT.2023.03.103.

[9] D. B. Miracle and O. N. Senkov, "A critical review of high entropy alloys and related concepts," *Acta Mater*, vol. 122, no. October, pp. 448-511, 2017. Doi: 10.1016/j.actamat.2016.08.081.

[10] J. Lu, G. Ren, Y. Chen, H. Zhang, L. Li, A. Huang, X. Liu, H. Cai, X. Shan, L. Luo, X. Zhang, and X. Zhao, "Unraveling the oxidation mechanism of an AlCoCrFeNi high-entropy alloy at 1100 °C," *Corros Sci*, vol. 209, pp. 110736, 2022. Doi: 10.1016/J.CORSCI.2022.110736.

[11] T. M. Butler and M. L. Weaver, "Oxidation behavior of arc melted AlCoCrFeNi multi-component high-entropy alloys," *J Alloys Compd*, vol. 674, pp. 229-244, 2016. Doi: 10.1016/j.jallcom.2016.02.257.

[12] T. M. Butler, M. J. Pavel, and M. L. Weaver, "The effect of annealing on the microstructures and oxidation behaviors of AlCoCrFeNi complex concentrated alloys," *J Alloys Compd*, vol. 956, pp. 170391, 2023. Doi: 10.1016/j.jallcom.2023.170391.

[13] S. Guo, C. Ng, J. Lu, and C. T. Liu, "Effect of valence electron concentration on stability of fcc or bcc phase in high entropy alloys," *J Appl Phys*, vol. 109, no. 10, 2011. Doi: 10.1063/1.3587228.

[14] A. Takeuchi and A. Inoue, "Calculations of mixing enthalpy and mismatch entropy for ternary amorphous alloys," *Materials Transactions, JIM*, vol. 41, no. 11, pp. 1372–1378, 2000. Doi: 10.2320/matertrans1989.41.1372.

[15] Y. Y. Liu, Z. Chen, Y. Z. Chen, J. C. Shi, Z. Y. Wang, S. Wang, and F. Liu, "Effect of Al content on high-temperature oxidation resistance of AlxCoCrCuFeNi high entropy alloys (x=0, 0.5, 1, 1.5, 2)," *Vacuum*, vol. 169, pp. 108837, 2019. Doi: 10.1016/J.VACUUM.2019.108837.

[16] J. Lee, H. Jeon, D. G. Oh, J. Szanyi, and J. H. Kwak, "Morphology-dependent phase transformation of γ-Al_2O_3," *Appl Catal A Gen*, vol. 500, pp. 58-68, 2015. Doi: 10.1016/J.APCATA.2015.03.040.

AUTHOR INDEX

SUBJECT INDEX